Institute of Thermoelectricity, Academy of Sciences and Ministry of Education and Science of Ukraine

Journal of THERMOELECTRICITY

International Research

Founded in December, 1993

published 6 times a year

No. 3 *2018*

Editorial Board

International Editorial Board

Founders – National Academy of Sciences, Ukraine
Institute of Thermoelectricity of National Academy of Sciences and Ministry of Education and Science of Ukraine

Certificate of state registration № КВ 15496-4068 ПР

Approved for printing by the Academic Council of Institute of Thermoelectricity of the National Academy of Sciences and Ministry of Education and Science, Ukraine

Address of editorial office:
Ukraine, 58002, Chernivtsi, General Post Office, P.O. Box 86.
Phone: +(380-372) 90 31 65.
Fax: +(380-3722) 4 19 17.
E-mail: jt@inst.cv.ua
http://www.jt.inst.cv.ua

Signed for publication 25.07.18. Format 70×108/16. Offset paper №1. Offset printing.
Printer's sheet 11.5. Publisher's signature 9.2. Circulation 400 copies. Order 5.

Printed from the layout original made by "Journal of Thermoelectricity" editorial board
in the printing house of "Bukrek" publishers,
10, Radischev Str., Chernivtsi, 58000, Ukraine

CONTENTS

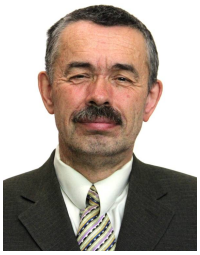

P.V. Gorskiy

P.V. Gorskiy, *Doctor Phys.-math. Science*[1,2]

Institute of Thermoelectricity of the NAS and MES of Ukraine,
1, Nauky str, Chernivtsi, 58029, Ukraine;
[2]Yu.Fedkovych Chernivtsi National University,
2, Kotsiubynskyi str., Chernivtsi, 58000, Ukraine
e-mail: anatych@gmail.com

INFLUENCE OF SURFACE PHENOMENA ON THE ORIENTATION OF CLEAVAGE PLANES OF BISMUTH TELLURIDE SINGLE CRYSTALS WITH RESPECT TO THE WIDE EDGES OF A SLOTTED CONTAINER

The paper considers the influence of surface phenomena on the orientation of cleavage planes of single-crystal plates of bismuth telluride-based thermoelectric materials with respect to the wide edges of the container when grown in flat slots by the Bridgman method. By solving the equation of mechanical equilibrium of solid phase nucleus on the vertical wall of a slotted container, a ratio is obtained for the angle between the single crystal cleavage planes with respect to the vertical walls of the container, when taking into account the action of both surface tension forces at the "container wall – nucleus", "container wall — melt" and "nucleus - melt" boundaries and the force of gravity. As a result of the analysis, it was shown that for the manufacture of containers or gaskets for them, whenever possible, such materials should be chosen, on the flat horizontal surface of which this mass of thermoelectric material, heated to the melting temperature, after spreading of the melt and its subsequent solidification forms a layer of the largest area, since the angle between the cleavage planes of the single crystal and the wide edges of the container is inversely proportional to the fourth power of this area. Bibl. 10, Fig. 5.

Key words: surface tension, contact angle, mechanical equilibrium of solid phase nucleus.

Introduction

The method of growing single crystals of thermoelectric materials in flat slots with the production of ingots in the form of parallelepipeds and the manufacture of thermoelectric modules from them is described in [1] and [2]. In particular, in patent [1] it is indicated that single crystals of bismuth telluride produced in the form of cylindrical ingots must be further cut into disks which are then cut along mutually perpendicular vertical planes. And since the cleavage planes are perpendicular to the disc planes, the discs are often destroyed. This forces to obtain thermoelectric legs from incomplete disks or their parts, which leads to the formation of a large amount of waste. Due to the arbitrary orientation of the cleavage planes of the ingot or the disc cut from it, it is difficult to obtain from such an ingot plate elements of the same length that have the same characteristics and the same cutting resistance. Therefore, it is desirable to have a cast plate of a layered structure with parallel cleavage planes, which could then be cut into plate elements and then into legs having the same characteristics. From the results of [1,2] it follows that if a single crystal in the form of such a plate is grown in a slotted container with flat walls, to achieve the aforementioned positive results, the angle between the wide edges of the container and the cleavage planes of the single crystal of bismuth telluride should not exceed 5^o. In contrast, the patent [3] describes the technology for creating thin-film thermoelectric elements, which, on the contrary, provides for the angle of inclination of the cleavage planes at an angle from 30^o to 90^o to the substrate. Because of this, the problem naturally

arises of analyzing the influence of various factors on the angle between the cleavage planes of a single crystal of bismuth telluride and the wide edges of a slotted container.

As is known, single-crystal bismuth telluride and its alloys have cleavage planes (hexagonal layers) along which they grow most rapidly. Due to the anisotropy of thermal conductivity and electrical conductivity of these single crystals, it is advantageous to manufacture thermoelectric modules so that the electric current density and temperature gradient vectors lie in the plane of layers. And this means that the planes of switching electrodes should be perpendicular to the planes of layers. The deviation from this perpendicularity should be as low as possible so that, on the one hand, the efficiency of the module is maximum, and on the other, it does not collapse when exposed to mechanical loads and temperature stresses caused by thermal expansion of the elements of the module when it is unevenly heated. To achieve these goals, it is also necessary to ensure a minimum angle between the cleavage planes of the single crystal and the wide edges of the slotted container. This can be achieved in several ways. On the one hand, it is possible to optimize the geometry of the container and the operation mode of the Bridgman unit in such a way as to minimize the transverse temperature gradient and properly relate it to the growth rate of a single crystal. On the other hand, it is possible to choose packing materials for the container that are in direct contact with the melt and the growing single crystal in such a way as to achieve the minimum angle between the cleavage planes of the bismuth telluride single crystal and the wide edges of the slotted container by controlling surface phenomena at the “container wall-melt” and “container wall-solid phase" boundaries. These approaches can be applied in combination with each other. However, the implementation of the first approach requires a detailed thermal calculation of the container and the installation as a whole, which is not the purpose of this paper.

The influence of surface phenomena on the formation of solid phase nuclei and their growth was considered in [4–8] and in the monograph [9]. However, this consideration was mainly concerned with the processes occurring during horizontal zone melting. At the same time, we showed in [10] that the anisotropy of the growth rate of bismuth telluride single crystals and its alloys and the resulting anisotropy of the surface tension coefficient at the “solid phase-melt” boundary causes uncompetitive growth of single crystals along cleavage planes. This makes it possible to obtain single-crystal flat plates of the aforementioned alloys in the process of vertical crystallization by the Bridgman method using special containers with cavities in the form of rectangular parallelepipeds.

In [7], the kinetics of nucleation in heterogeneous systems was considered with allowance for capillary phenomena. However, in this work the container wall was also assumed to be located horizontally. We will consider this process with the vertical arrangement of the wide edges of the container, which takes place, for example, with vertical recrystallization by the Bridgman method. In this case, there is a need for additional consideration of the effect of gravity.

Thus, the goal is to consider surface phenomena at the “container wall - melt” and “container wall - solid phase” boundaries during vertical crystallization, i.e. under the influence of gravity, and their influence on the angle between the cleavage planes of the single crystal of bismuth telluride and the wide edges of the slotted container.

Analysis of the conditions for mechanical equilibrium of the solid phase nucleus at the boundary with the container wall and the derivation of the expression for the angle

The physical model of the considered problem of the mechanical equilibrium of the solid phase nucleus on a vertically located flat wall of the container is shown in Fig.1.

Projecting the forces acting on the solid phase nucleus, on the vertical direction, and considering the nucleus as a spherical segment, we obtain the condition for mechanical equilibrium of the nucleus on the vertical flat wall of the container in the following form:

$$\gamma_{13} + \frac{\rho g r^2}{6}\left[\frac{2(1-\cos\theta)}{\sin^3\theta} - \mathrm{ctg}\theta\right] = \gamma_{23}\cos\theta + \gamma_{12}, \qquad (1)$$

where γ_{12}, γ_{13}, γ_{23} are surface tension coefficients at the "container wall – nucleus", "container wall- melt" and "nucleus-melt" boundaries, respectively, ρ is solid phase density, g is free fall acceleration, r is the radius of the spherical segment base.

With small θ, restricting ourselves in Eq.(1) to the first nonzero term by θ, we obtain:

$$|\theta| = \frac{8|\gamma_{13} - \gamma_{23} - \gamma_{12}|}{\rho g r^2}. \tag{2}$$

From Eq. (2) it follows that under the condition $\gamma_{13} - \gamma_{12} = \gamma_{23}$ the orientation of the cleavage planes will be the best, since they will be perfectly parallel to the wide edges of the container.

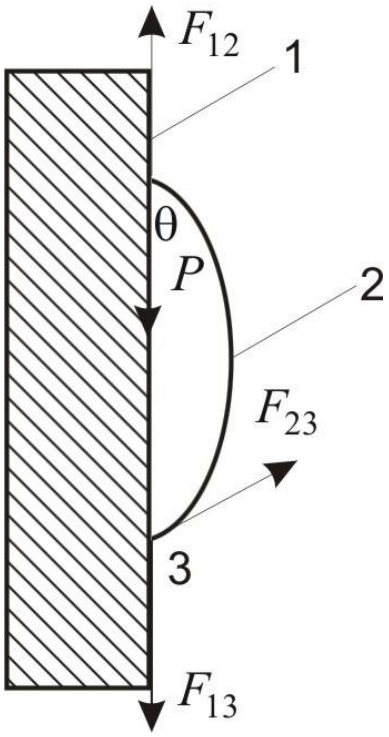

Fig.1 Physical model of the problem. 1-container wall, 2-solid phase nucleus, 3-melt, θ - contact angle, P – nucleus weight, F_{12}, F_{13}, F_{23} - surface tension forces at the "container wall- nucleus", "container wall – melt" and "nucleus-melt" boundaries, respectively.

To this end, we first estimate the surface tension coefficient γ_{23} at the "nucleus – melt" boundary without taking into account the anisotropy for bismuth telluride, for which purpose we will use the semi-empirical approach developed in [5]. From its results it follows that this coefficient with sufficient accuracy is a linear function of the heat of formation of the compound ΔH_f and is equal to:

$$\gamma_{23} = \frac{0.385 \Delta H_f \rho^{2/3}}{M^{2/3} N_A^{1/3}}, \tag{4}$$

where ρ – the density of the crystal, M – its molecular weight, N_A – the Avogadro number. Regarding the empirical coefficient of 0.385, we note that due to the lack of specific experimental data on the nucleation in small drops of the melt of bismuth telluride, this coefficient is taken to be equal to the arithmetic average of the highest and lowest values given in [4]. The values of the heat of formation and the density of bismuth telluride are taken from monograph [9]. After substituting the numerical values in formula (4), we obtain $\gamma_{23} = 0.158\ \text{J/m}^2$. With regard to this result, we note that it is within the range of values of the

surface tension coefficient at the "nucleus – melt" boundary given in [5] for a number of other materials, namely, ice, metals, and some elemental semiconductors (0.024 ÷ 0.240 J/m^2), but coincides with none of them.

Further, in order to exclude unknown quantities γ_{12} and γ_{13} from expression (2) and unambiguously expressing the angle between the cleavage planes of bismuth telluride single crystal and the wide edges of the slotted container when growing by the Bridgman method through γ_{23}, we consider additionally the equilibrium condition of the nucleus in the form of a spherical segment on the horizontal flat surface. It is obtained from condition (1) with $g = 0$. It follows from it that Eq.(2) for this angle can be represented as follows:

$$|\theta| = \frac{216m^2\gamma_{23}}{\pi^2 r_h^6 \rho^3 g r_v^2}, \tag{5}$$

where m is the mass of the nucleus, r_h – the radius of the base of the nucleus formed on the container wall at its horizontal arrangement, r_v – the radius of the base of the nucleus formed on the container wall at its vertical arrangement. Hence it is clear that, if possible, for containers or gaskets, such materials should be chosen on a horizontal flat surface of which a given mass of thermoelectric material, being heated to the melting temperature, during subsequent spreading of the melt and its solidification forms a layer of the largest area, since the angle between the cleavage planes of the single crystal and the wide edges of the container is inversely proportional to the cube of this area. But in the case of a vertical surface for the same mass there holds an inequality $r_v^2 \geq r_h^2$, since the action of gravity contributes to the spreading of the melt. Therefore, we can write the following inequality:

$$|\theta| \leq \frac{216m^2\gamma_{23}}{\pi^2 r_h^8 \rho^3 g}. \tag{6}$$

Therefore, it turns out that the angle between the cleavage planes of a single crystal of bismuth telluride and the wide edges of the container when it is grown in a vertical slotted crystallizer is inversely proportional to the eighth power of the radius or the fourth power of the layer formed during the spreading and subsequent solidification of the given mass of melt on a horizontal surface. Thus, for example, an increase in the layer radius by 10% means a decrease in the angle between the cleavage planes of the single crystal and the wide edges of the slotted container by about 2 times. Substituting the previously specified value γ_{23} and the density of the material $\rho = 6809$ kg/m^3, and also assuming that $\theta = 5^0$, we obtain the following dependence between the mass of the material and the radius of the layer which it forms after bringing to the melting temperature, spreading of melt and its subsequent solidification:

$$r_h = 1.04m^{0.25}, \tag{7}$$

where r_h is measured in centimeters, and m – in grams. This dependence is depicted in Fig. 2

From this dependence it follows that, for example, a cylindrical sample with a diameter of 11 mm and a height of 3.4 mm, having a mass of 2.2 g, with an angle between the cleavage planes and the wide edges of the slotted container equal to 5^o, provided that the above estimate of the surface tension coefficient at the "melt-solid phase" boundary is valid, after melting and subsequent solidification on a horizontal surface, should form a layer with a diameter of about 25 mm. But this is the most stringent requirement, the fulfillment of which guarantees the achievement of the required or smaller angle between the cleavage planes and the wide edge of the slotted container. In order to make it different, it is necessary to know the relationship between radii r_h and r_v. However, for the radius of the layer on the horizontal surface, which guarantees achievement of the specified angle of inclination of the cleavage planes to the plane of the wide

edge of the container, to be reduced, for instance, by half, the radius of the layer on the vertical surface, should be 16 times higher than the radius of the layer on the horizontal surface, which is hardly the case in reality. And if these radii are comparable, then the dependence shown in Fig. 2 determines the area in which the desired orientation of the single crystal cleavage planes with respect to the wide edges of the slotted container is achievable by virtue of the anisotropy of the single crystal growth rate. The specified area lies above the curve shown in Fig.2. But if the real dependence $r_h(m)$ lies below this curve, then it should be assumed that by itself the growth anisotropy of a single crystal based on bismuth telluride can only provide parallelism of its cleavage planes to each other, but not to the plane of the container. This is because equality $\gamma_{13} - \gamma_{23} - \gamma_{12} = 0$ is not satisfied. Therefore, an acceptable orientation of the cleavage planes of the single crystal with respect to the wide edges of the slotted container during vertical crystallization can be ensured only by force, using a seed or spike. At first glance, this statement contradicts the conclusions of [10], but this contradiction is apparent, since in this work only surface phenomena were considered at the "solid phase – melt" boundary, but not at the interface between the solid phase and the melt with the container wall.

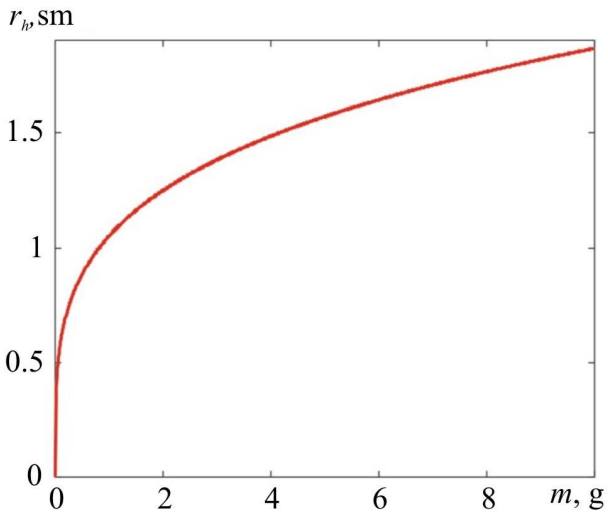

Fig. 2. Dependence of the radius of the layer formed by bismuth telluride-based thermoelectric material on the horizontal surface after melting, spreading of melt and subsequent solidification of the material sample mass, corresponding to the angle between the cleavage planes of the single crystal and the wide edges of the slotted container equal to 5^o

The results obtained can be generalized for the case of an arbitrary angle of inclination of the cleavage planes of the single crystal to the planes of the wide edges of the slotted container. The dependence obtained for this case of the aforementioned angle on the radius of the layer formed after melting and subsequent solidification by the sample weight of 2 g on the horizontal surface is shown in Fig.3. The calculation is made for the worst case, i.e. under the assumption that the radii of the layers formed on the horizontal and vertical surfaces are the same.

From the obtained dependence it follows that if the radius of the aforementioned layer exceeds 7.65 mm, then the angle between the cleavage planes does not exceed 5^0.

However, if we take into account the effect of gravity on the layer radius, then, considering the solid phase nucleus as a spherical segment, we obtain the following equation for determining the angle of inclination of the cleavage planes with respect to the wide edges of the slotted container:

$$2\pi\gamma_{23}(\cos\theta - \cos\theta_0)\cdot\sqrt[3]{m/[\pi\rho f(\theta)]} - mg = 0\,, \qquad (8)$$

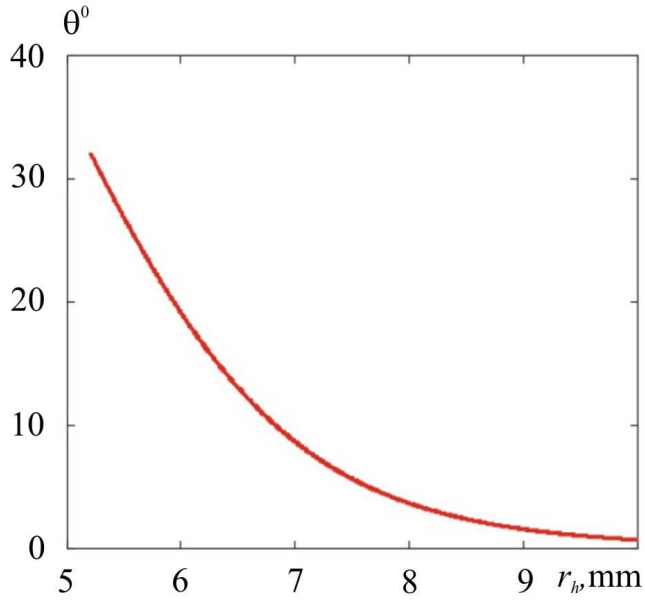

Fig.3. The dependence of the angle between the cleavage planes of the single crystal and the wide edge of the slotted container on the radius of the layer formed on the horizontal flat surface for arbitrary angles

where function $f(\theta)$ is given by:

$$f(\theta)=\frac{2(1-\cos\theta)}{3\sin^3\theta}-\frac{\mathrm{ctg}\,\theta}{3}, \tag{9}$$

and the angle θ_0 is determined from the condition $m/\pi\rho r_h^3 f(\theta_0)=1$. The results of this calculation are represented in Fig.4.

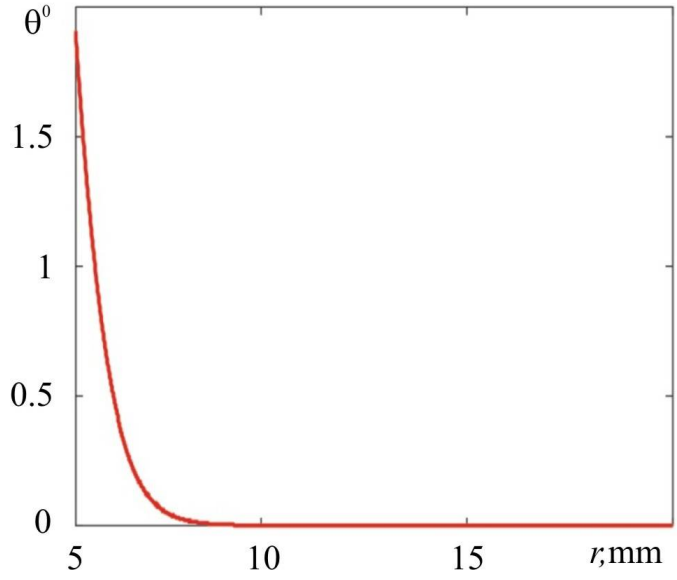

Fig. 4. Dependence of the angle between the cleavage planes of the single crystal and the wide edge of the slotted container on the radius of the layer formed on the horizontal flat surface, with regard to the effect of gravity on the radius of the layer formed on the vertical flat surface.

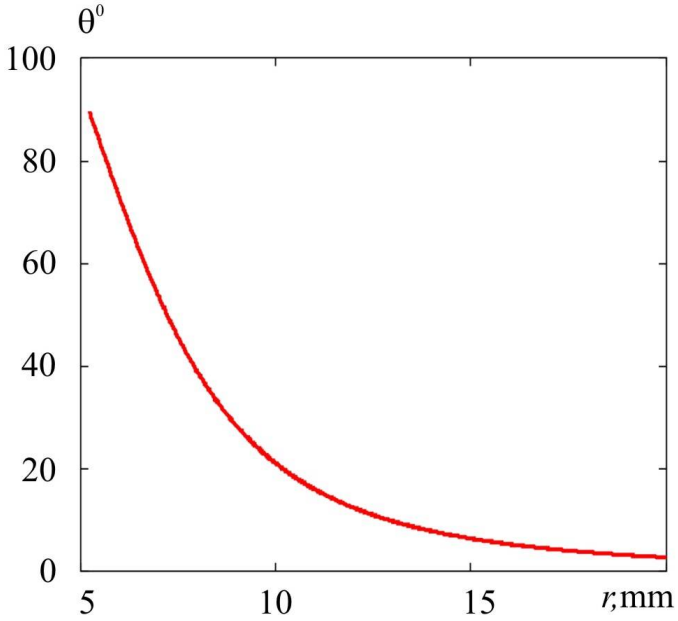

Fig. 5. Dependence of the angle of rotation of the cleavage planes of a single crystal around the vertical axis of the container on the radius of the layer formed on the horizontal flat surface

From Fig. 4, at first glance it may seem that the very effect of gravity during vertical recrystallization automatically provides an acceptable inclination of the cleavage planes of the single crystal to the wide edge of the slotted container. But in reality, the action of gravity takes place only in the vertical direction and determines the orientation of the cleavage planes only in relation to this direction. However, they can prove to be definitely rotated around an axis that coincides with the vertical axis of the container. Gravity does not affect this angle of rotation, and it is determined by the dependence characteristic of the horizontal surface. This dependence is shown in Fig.5.

And from this dependence it follows that for the aforementioned angle of rotation not to exceed 5^0, the radius of the layer must be at least 16.5 mm. Otherwise, the required orientation should be created by force, using, for example, seed.

Conclusion

1. By solving the one-dimensional diffusion equation, a stationary distribution of the concentration of nickel particles in bismuth telluride over the depth of the transient layer was found.
2. Using the theory of composites, the electrical and thermal contact resistances, the thermoEMF, the power factor and the figure of merit of transient layer were calculated depending on the intensity of arrival of nickel particles with stationary diffusion.
3. It was established that with increasing the intensity of arrival of nickel particles, the electrical and thermal contact resistances and the thermoEMF of transient contact layer decrease, and the power factor and the thermoelectric figure of merit increase.
4. In the considered intensity range of nickel particles arrival with stationary diffusion at transient layer thicknesses 20 – 150 μm the electrical contact resistance can vary in the range from $1.16 \cdot 10^{-5}$ to $4.41 \cdot 10^{-7}$ $\Omega \cdot sm^2$, the thermal contact resistance – in the range from 0.674 to 0.032 $(K \cdot cm^2)/W$, the thermoEMF – in the range from 199.5 to 198.5 μV/K, the power factor – in the range from $5 \cdot 10^{-5}$ to $1.8 \cdot 10^{-4}$ $W/(m \cdot K^2)$, and the thermoelectric figure of merit – in the range from

$2.35 \cdot 10^{-3}$ to $2.9 \cdot 10^{-3}$ K^{-1}. The intervals of change in the electrical and thermal contact resistances can vary and expand on the one hand due to the presence of potential barriers between TEM and metal, which are overcome by tunneling or emission, on the other, due to the presence of a thin oxide film on the TEM surface, but these factors in this paper are not considered.

References

1. *Patent of Russia and Japan* (2000). Belov Yu.M., Maekawa N. Cast plate made of thermoelectric material.
2. Belov Yu. M., Maniakin S.M., Morgunov I.V. (2006). Review of methods of thermoelectric materials mass production. In: *Thermoelectric handbook. Macro to nano.* D. M. Rowe (Ed.). Boca Raton (FL): CRC Press.
3. Patent DE10230080A1. (2002). Böttner H., Künzel C., Numus J., Shubert A. A method for making a thermoelectric view structure and elements of a thermoelectric layer structure.
4. Hillig W., Turnbull D. (1956). Theory of crystal growth in undercooled pure liquids. *J. Chem. Phys.*, 24, 914.
5. Turnbull D., Fischer J.C. (1949). Rate of nucleation in condensed systems. *J. Chem. Phys.*, 17, P. 71-73.
6. Turnbull D. (1950). Formation of crystal nuclei in liquid metals. *J. Appl. Phys*., 21, 1022-1028.
7. Turnbull D. (1950). Kinetics of heterogeneous nucleation. *J. Chem. Phys*., 18, 198-203.
8. Tiller V. (1962*). V sbornike: Zhidkiie metally i zatverdevaniie [In: Liquid metals and solidification]*. Moscow: Metallurgizdat [in Russian].
9. Avdonin N.A. (1980). *Matematicheskoie opisaniie protsessov kristallizatsii [Mathematical description of crystallization processes]*. Riga: Zinatne [in Russian]. .
10. Gorskiy P.V. (2018). The role of elementary growth processes in the formation of single crystals of thermoelectric materials based on bismuth telluride. *J.Thermoelectricity*, 1, 18-26.
11. Goltsman B.M., Kudinov V.A., Smirnov I.A. (1972). *Poluprovodnikovyie termoelektricheskiie materialy na osnove Bi_2 Te_3 [Semiconductor thermoelectric materials based on Bi_2 Te_3]*. Moscow: Nauka [in Russian].

Submitted 02.06.2018

Горський П.В. *докт. фіз.-мат. наук*[1,2]

Інститут термоелектрики НАН і МОН України,
вул. Науки, 1,Чернівці, 58029, Україна,
[2]Чернівецький національний університет
імені Юрія Федьковича, вул. Коцюбинського 2,
Чернівці, 58012, Україна
e-mail: anatych@gmail.com

ОЦІНКА ЕЛЕКТРИЧНОГО ТА ТЕПЛОВОГО КОНТАКТНИХ ОПОРІВ ТА ТЕРМОЕРС ПЕРЕХІДНОГО КОНТАКТНОГО ШАРУ«ТЕРМОЕЛЕКТРИЧНИЙ МАТЕРІАЛ-МЕТАЛ» НА ОСНОВІ ТЕОРІЇ КОМПОЗИТІВ

Теоретично досліджено електричний та тепловий контактні опори, термоЕРС, фактор потужності та термоелектричну добротність перехідного контактного шару «термоелектричний матеріал-метал», зумовленого дифузією частинок металу у напівпровідник без утворення нових фаз. Дослідження виконано на основі теорії композитів на прикладі пари «телурид вісмуту – нікель». Встановлено, що термоелектричні характеристики перехідного контактного шару залежать як від його товщини, так і від режиму створення, за основну характеристику якого взято інтенсивність дифузії металу у напівпровідник. При цьому як від товщини так і від режиму створення істотно залежать електричний і тепловий контактні опори,фактор потужності та добротність перехідного шару, в той час, як термоЕРС не залежить від товщини шару і мало залежить від режиму створення. В інтервалі товщин перехідного шару від 20 до 150 мкм за розглянутих режимів створення електричний контактний опір змінюється в інтервалі від 1.16·10-5 до 4.41·10-7Ом·см^2, тепловий контактний опір змінюється в інтервалі від 0.674 до 0.032(К•см2)/Вт, термоЕРС – в інтервалі від 199.5 до 198.5мкВ/К, фактор потужності – в інтервалі від 5·10-5 до 1.8·10-4 Вт/(м·К^2), термоелектрична добротність – в інтервалі від 2.35 10-3 до 2.9 10-3 К-1. Бібл. 10, рис. 5.

Ключові слова: електричний контактний опір, тепловий контактний опір, термоЕРС, перехідний шар, композит, дифузія, інтенсивність дифузії.

Горский П.В., *докт. физ.-мат. наук*[1,2]

Институт термоэлектричества, ул. Науки, 1, Черновцы, 58029, Украина
[2]Черновицкий национальный университет им. Юрия Федьковича,
ул. Коцюбинского, 2, Черновцы,
58000, Украина
e-mail: anatych@gmail.com

ОЦЕНКА ЭЛЕКТРИЧЕСКОГО И ТЕПЛОВОГО КОНТАКТНЫХ СОПРОТИВЛЕНИЙ И ТЕРМОЭДС ПЕРЕХОДНОГО КОНТАКТНОГО СЛОЯ«ТЕРМОЭЛЕКТРИЧЕСКИЙ МАТЕРИАЛ-МЕТАЛЛ» НА ОСНОВЕ ТЕОРИИ КОМПОЗИТОВ

Теоретически исследованы электрический и тепловой контактные сопротивления, термоЭДС, фактор мощности и термоэлектрическая добротность переходного контактного слоя «термоэлектрический материал-металл», обусловленного диффузией частиц металла в полупроводник без образования новых фаз. Исследование выполнено на основе теории композитов на примере пары «телурид висмута – никель». Установлено, что термоэлектрические характеристики переходного контактного слоя зависят как от его толщины, так и от режима создания, в качестве основной характеристики которого взята интенсивность диффузии металла в полупроводник. При этом как от толщины, так и от режима создания существенно зависят электрический и тепловой контактные сопротивления, фактор мощности и добротность переходного слоя, в то время, как термоЭДС не зависит от толщины слоя и мало зависит от режима создания. В интервале толщин переходного слоя от 20 до 150 мкм при рассмотренных режимах создания электрическое контактное сопротивление изменяется в интервале от 1.16·10-5 до 4.41·10-7Ом·см2, тепловое контактное сопротивление изменяется в интервале от 0.674 до 0.032(К·см2) /Вт, термоЕРС – в интервале от 199.5 к 198.5мкВ/К, фактор мощности – в интервале от 5·10-5 до 1.8·10-4 Вт/(м·К^2), термоэлектрическая добротность – в интервале от 2.35·10-3 до 2.9·10-3 К-1. Библ. 10, рис. 5.

Ключевые слова: электрическое контактное сопротивление, тепловое контактное сопротивление, термоЕРС, переходный слой, композит, диффузия, интенсивность диффузии.

References

1. Alieva T.D., Barkhalov B.Sh., Abdinov D.Sh. (1995). Struktura i elektricheskie svoistva granits razdela kristallov $Bi_{0.5}Sb_{1.5}Te_3$ i $Bi_2Te_{2.7}Se_3$ s nekotorymi splavami [Structure and electrical properties of interfaces of $Bi_{0.5}Sb_{1.5}Te_3$ and $Bi_2Te_{2.7}Se_3$ crystals with some alloys]. *Neorganicheskie materialy – Inorganic Materials*, 31(2), 194-198 [in Russian].
2. Chuang C.-H., Lin Y.-C., Lin C.-W. (2016). Intermetallic reactions during the solid-liquid interdiffusion bonding of $Bi_2Te_{2.55}Se_{0.45}$ thermoelectric materials with Cu electrodes using a Sn interlayer. *Metals*, 6(92), 1-10. (doi: 103390/met.6040092).
3. Sabo E.P. (2011). Technology of chalkogen thermoelements. Physical foundations. Section 3. Technology of connection of thermoelement legs. Continuation. 3.5. Electrochemical metallization. *J.Thermoelectricity*, 1, 26-35.
4. Kuznetsov G.D., Polystanskiy Y.G., Evseev V.A. (1995). The metallization of the thermoelement branches by ionic sputtering of the nickel and cobalt. *Proc. of XIV International Conference on Thermoelectrics* (Russia, St.Petersburg, June 27-30, 1995) (pp.166-167).
5. Bublik V.T., Voronin A.I., Ponomarev V.F., Tabachkova N.Yu. (2012). Izmeneniie struktury prikontaktnoi oblasti termoelektricheskikh materialov na osnove telluride vismuta pri povyshennykh temperaturakh [Change in the structure of near-contact area of thermoelectric materials based on bismuth telluride at elevated temperatures] *Izvestiia vysshykh uchebnykh zavedenii*. Materialy elektronnoi tekhniki - *News of Higher Educational Institutions. Electronic Technique Materials,* 2, 17-20 [in Russian].
6. Snarskiy A.O., Zhenirovskiy M.I., Bezsudnov I.V. (2006). On the law of Wiedemann-Franz in thermoelectric composites. *J.Thermoelectricity*, 3, 59-65.
7. Tikhonov A.N., Samarskii A.A. (1972). *Uravneniia matematicheskoi fiziki [Equations of Mathematical Physics]*. Moscow: Nauka [in Russian].
8. Kittel Charles. *Vvedeniie v fiziku tverdogo tela [Introduction to Solid State Physics]*. Moscow: Nauka, 1978 [Russian transl].
9. Gupta R.P., McCarty R., Sharp J. (2013). Practical contact resistance measurement method for bulk Bi_2Te_3-based thermoelectric devices. *J. of Electron. Mat*., 1-5 (doi: 10.10007/s11664-013-2806-6).
10. Drabkin I.A., Osvenskiy V.B., Sorokin A.I. et al. (2017). Kontaktnyie soprotivleniia v sostavnykh termoelektricheskikh vetviakh [Contact resistances in composite thermoelectric legs]. *Fizika i Tekhnika Poluprovodnikov – Semiconductors,* 51 (8), 1038-1040.

Submitted 02.06.2018

L.I. Nykyruy *Ph.D. Proffesor*[1], **O.M. Voznyak** *Ph.D. Proffesor*[1],
Y.S. Yavorskiy *Ph.D*[1], **V.A. Shenderovskiy** *Dr.Sci., Professor*[2],
R.O. Dzumedzey[1], **O.B. Kostyuk**[1], **R.I. Zapukhlyak** *Ph.D.*[1]

[1]Vasyl Stefanyk Precarpathian National University, 57, Shevchenko Str.,
Ivano-Frankivsk, 76018, Ukraine,
[2]Institute of Physics NAS of Ukraine, 46, Nauky Av., Kyiv, 02000, Ukraine

INFLUENCE OF THE BEHAVIOR OF CHARGE CARRIERS ON THE THERMOELECTRIC PROPERTIES OF *PbTe:Bi* THIN FILMS

The influence of technological factors of thin film deposition by the method of open evaporation in vacuum on the realization of charge carrier scattering processes is investigated. The contribution to the transport phenomena of carrier scattering for PbTe:Bi films deposited on the muscovite mica and glass ceramic (sitall) (0001) substrates are determined. In particular, the surface-bound carriers (Fuchs and Sondheimer theory) and grain boundaries (Meijdes and Shatskis theory) are analyzed. The choice of the type of substrate material and the temperature modes of the deposition changed the structure of the film surface and, accordingly, the values of thermoelectric parameters of the initial material. In particular, the selection of experimental modes allows manipulating the grain size and the thickness of the film. Glass ceramic (sitall) substrates contribute to a significantly smaller grain size compared with the use of mica substrates. It is shown that the effects of grain boundaries scattering are dominant for all films. The surface effects are only significant for sufficiently thin films the thickness of which is commensurate with the mean free path of charge carriers. Bibl. 46, Fig. 3, Table 3.
Key words: thermoelectricity, thin films, surface, grain boundaries, charge carrier scattering.

Introduction

The thermoelectric energy conversion annually increases the potential of its practical application. This is caused by a number of factors: the possibility of direct conversion of heat into electricity without the use of mobile mechanisms, positive environmental impact, reliability and accuracy in operation [1, 2]. Thus, the conversion of the heat of exhaust gases into electric energy at combustion of various types of fuels has a positive effect on the global reduction of the greenhouse effect [3 – 5]. Sometimes only thermoelectricity allows electricity generation when there are no other available sources, such as power lines.

The quality of final devices – thermoelectric modules, or individual thermoelements, is conventionally determined by the value of the dimensionless thermoelectric figure of merit ZT:

$$ZT = \frac{S^2\sigma}{\chi}T, \qquad (1)$$

where S is the Seebeck coefficient, σ is the electrical conductivity, χ is the coefficient of thermal conductivity, T is the absolute temperature, Z is the thermoelectric figure of merit of the thermoelectric material.

The value of *ZT* for most modern industrial thermoelements is 0.4 – 0.7 [6] or for the best within 1.0 [7]. For the studies of laboratory materials, this value is significantly higher: 1.1 for doped *SnTe* [8, 9] 1.6 – 1.8 for $PbTe_{1-x}Se_x$ [10], 1.7 for Mg_3Sb_2 [11] or 2.2 for $Pb_{18}Ag_2Te_{20}$ [12, 13].

Concerning final industrial devices – thermoelectric generators, their efficiency values are (4 – 6) % [6, 14]. These are sufficiently high values taking into account almost free of charge sources of heat for the generation of thermoelectric energy. These efficiency values provide a decent economic competition for thermoelectric generating devices to other alternative energy sources. On the other hand, thermoelectric devices are characterized by the reliability, durability in operation and have a positive effect on the improvement of environmental situation.

The thin-film thermoelectric devices deserve special attention [15 – 18]. They have a number of features. On the one hand, they generate several fold less energy than traditional macroscopic devices. But, on the other hand, the thin-film micro-generators of energy are indispensable for use in miniature devices, for example, for medicine or electronics. Also, one should note their significantly lower cost and higher technical characteristics. Thus, [19] shows the possibility of achieving $ZT \sim 2.5$ for $PbSe_{0.98}Te_{0.02}$ / *PbTe*, *PbSnSeTe* / *PbTe* or Bi_2Te_3 / Sb_2Te_3 quantum dot heterostructures. The thin films arouse the interest of researchers due to their different peculiarities. On the one hand, it is the possibility of significant improvement of certain features, in particular, thermoelectric properties, due to diminishing their size [20 – 24]. On the other hand, an important role is played by the miniaturization of final devices. On the basis of thin films it is possible to create thermoelectric micro-modules that will have practical use in miniature devices, where conventional thermoelectric modules cannot be placed due to their dimensions [25 – 27].

This paper analyzes the possibility of using bismuth doped *PbTe* thin films for thermoelectric energy conversion. For this purpose, the study of the thermoelectric properties of *PbTe*:*Bi* thin films deposited on mica and sitall substrates was performed.

Experiment

The *PbTe:Bi* doped films were obtained by vapour phase deposition using open vacuum evaporation method. As materials, freshly cleaved muscovite mica and sitall (0001) substrates were chosen. For the films on mica substrates the following technological modes were used: the temperature of evaporator was $T_E = 970$ K, and the temperature of the substrates varied $T_S = (420 – 470)$ K. The thickness of thin films within (0.08 – 1.2) μm was sometimes set by the time of deposition (5 – 45) min and determined using microinterferometer MII-4 and the Dektak XT profilograph with application of the digital image processing methods. When the films were deposited on the sitall substrates, the temperature of the evaporator varied in the range of $T_E = (920 – 1020)$ K, the temperature of the substrates varied in range of $T_S = (420 – 520)$ K, and the deposition time was chosen from $\tau = 3$ sec to 120 sec. The presence of specially designed oven that included five heaters of substrates made it possible to obtain films of different thicknesses in one technological process.

Four Hall and two current contacts were applied on the measurement sample. Electrical parameters were measured in constant electric and magnetic fields. The magnetic field is directed perpendicular to the film surface at induction of 2 T. Silver films were used as ohmic contacts. The current through the sample was ~ 3 mA.

The structure of the films was investigated by Atomic Force Microscopy (AFM) methods using Nanoscope 3a Dimension 3000 (Digital Instruments USA). Measurements were made in the central part of the samples using serial silicon probes NSG-11. The AFM data were processed in the Gwyddion program (surface topology, nanocrystal size, etc.). The AFM images of the surface of obtained films are shown in Fig. 1, and the technological modes for these *PbTe:Bi* films are given in Table 1. The grain sizes on the

surface of the crystallites were determined by processing the images obtained on Nexus 412 A microscope using the specialized INNOVATEST Hardworx software package.

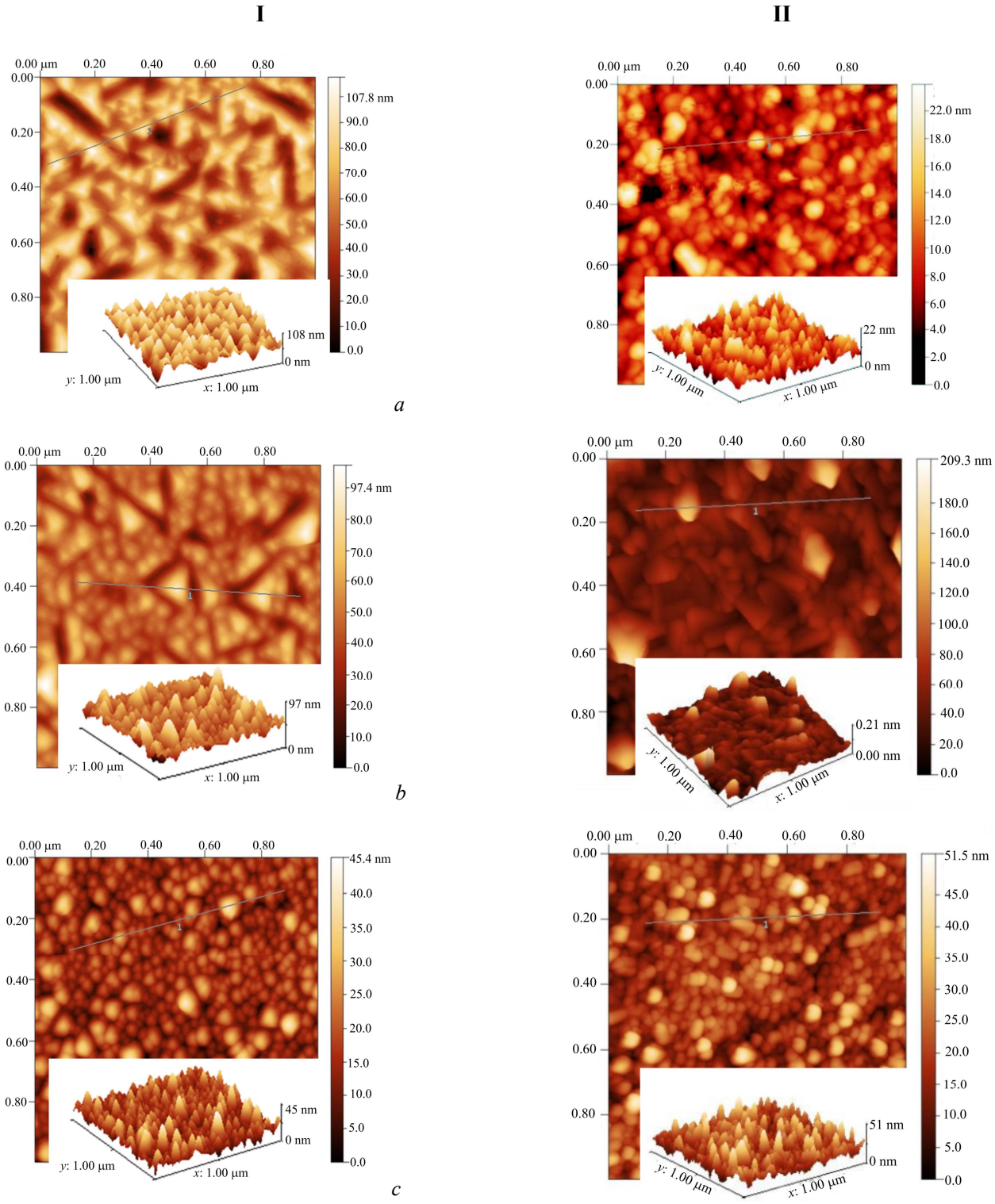

Fig. 1. *2D and 3D AFM-images of PbTe:Bi surface condensates deposited on (0001) cleavages of muscovite mica (I) and sitall (II) substrates in different technological modes:*
a: T_S = 420 K, T_E = 970 K, τ = 900 sec (I), τ = 60 sec (II);
b: T_S = 470 K, T_E = 970 K, τ = 900 sec (I), τ = 60 sec (II);
c: T_S = 470 K, T_E = 970 K, τ = 300 sec (I), τ = 15 sec (II).

Table 1

Technological modes for the PbTe:Bi thin films deposited on (0001) fresh cleavages of muscovite mica and sitall substrates and their morphological characteristics

Sample №	Substrate material	Evaporator temperature T_E, K	Substrate temperature T_E, K	Deposition time τ, sec	Thickness d, nm	Average height h_{av}, m	Average roughness R, nm
2m	mica	970	470	300	320	16	1.8
4m	mica	970	470	900	670	47	2.2
7m	mica	970	420	900	1080	35	1.2
4c	sitall	970	420	15	108	14	1.3
5c	sitall	970	420	60	540	9	0.6
14c	sitall	970	470	60	890	53	3.2

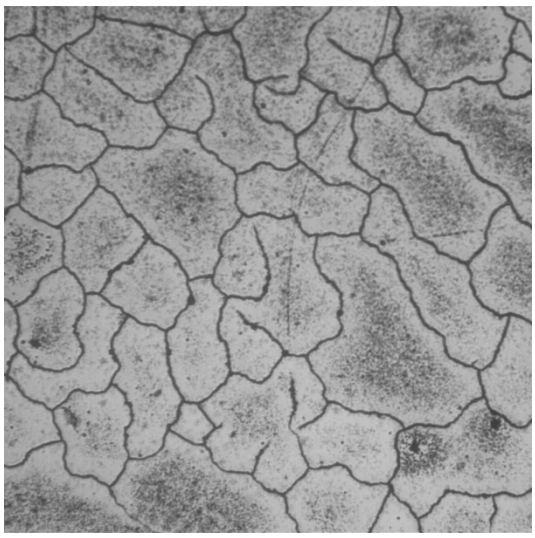

a)

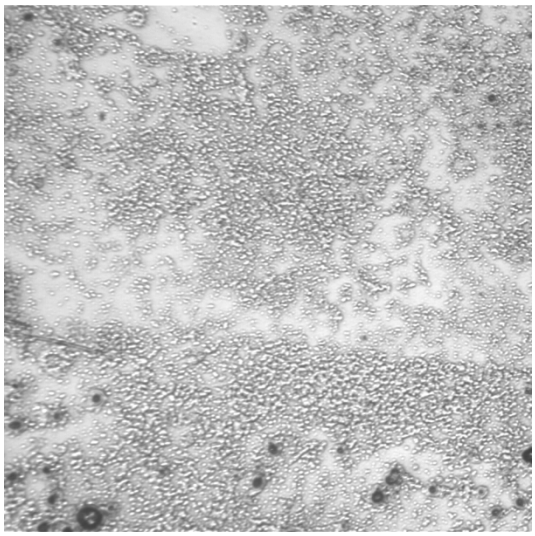

b)

Fig. 2. The image of the surface of the PbTe:Bi films deposited on mica (a, sample 4m, Table 1) and sitall (b, sample 14c, Table 1) substrates. Surface image obtained at 400x magnification with Nexus 412 A optical microscope (INNOVATEST).

Theory

To optimize the parameters of thermoelectric material, it is necessary to correctly describe the dynamics of the electron and phonon subsystems of the material. As regards the bulk materials, these issues are well described, for example, in surveys [28 – 32]. Often, with sufficiently high accuracy, we can restrict ourselves to taking into account the scattering of charge carriers by acoustic phonons. Sometimes, the interaction of charge carriers with optical phonons or vacancies can play a certain role, especially when the inelastic effects of electron-phonon interaction are significant or a strongly degenerate material is considered.

If thin films are under study, then additional mechanisms should be considered that determine the total contribution of charge carriers scattering. In particular, this is the influence of the surface and grain boundaries.

The consideration of the surface scattering, as well as size-related effects, can have a significant effect on the finite material properties [33]. The first explanations of these effects were given by Fuchs and Sondheimer [34, 35] by the example of metallic films. As shown in these papers, the influence of the surface and interfaces is determined by the corresponding inelastic scattering of the carriers. The mean free path of the carriers is statistically uniformly distributed over the bulk of material. Therefore, it is considered that the surface itself plays a dominant role in such distribution of the values of the mean free path values. According to this model, the resistivity is determined by next ratio:

$$\frac{\rho_0}{\rho_{FS}} = \frac{k}{\Phi_p(k)} \tag{2}$$

where

$$\frac{k}{\Phi_p(k)} = \frac{1}{k}\frac{3}{2k^2}(1-p)\int_1^{\infty}\left(\frac{1}{t^3}-\frac{1}{t^5}\right)\frac{1-e^{-kt}}{1-pe^{-kt}}dt \tag{3}$$

Here, $\rho_{FS}$is the resistivity due to the influence of the film surface, p_0 is the value of resistance for the bulk material, $k = t/\lambda_0$ is the ratio where λ_0 is mean free path in the bulk material, p – the proportion of elastically scattered electrons by the film surface. If $p = 0$, we obtain the maximum value for p, which completely corresponds to the surface scattering. Assuming that $p = 1$ we have mirror surfaces, which indicates the dominance of volume scattering and neglecting the surface influence.

Analytically, the contribution of these mechanisms to total mobility can be expressed by following ratio:

$$\frac{\mu}{\mu_{bulk}} = 1 - \frac{3\lambda}{8D}(1-p), \tag{4}$$

where λ is mean free path, D is film thickness, p is surface reflection coefficient .

Mayadas and M. Shatzkes developed the Fuchs and Sondheimer theory for the case of taking into account carrier scattering on grain boundaries [36]. The main parameter in this case was the grain size D:

$$\frac{\rho_0}{\rho_{MS}} = \left[1 - \frac{2}{3}\alpha + 3\alpha^2 - 3\alpha^3 \ln\left(1+\frac{1}{\alpha}\right)\right]^{-1} \tag{5}$$

where $\alpha = \frac{\lambda}{D}\left(\frac{R}{1-R}\right)$, R is grain boundary reflection coefficient which takes on the values from 0 to 1.

Then, taking into account the influence of grain boundaries on the charge carrier mobility is determined by ratio [36]:

$$\frac{\mu}{\mu_{bulk}} = \frac{1}{1+1.34\left(\frac{R}{R-1}\right)\frac{\lambda}{d_{grain}}}, \quad (6)$$

where d_{grain} is the average grain size.

In [37], a certain combined model was proposed for thin films. The values of the p and R coefficients were taken in this case from the experimental results. Accordingly, the total resistance was determined:

$$\rho_{sum} = \rho_{FS} + \rho_{MS} - \rho_0. \quad (7)$$

The appropriate combinations of values p and R were selected [38] for the best agreement with the experimental data.

Results and discussion

The analysis of the AFM images was performed for reasons of determining the influence of surface temperature, deposition time, and substrate material on the surface of the resulting condensates. In this way one can get information on the mechanisms of the nucleation and growth of the obtained thin films. The theoretical basis for explaining these processes is rather fully formulated in [39, 40].

As can be seen from Fig.1, irrespective of the deposition conditions and substrate material, the PbTe:Bi thin films tend to formation and growth of individual pyramidal structures. The formation of three-dimensional individual initial islands indicates the implementation of the Folmer-Weber growth mechanism. However, there are some differences, depending on the choice of substrate material. Thus, it is clearly seen that pyramidal nanoislands of correct cut with a triangular basis grow on mica crystalline substrates. No formation of the objects of clear symmetry group is observed on polycrystalline sitall substrates. However, in both cases, it can be argued that there is certain degree of uniformity in the distribution of nanoobjects along the film surface, for which, both normal and lateral dimensions exceed the mean free path of charge carriers and make up (50 – 200) nanometers.

The analysis of the deposition time shows a certain pattern. The time of deposition is the most significant factor that forms the geometry of nanostructures surface. The change in the substrate temperature slightly changes their average height, while the change in the deposition time (in particular, decrease) causes the formation of several fold smaller nanoislands in the lateral direction. As regards the substitution of substrate for sitall, it can be seen that the dimensions of pyramidal structures are affected by the change in the deposition time and the change in the substrate temperature. Still, the choice of substrate temperature is more decisive in their geometry. Thus, a slight change in temperature can cause an increase in the size of nanoislands by almost 10 times. Therefore, in the case of sitall, one can definitely assert the implementation of the Folmer-Weber mechanism of nucleation. As for monocrystalline mica substrates, the growth rate is slightly slower, although the deposition time was much longer. But on the basis of the fact that monocrystalline substrates are more structurally perfect, one can assume that in this case the implementation of the nucleation mechanism of the Stranky-Krastanov can be more obvious. When this occurs, the layer growth is first realized, and then three-dimensional islands are formed on the surface.

On the other hand, the logarithmic normal distribution is observed along the heights of surface nanostructures for both substrate materials, which is confirmed by the AFM data and described in [41]. This indicates the perfection of the deposited material within the grain. Therefore, when considering thermoelectric parameters, the effects that are realized in the bulk materials and the specific effects associated with the surface are more significant.

As shown in [42], the transition from the bulk materials to films substantially reduces the value of the coefficient of thermal conductivity. According to (1), this leads to significant increase of the thermoelectric *Q*-factor.

The scattering mechanisms for the bulk materials that determine thermoelectric parameters are studied in detail, for example, in [31]. Therefore, in this publication an estimation of the effects associated with the contribution of surface to total scattering of charge carriers was made. In particular, the influence of the surface according to with expression (4) and the influence of grain boundaries according to expression (6) were estimated. The analysis was performed for thin films deposited on different substrates, since different structure of substrates can contribute to the implementation of various scattering mechanisms.

As for the calculated values, it is necessary to pay special attention to the values of the mean free path of carriers. Different papers presented different meanings, which were, however, approximately of the same order. In particular, a λ value of 40 nm [43], 10 nm [44], or an interval from 10 nm to 100 nm [45] were obtained. The first two values are calculated, derived from the *ab initio* methods. Our calculations, according to method [46] showed a value of 72 nm, which is in good agreement with the results of the above studies.

The grain size was determined using a Nexus 412 A (INNOVATEST) optical microscope.

The technological modes and characteristics of deposited films are presented in Tables 2-3.

Table 2

Technological parameters of the deposited PbTe:Bi thin films obtained on muscovite mica (samples 2m, 4m, 7m) and sitall (samples 4c, 5c, 14c) substrates.

No samples	Substrate	Evaporator temperature T_E, K	Substrate temperature T_S, K	Deposition time τ, sec	Thickness *d*, nm	Grain size, μ*m*	Average height value of nanostructures h_c, nm	Average roughness *R*, nm
2m	mica	970	470	300	320	60	16	1.8
4m	mica	970	470	900	670	80	47	2.2
7m	mica	970	420	900	1080	65	35	1.2
4c	sitall	970	420	15	108	0.4	14	1.3
5c	sitall	970	420	60	540	0.8	9	0.6
14c	sitall	970	470	60	890	3	53	3.2

Table 3

Experimental values of specific conductivity σ, the Hall coefficient R_H, carrier concentration n (p), and charge carrier mobility μ of PbTe:Bi thin films obtained on muscovite mica (samples 2m, 4m, 7m) and sitall (samples 4c, 5c, 14c) substrates.

Sample №	σ, $\Omega^{-1}cm^{-1}$	R_H, cm^3/C	n (p), cm^{-3}	μ, $cm^2/V\ s$
2m	627	-0.039	$-1.6\cdot10^{20}$	24.2
4m	480	-0.030	$-2.1\cdot10^{20}$	14.4
7m	44.0	-0.101	$-6.2\cdot10^{20}$	4.4
4c	6.60	3.49	$8.3\cdot10^{19}$	23
5c	74.5	0.27	$8.3\cdot10^{19}$	20
14c	384	0.13	$8.3\cdot10^{19}$	51

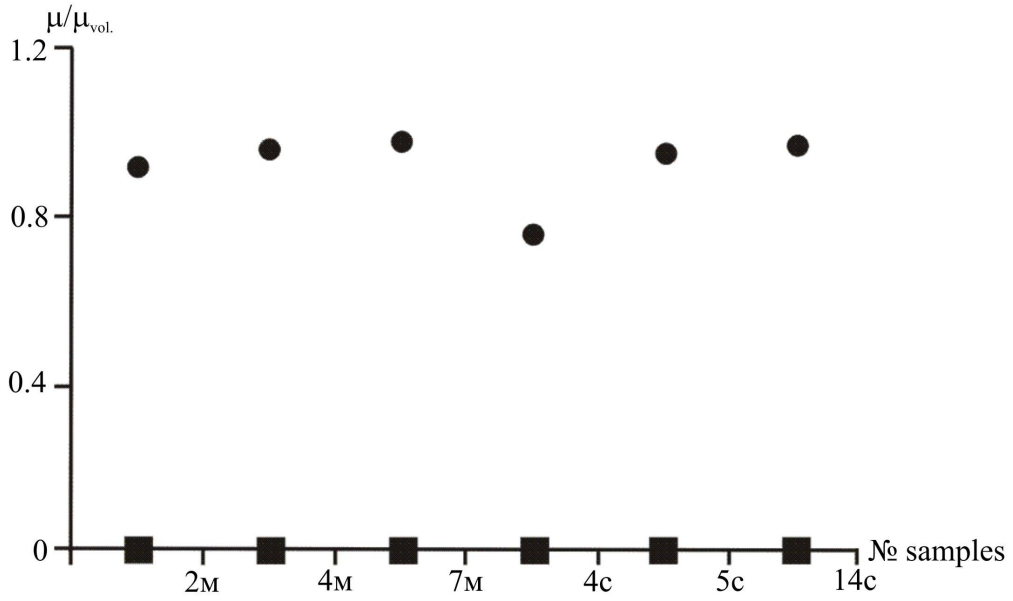

Fig. 3. The relation of $\frac{\mu}{\mu_{bulk}}$, obtained by taking into account the influence of the surface (circles) and intergrain boundaries (squares).

The estimate of the effect of charge carrier scattering on the surface and at the intergrain boundaries is shown in Fig. 3. The proximity of the ratio μ/μ_{bulk} to unity indicates that the total mobility obtained by the Mattisen rule is determined mainly by the scattering mechanisms inherent in the bulk materials (carrier scattering on phonons or vacancies). The greater the deviation from the unity, the greater the influence of surface effects. As can be seen in Fig. 3, account of the surface mobility μ_{FS} (the Fuchsian and Zondheim

theory) is significant for the sample 4c. This is well explained if we analyze the thickness of all studied films. It is for this sample that the thickness is the smallest and is 108 nm (Table 2).

If we consider the influence of intergrain boundaries, this effect will be dominant for all films (curve 2 – Fig. 3) and determined by mobility μ_{MS} (the Mayadas and Shatzkes theory).

The effect of film thickness D is in good agreement with the experimental data and the use of a combined model ($\mu_{MS} + \mu_{FS}$) for quantitative estimation of the contributions of surface and grain boundaries to the values of mobility and electrical conductivity. The good agreement between the calculated and the experimental data occurs, provided that the reflection coefficients p and R vary with thickness. This can happen when the main contribution to the measured values causes the grain boundaries to be taken into account. That is, it can be assumed that with increasing film thickness, in the first stages the key role is played by the nucleation processes of the film, which are responsible for the formation of grain boundaries and lead to high values of electrical conductivity (samples *PbTe:Bi* deposited on mica 2m, 4m, Table 2). These results are in good agreement with the data [38], where the authors analyze correlations between the thickness and size of surface formations with the time of growth.

Conclusion

The role of the effects associated with the surface in the analysis of charge carrier scattering mechanisms and, consequently, their influence on the thermoelectric properties of thin films are determined. The dominant influence of carrier scattering on intergrain boundaries (the Mayadas and Shatzkes theory) is established, regardless of the grain size. The influence of the surface effects, which is described by the Fuchs and Sondheimer theory, becomes significant with decreasing the thickness of films. In particular, for *PbTe:Bi*, the surface of the film substantially affects transport phenomena for thicknesses ~ 100 nm, that is, for thin films whose thickness is commensurate with the mean free path. The obtained results allow setting the technological regimes for optimization of the material parameters in order to obtain the maximum values of thermoelectric figure of merit *ZT*.

References

1. Anatychuk L. I. (2007). Current status and some prospects of thermoelectricity. *J. Thermoelectricity*, 2, 7.
2. Rowe D. M. (2005). *Thermoelectrics handbook: macro to nano*. CRC press.
3. Bell L. E. (2008). Cooling, heating, generating power, and recovering waste heat with thermoelectric systems. *Science*, 321(5895), 1457-1461.
4. Mamur H., Ahiska R. (2014). A review: Thermoelectric generators in renewable energy. *International Journal of Renewable Energy Research (IJRER)*, 4(1), 128-136.
5. Anatychuk L. I., Rozver Y. Y., Misawa K., & Suzuki N. (1997). Thermal generators for waste heat utilization. *Proceedings of XVI International Conference on Thermoelectrics (Dresden, Germany, August 1997) (pp. 586-587)*.
6. LeBlanc S., Yee S. K., Scullin M. L., Dames C., & Goodson K. E. (2014). Material and manufacturing cost considerations for thermoelectrics. *Renewable and Sustainable Energy Reviews*, 32, 313-327.
7. Snyder G. J. and Toberer E. S. (2008). Complex thermoelectric materials. *Nature Materials* 7, 105-114.
8. Zhang Q., Liao B., Lan Y., Lukas K., Liu W., Esfarjani K., ... & Ren Z. (2013). High thermoelectric performance by resonant dopant indium in nanostructured SnTe. *Proceedings of the National Academy of Sciences*, 110(33), 13261-13266.
9. Ren Z., Zhang Q., & Chen G. U.S. Patent No. 9,905,744. Washington, DC: U.S. Patent and Trademark Office, 2018.

10. Pei Y. Z., Shi X. Y., LaLonde A., Wang H., Chen L. D. and Snyder G. J. (2011). Convergence of electronic bands for high performance bulk thermoelectrics. *Nature*, 473, 66-69.
11. Mao J., Shuai J., Song S., Wu Y., Dally R., Zhou J., ... & Wilson S. (2017). Manipulation of ionized impurity scattering for achieving high thermoelectric performance in n-type Mg_3Sb_2-based materials. *Proceedings of the National Academy of Sciences*, 2017, 201711725.
12. Horichok I., Ahiska R., Freik D., Nykyruy L., Mudry S., Matkivskiy O., & Semko T. (2016). Phase content and thermoelectric properties of optimized thermoelectric structures based on the Ag-Pb-Sb-Te system. *J.Electronic Materials*, 45(3), 1576-1583.
13. Haluschak M.O., Mudryi S.I., Lopyanko M.A., et al. (2016). Phase composition and thermoelectric properties of materials in Pb-Ag-Te system. *J. Thermoelectricity*, 3, 34-39.
14. Shostakovski P. (2016). The manufactured thermoelectric generators. *Modern Electronics*, 1, 2-5.
15. Dashevsky Z., Kreizman R., & Dariel M. P. (2005). Physical properties and inversion of conductivity type in nanocrystalline PbTe films. *J. Applied Physics*, 98(9), 094309.
16. Freik D.M., Chobanyuk V.M., Nykyruy L.I. (2006). Semiconductors thin films – modern state (the review). *Physics and Chemistry of Solid State*, 7(3), 405-417.
17. Bulman G., Barletta P., Lewis J., Baldasaro N., Manno M., Bar-Cohen A., & Yang B. (2016). Superlattice-based thin-film thermoelectric modules with high cooling fluxes. *Nature Communications*, 7, 10302.
18. Baumgart H., Chen X., Lin P., & Zhang K. (2017). Review of recent progress in nanoscaled thermoelectric thin films. *The Electrochemical Society Meeting Abstracts* (2017, September) (No. 27, pp. 1166-1166).
19. Böttner H., Chen G., & Venkatasubramanian R. (2006). Aspects of thin-film superlattice thermoelectric materials, devices, and applications. *MRS Bulletin*, 31(3), 211-217.
20. Hicks L. D., & Dresselhaus M. S. (1993). Effect of quantum-well structures on the thermoelectric figure of merit. *Physical Review B*, 47(19), 12727.
21. Lan Y., Minnich A. J., Chen G., & Ren Z. (2010). Enhancement of thermoelectric figure of merit by a bulk nanostructuring approach. *Advanced Functional Materials*, 20(3), 357-376.
22. Anatychuk L. I. & Luste O. J. (1996). Physical principles of microminiaturization in thermoelectricity. *Proc Fifteenth International Conference on Thermoelectrics* (Pasadena, USA, 1996, March) (pp. 279-287).
23. Alam H., & Ramakrishna S. (2013). A review on the enhancement of figure of merit from bulk to nano-thermoelectric materials. *Nano Energy*, 2(2), 190-212.
24. Ding D., Wang D., Zhao M., Lv J., Jiang H., Lu C., & Tang Z. (2017). Interface engineering in solution of processed nanocrystal thin films for improved thermoelectric performance. *Advanced Materials*, 29(1), 1603444.
25. Venkatasubramanian R., Silvola E., Colpitts T., & O'quinn B. (2011). Thin-film thermoelectric devices with high room-temperature figures of merit. In *Materials for Sustainable Energy: A Collection of Peer-Reviewed Research and Review Articles from Nature Publishing Group (pp. 120-125) (2011); Moorthy, S. B. K. (Ed.). Thin film structures in energy applications. Springer, 2015.*
26. Moskalyk I. A. (2015). About the use of thermoelectric devices in cryosurgery. *Physics and Chemistry of Solid State*, 16(4), 742-746.
27. Bulman G., Barletta P., Lewis J., Baldasaro N., Manno M., Bar-Cohen A., & Yang B. (2016). Superlattice-based thin-film thermoelectric modules with high cooling fluxes. *Nature Communications*, 7, 10302.
28. Zayachuk D.M. (1997). On the question of the dominant scattering mechanisms in lead telluride. *Semiconductors*, 31, 217–220.
29. Bilc D. I., Mahanti S. D., and Kanatzidis M. G. (2006). Electronic transport properties of PbTe and

AgPb m SbTe 2+ m systems. *Physical Review B 74*, 12, 125202.

30. Ahmad Salameh, and Mahanti S. D. (2010). Energy and temperature dependence of relaxation time and Wiedemann-Franz law on PbTe. *Physical Review B* 81, 16, 165203.
31. Freik D.M., Nykyruy L.I., Ruvinskiy M.A., Shperun V.M. and Nyzhnykevych V.V. (2001). Scattering of current carriers in n-type lead chalcogenides crystals. *Physics and Chemistry of Solid State*, 2(4), 681-685.
32. Lee HoSung. (2016). A theoretical model of thermoelectric transport properties for electrons and phonons. *J. Electronic Materials* 45, 2, 1115-1141.
33. Panchenko O.A., Sologub S.V. (2003). Dimensional phenomena and surface scattering of current carriers in metals (review). *Physics and Chemistry of Solid State,* 4(1), 7-42.
34. Fuchs K. (1938). The conductivity of thin metallic films according to the electron theory of metals. *Proc. Camb. Phil. Soc*., 34, 100.
35. Sondheimer E. H. (1952). The mean free path of electrons in metals. *Adv. Phys*. 1, 1.
36. Mayadas A. F. and Shatzkes M. (1970). Electrical resistivity model for polycrystalline films: the case of arbitrary reflection at external surfaces. *Phys. Rev. B*, 1, 1382.
37. Durkan C., Welland M.E. (2000). Size effects in the electrical resistivity of polycrystalline nanowires. *Phys. Rev. B*, 61, 14215.
38. Camacho J.M., Oliva A.I. (2006). Surface and grain boundary contributions in the electrical resistivity of metallic nanofilms. *Thin Solid Films* 515(4), 1881-1885.
39. Vengrenovych R.D., Ivanskyy B.V., Moskalyuk A.V. (2009). The theory of Lifshitz-Slyozov-Wagner. *Physics and Chemistry of Solid State*, 10(1), 19-23.
40. Ivanskii B. V., Vengrenovich R. D., Kryvetskyi V. I., & Kushnir Y. M. (2017). Ostwald ripening of the InAsSbP/InAs (100) quantum dots in the framework of the modified LSW theory. *J. Nano-and Electronic Physics*, 9(2), 2025-1.
41. Saliy Y., Ruvinskiy M. and Nykyruy L. (2017). Statistics of nano-objects characteristics on the surface of PbTe: Bi condensate deposited on ceramic. *Modern Physics Letters B*, 31(03), 1750023.
42. Nykyruy L.I., Ruvinskiy M.A., Ivakin E.V., Kostyuk O.B., Horichok I.V., Kisialiou I.G., Yavorskyy Y.S., Hrubyak A.B. (2018). Low-dimensional systems on the base of PbSnAgTe compounds for thermoelectric application. *Physica E: Low-dimensional systems and nanostructures* (in print); doi: 10.1016/j.physe.2018.10.020.
43. Song Q., Liu T.H., Zhou J., Ding Z. and Chen G. (2017). Ab initio study of electron mean free paths and thermoelectric properties of lead telluride. *Materials Today Physics*, 2, 69-77.
44. Peng-Xian L. and Ling-Bo Q. (2013). Electronic structure, lattice dynamics and thermoelectric properties of PbTe from first-principles calculation. *Chinese Physics Letters*, 30(1), 017101.
45. Liu T.H., Zhou J., Li M., Ding Z., Song Q., Liao B., Fu L. and Chen G. (2018). Electron mean-free-path filtering in Dirac material for improved thermoelectric performance. *Proceedings of the National Academy of Sciences*, 201715477.
46. Ruvinskii M.A., Kostyuk O.B. and Dzundza B.S. (2015). Classic size effects in n-PbTe films. *Physics and Chemistry of Solid State*, 16(4), 661-666.

Submitted 12.06.2018

Никируй Л.І. *канд. фіз.-мат. наук*, *професор*[1],
Возняк О.М. *канд. фіз.-мат. наук* [1],
Яворський Я.С. *канд. фіз.-мат. наук* [1],
Шендеровський В.А. *доктор фіз.-мат. наук,професор* [2],
Дзумедзей Р.О.[1], **Костюк О.Б.**[1],
Запухляк Р.І. *канд. фіз.-мат. наук*, *доцент*[1]

[1]Прикарпатський національний університет імені Василя Стефаника,
вул. Шевченка, 57, м. Івано-Франківськ, 76018, Україна,
[2]Інститут фізики НАН України, пр. Науки, 46, м. Київ, 02000, Україна

ВПЛИВ ПОВЕДІНКИ НОСІЇВ ЗАРЯДУ НА ТЕРМОЕЛЕКТРИЧНІ ВЛАСТИВОСТІ ТОНКИХ ПЛІВОК *PbTe*:*Bi*

Досліджено вплив технологічних факторів осадження тонких плівок методом відкритого випаровування у вакуумі на реалізацію процесів розсіювання носіїв заряду. Для плівок PbTe:Bi, осаджених на підкладки (0001) слюди-мусковіт та ситалу визначено внесок у транспортні явища механізмів розсіювання носіїв, пов'язаних із поверхнею (теорія Фукса і Зондгеймера) та із межами зерен (теорія Мейядеса та Шацкиса). Вибором типу матеріалу підкладки та температурних режимів осадження змінювали структуру поверхні плівки та, відповідно, термоелектричні параметри вихідного матеріалу. Зокрема, підбір експериментальних режимів дозволяє маніпулювати розмірами зерен та товщиною плівки. Скло-керамічні підкладки із ситалу сприяють отриманню суттєво менших розмірів зерен у порівнянні із використанням підкладок із слюди. Показано, що ефекти, пов'язані із розсіюванням на межах зерен є домінуючими для всіх плівок. Поверхневі ж ефекти стають суттєвими лише для достатньо тонких плівок, для яких товщина співмірна із довжиною вільного пробігу носії заряду. Бібл.46, рис.3, табл.2.

Ключові слова: термоелектрика, тонкі плівки, поверхня, межі зерен, механізми розсіювання носіїв.

Никируй Л.И. *канд. физ.-мат. наук*, *професор*[1],
Возняк О.М. *канд. физ.-мат. наук* [1],
Яворский Я.С. *канд. физ.-мат. наук* [1],
Шендеровский В.А. *доктор физ.-мат. наук,професор* [2],
Дзумедзей Р.О.[1], **Костюк О.Б.**[1],
Запухляк Р.И. *канд. физ.-мат. наук*, *доцент*[1]

[1]Прикарпатский национальный университет имени Василия Стефаныка,
ул. Шевченка, 57, г. Ивано-Франковск, 76018, Украина,
[2]Институт физики НАН Украины, пр. Науки, 46,
г. Киев, 02000, Украина

ВЛИЯНИЕ ПОВЕДЕНИЯ НОСИТЕЛЕЙ ЗАРЯДА НА ТЕРМОЭЛЕКТРИЧЕСКИЕ СВОЙСТВА ТОНКИХ ПЛЕНОК *PbTe*:*Bi*

Исследовано влияние технологических факторов осаждения тонких пленок методом открытого испарения в вакууме на реализацию процессов рассеяния носителей заряда. Для пленок PbTe:Bi, осажденных на подложки (0001) слюды-мусковит и ситалла определен взнос в транспортные явления механизмов рассеяния носителей, связанных с поверхностью (теория Фукса и Зондгеймера) и с границами зерен (теория Мейядеса и Шацкиса). Выбором типа материала подложки и температурных режимов осаждения изменяли структуру поверхности пленки и, соответственно, значения термоэлектрических параметров исходного материала. В частности, подбор экспериментальных режимов позволяет манипулировать размерами зерен и толщиной пленки. Стеклокерамические подложки из ситалла способствуют получению существенно меньших размеров зерен исходных пленок в сравнении с использованием подложек из слюды. Показано, что эффекты, связанные с рассеянием на границах зерен, являются доминирующими для всех пленок. Поверхностные же эффекты становятся существенными только для достаточно тонких пленок, толщина которых соразмерна с длиной свободного пробега носителей заряда. Библ.46, рис.3, табл.2.

Ключевыеслова: термоэлектричество, тонкиепленки, поверхность, границы зерен, рассеяние носителей заряда.

References

1. Anatychuk L. I. (2007). Current status and some prospects of thermoelectricity. *J. Thermoelectricity*, 2, 7.
2. Rowe D. M. (2005). *Thermoelectrics handbook: macro to nano*. CRC press.
3. Bell L. E. (2008). Cooling, heating, generating power, and recovering waste heat with thermoelectric systems. *Science*, 321(5895), 1457-1461.
4. Mamur H., Ahiska R. (2014). A review: Thermoelectric generators in renewable energy. *International Journal of Renewable Energy Research (IJRER)*, 4(1), 128-136.
5. Anatychuk L. I., Rozver Y. Y., Misawa K., & Suzuki N. (1997). Thermal generators for waste heat utilization. *Proceedings of XVI International Conference on Thermoelectrics (Dresden, Germany, August 1997) (pp. 586-587)*.
6. LeBlanc S., Yee S. K., Scullin M. L., Dames C., & Goodson K. E. (2014). Material and manufacturing cost considerations for thermoelectrics. *Renewable and Sustainable Energy Reviews*, 32, 313-327.
7. Snyder G. J. and Toberer E. S. (2008). Complex thermoelectric materials. *Nature Materials* 7, 105-114.
8. Zhang Q., Liao B., Lan Y., Lukas K., Liu W., Esfarjani K., ... & Ren Z. (2013). High thermoelectric performance by resonant dopant indium in nanostructured SnTe. *Proceedings of the National Academy of Sciences*, 110(33), 13261-13266.
9. Ren Z., Zhang Q., & Chen G. U.S. Patent No. 9,905,744. Washington, DC: U.S. Patent and Trademark Office, 2018.
10. Pei Y. Z., Shi X. Y., LaLonde A., Wang H., Chen L. D. and Snyder G. J. (2011). Convergence of electronic bands for high performance bulk thermoelectrics. *Nature*, 473, 66-69.
11. Mao J., Shuai J., Song S., Wu Y., Dally R., Zhou J., ... & Wilson S. (2017). Manipulation of ionized impurity scattering for achieving high thermoelectric performance in n-type Mg_3Sb_2-based materials. *Proceedings of the National Academy of Sciences*, 2017, 201711725.
12. Horichok I., Ahiska R., Freik D., Nykyruy L., Mudry S., Matkivskiy O., & Semko T. (2016). Phase content and thermoelectric properties of optimized thermoelectric structures based on the Ag-Pb-Sb-Te system. *J.Electronic Materials*, 45(3), 1576-1583.

13. Haluschak M.O., Mudryi S.I., Lopyanko M.A., et al. (2016). Phase composition and thermoelectric properties of materials in Pb-Ag-Te system. *J. Thermoelectricity*, 3, 34-39.
14. Shostakovski P. (2016). The manufactured thermoelectric generators. *Modern Electronics*, 1, 2-5.
15. Dashevsky Z., Kreizman R., & Dariel M. P. (2005). Physical properties and inversion of conductivity type in nanocrystalline PbTe films. *J. Applied Physics*, 98(9), 094309.
16. Freik D.M., Chobanyuk V.M., Nykyruy L.I. (2006). Semiconductors thin films – modern state (the review). *Physics and Chemistry of Solid State*, 7(3), 405-417.
17. Bulman G., Barletta P., Lewis J., Baldasaro N., Manno M., Bar-Cohen A., & Yang B. (2016). Superlattice-based thin-film thermoelectric modules with high cooling fluxes. *Nature Communications*, 7, 10302.
18. Baumgart H., Chen X., Lin P., & Zhang K. (2017). Review of recent progress in nanoscaled thermoelectric thin films. *The Electrochemical Society Meeting Abstracts* (2017, September) (No. 27, pp. 1166-1166).
19. Böttner H., Chen G., & Venkatasubramanian R. (2006). Aspects of thin-film superlattice thermoelectric materials, devices, and applications. *MRS Bulletin*, 31(3), 211-217.
20. Hicks L. D., & Dresselhaus M. S. (1993). Effect of quantum-well structures on the thermoelectric figure of merit. *Physical Review B*, 47(19), 12727.
21. Lan Y., Minnich A. J., Chen G., & Ren Z. (2010). Enhancement of thermoelectric figure of merit by a bulk nanostructuring approach. *Advanced Functional Materials*, 20(3), 357-376.
22. Anatychuk L. I. & Luste O. J. (1996). Physical principles of microminiaturization in thermoelectricity. *Proc Fifteenth International Conference on Thermoelectrics* (Pasadena, USA, 1996, March) (pp. 279-287).
23. Alam H., & Ramakrishna S. (2013). A review on the enhancement of figure of merit from bulk to nano-thermoelectric materials. *Nano Energy*, 2(2), 190-212.
24. Ding D., Wang D., Zhao M., Lv J., Jiang H., Lu C., & Tang Z. (2017). Interface engineering in solution of processed nanocrystal thin films for improved thermoelectric performance. *Advanced Materials*, 29(1), 1603444.
25. Venkatasubramanian R., Silvola E., Colpitts T., & O'quinn B. (2011). Thin-film thermoelectric devices with high room-temperature figures of merit. In *Materials for Sustainable Energy: A Collection of Peer-Reviewed Research and Review Articles from Nature Publishing Group (pp. 120-125) (2011); Moorthy, S. B. K. (Ed.). Thin film structures in energy applications. Springer, 2015.*
26. Moskalyk I. A. (2015). About the use of thermoelectric devices in cryosurgery. *Physics and Chemistry of Solid State*, 16(4), 742-746.
27. Bulman G., Barletta P., Lewis J., Baldasaro N., Manno M., Bar-Cohen A., & Yang B. (2016). Superlattice-based thin-film thermoelectric modules with high cooling fluxes. *Nature Communications*, 7, 10302.
28. Zayachuk D.M. (1997). On the question of the dominant scattering mechanisms in lead telluride. *Semiconductors*, 31, 217–220.
29. Bilc D. I., Mahanti S. D., and Kanatzidis M. G. (2006). Electronic transport properties of PbTe and AgPb m SbTe 2+ m systems. *Physical Review B 74*, 12, 125202.
30. Ahmad Salameh, and Mahanti S. D. (2010). Energy and temperature dependence of relaxation time and Wiedemann-Franz law on PbTe. *Physical Review B* 81, 16, 165203.
31. Freik D.M., Nykyruy L.I., Ruvinskiy M.A., Shperun V.M. and Nyzhnykevych V.V. (2001). Scattering of current carriers in n-type lead chalcogenides crystals. *Physics and Chemistry of Solid State*, 2(4), 681-685.

32. Lee HoSung. (2016). A theoretical model of thermoelectric transport properties for electrons and phonons. *J. Electronic Materials* 45, 2, 1115-1141.
33. Panchenko O.A., Sologub S.V. (2003). Dimensional phenomena and surface scattering of current carriers in metals (review). *Physics and Chemistry of Solid State,* 4(1), 7-42.
34. Fuchs K. (1938). The conductivity of thin metallic films according to the electron theory of metals. *Proc. Camb. Phil. Soc*., 34, 100.
35. Sondheimer E. H. (1952). The mean free path of electrons in metals. *Adv. Phys*. 1, 1.
36. Mayadas A. F. and Shatzkes M. (1970). Electrical resistivity model for polycrystalline films: the case of arbitrary reflection at external surfaces. *Phys. Rev. B*, 1, 1382.
37. Durkan C., Welland M.E. (2000). Size effects in the electrical resistivity of polycrystalline nanowires. *Phys. Rev. B*, 61, 14215.
38. Camacho J.M., Oliva A.I. (2006). Surface and grain boundary contributions in the electrical resistivity of metallic nanofilms. *Thin Solid Films* 515(4), 1881-1885.
39. Vengrenovych R.D., Ivanskyy B.V., Moskalyuk A.V. (2009). The theory of Lifshitz-Slyozov-Wagner. *Physics and Chemistry of Solid State*, 10(1), 19-23.
40. Ivanskii B. V., Vengrenovich R. D., Kryvetskyi V. I., & Kushnir Y. M. (2017). Ostwald ripening of the InAsSbP/InAs (100) quantum dots in the framework of the modified LSW theory. *J. Nano-and Electronic Physics*, 9(2), 2025-1.
41. Saliy Y., Ruvinskiy M. and Nykyruy L. (2017). Statistics of nano-objects characteristics on the surface of PbTe: Bi condensate deposited on ceramic. *Modern Physics Letters B*, 31(03), 1750023.
42. Nykyruy L.I., Ruvinskiy M.A., Ivakin E.V., Kostyuk O.B., Horichok I.V., Kisialiou I.G., Yavorskyy Y.S., Hrubyak A.B. (2018). Low-dimensional systems on the base of PbSnAgTe compounds for thermoelectric application. *Physica E: Low-dimensional systems and nanostructures* (in print); doi: 10.1016/j.physe.2018.10.020.
43. Song Q., Liu T.H., Zhou J., Ding Z. and Chen G. (2017). Ab initio study of electron mean free paths and thermoelectric properties of lead telluride. *Materials Today Physics*, 2, 69-77.
44. Peng-Xian L. and Ling-Bo Q. (2013). Electronic structure, lattice dynamics and thermoelectric properties of PbTe from first-principles calculation. *Chinese Physics Letters*, 30(1), 017101.
45. Liu T.H., Zhou J., Li M., Ding Z., Song Q., Liao B., Fu L. and Chen G. (2018). Electron mean-free-path filtering in Dirac material for improved thermoelectric performance. *Proceedings of the National Academy of Sciences*, 201715477.
46. Ruvinskii M.A., Kostyuk O.B. and Dzundza B.S. (2015). Classic size effects in n-PbTe films. *Physics and Chemistry of Solid State*, 16(4), 661-666.

Submitted 12.06.2018


G.P. Gaidar

G.P. Gaidar[1], *Doctor of Physical and Mathematical Sciences*, *Senior Researcher*
P.I. Baranskii[2], *Doctor of Physical and Mathematical Sciences, Professor*


P.I. Baranskii

[1]Institute for Nuclear Research of the NAS of Ukraine,
Nauky Ave., 47, Kyiv, 03028, Ukraine,
e-mail: gaydar@kinr.kiev.ua
[2]V. Lashkaryov Institute of Semiconductor Physics of the NAS of Ukraine,
Nauky Ave., 45, Kyiv, 03028, Ukraine

CONCENTRATION AND TEMPERATURE DEPENDENCES OF THERMOELECTRIC CHARACTERISTICS OF THE ELASTICALLY DEFORMED SILICON

The concentration and temperature dependences of thermo-EMF, tenso-thermo-EMF, thermo-EMF anisotropy and thermoelectric figure of merit of the undeformed and uniaxially elastically deformed n-Si crystals were studied. It was found that despite high thermal conductivity which is increased in n-Si with decreasing temperature, these crystals (in the elastically deformed state) can have thermoelectric figure of merit which is comparable to the figure of merit of the most common thermoelectrically anisotropic materials. It is shown that thermo-EMF anisotropy of the deformed n-Si, which determines the sensitivity of anisotropic thermoelement, exceeds $\Delta\alpha$ for the traditional thermoelectrically anisotropic materials by two-three orders of magnitude. Bibl. 23, Fig. 5, Tables 3.
Key words: silicon, uniaxial elastic deformation, thermoelectromotive force (thermo-EMF), tenso-thermo-EMF, thermo-EMF anisotropy, thermoelectric figure of merit.

Introduction

In recent years, fundamentally new results have been obtained in the field of thermoelectric conversion concerning the development of highly efficient thermoelectric materials, methods for calculating and optimizing thermoelectric devices, creation of new types of thermoelements, etc. [1 – 3]. Thermoelectric phenomena are gaining ever-widening applications [4]. Today, the problem of increasing the efficiency of thermoelectric converters ($ZT > 1$) based on both traditional bulk semiconductors and spatially-inhomogeneous materials whose inhomogeneities are comparable in size to the characteristic electron or phonon wavelengths, is very relevant and promising [5, 6].

Creation of effective thermoelectric converters imposes rather complex requirements on modern materials of electronic technology, which are not limited to considering the dynamics of electrons, but equally apply to the phonon subsystem [7]. Indeed, apart from the differential thermo-EMF α and electrical conductivity σ, the dimensionless thermoelectric figure of merit $ZT = \alpha^2 \sigma T / \chi$ is also determined by thermal conductivity χ of the material. Thus, thermoelectric materials should be good conductors and at the same time have low thermal conductivity.

Until recently it was believed that for thermoelectric applications, silicon is completely unsuitable, since its thermal conductivity is rather high due to large phonon contribution. However, a new generation of thermoelectric silicon (in the form of silicon nanostructures and nanowires) can significantly improve

some of the existing devices (including fuel cells), and also provide new products on the global consumer electronics market [7 – 11].

In order to use semiconductor materials which today are not considered highly effective thermoelectrically, it is necessary to look for fundamentally new approaches that not only increase thermo-EMF α or its anisotropy $\Delta\alpha$, but also substantially reduce thermal conductivity χ of the system, which will likely provide an increase in the thermoelectric figure of merit Z, even on the basis of materials similar to silicon (or silicon itself). The reserve in this respect is the ability of the directed elastic deformation to substantially increase the thermo-EMF anisotropy $\Delta\alpha$ in those cases when the technical difficulties associated with the need to use the above deformation of the crystals will not be significant. It is worth noting that in the study of uniaxially deformed semiconductors, experiments carried out in the field of the manifestation of the effect of electron-phonon drag allow us to determine the important parameters and characteristics of electron-phonon interaction and may have an important applied value.

The purpose of this work was to establish the peculiarities of the concentration and temperature dependences of thermoelectric characteristics (thermo-EMF, tenso-thermo-EMF, thermo-EMF anisotropy, thermoelectric figure of merit) of uniaxially elastically deformed *n-Si* single crystals, that must be taken into account when calculating various effects on the basis of anisotropic scattering theory.

Dependences of thermoelectric characteristics on the concentration of electrons in the elastically deformed *n-Si* crystals

The search for new thermoelectric materials and methods for creating thermo-EMF anisotropy is an important task, since the number of thermoelectrically anisotropic materials is limited. In addition, thermo-EMF anisotropy of these materials $\Delta\alpha$ usually does not exceed 0.2 ÷ 0.3 mV / K (at temperatures of 300 ÷ 400 K [12]) (see *Table 1*), and in the case of temperature decrease, thermo-EMF anisotropy decreases (and in some materials even changes its sign [12, 13]) and at T = 150 ÷ 200 K it is several tens of μV / K.

The existing thermoelements, depending on their operating principle, can be arbitrarily divided into two categories: a) conventional (the so-called isotropic) thermoelements, b) anisotropic thermoelements that are based on thermoelectrically anisotropic crystals.

Table 1

Characteristics of some thermoelectrically anisotropic materials [12]

Material	*T*, K	$\Delta\alpha$, μV/K	σ, $\Omega^{-1}\cdot cm^{-1}$	χ, $W\cdot cm^{-1}\cdot K^{-1}$	Z_a, K^{-1}
Bi	350	0.054	$9.9 \cdot 10^{3}$	$8 \cdot 10^{-2}$	$0.9 \cdot 10^{-4}$
Sb	300	$2.6 \cdot 10^{-3}$	$2.9 \cdot 10^{4}$	0.18	$2.7 \cdot 10^{-5}$
Cd	300	$3.2 \cdot 10^{-3}$	$1.4 \cdot 10^{5}$	0.92	$3.8 \cdot 10^{-7}$
CdSb	400	0.280	$4 \cdot 10$	$1.2 \cdot 10^{-2}$	$6.1 \cdot 10^{-6}$
$MnSi_{1.7}$	300	0.055	490	$3.8 \cdot 10^{-2}$	$9.6 \cdot 10^{-6}$
Te	300	0.130	4.0	$2.9 \cdot 10^{-2}$	$9.3 \cdot 10^{-7}$
$Zn_{0.1}Cd_{0.9}Sb$	400	0.190	5	$1.1 \cdot 10^{-2}$	$4.1 \cdot 10^{-6}$

The thermoelectric figure of merit *Z* of a conventional thermoelement is determined by the thermoelectric figure of merit of its legs [14].

$$Z = \left[\frac{\alpha_1 + \alpha_2}{\alpha_1 / \sqrt{Z_1} + \alpha_2 / \sqrt{Z_2}} \right]^2, \quad (1)$$

whereby

$$Z_1 = \frac{\sigma_1}{\chi_1} \alpha_1^2, \; Z_2 = \frac{\sigma_2}{\chi_2} \alpha_2^2 \quad (2)$$

(Z_i, α_i, σ_i and χ_i, where i = 1 or 2, is the figure of merit, thermo-EMF, electrical conductivity and thermal conductivity of the respective thermoelement leg).

The most important characteristics that determine the suitability of thermoelectric anisotropic materials for their practical use are thermo-EMF anisotropy $\Delta\alpha$ and thermoelectric figure of merit Z_a. The thermo-EMF anisotropy is determined by the difference in the principal values of thermo-EMF tensor:

$$\Delta\alpha = \alpha_{ii} - \alpha_{kk}. \quad (3)$$

The thermoelectric figure of merit of anisotropic thermoelements is mainly determined by thermo-EMF anisotropy [15]:

$$Z_a = \frac{\overline{\sigma}}{4\overline{\chi}} \left(\Delta\alpha \right)^2, \quad (4)$$

where $\overline{\sigma}$ and $\overline{\chi}$ are certain combinations of components of electrical and thermal conductivity tensors. The appearance of these combinations depends both on the semiconductor properties and on the design of thermoelement on its basis.

For the anisotropic thermoelement *n*-Si and some types of eddy thermoelements [1] the combination of components of the electrical conductivity tensor which enters (4), can be represented as:

$$\overline{\sigma} = 2 \frac{\sigma_\parallel \sigma_\perp}{\sigma_\parallel + \sigma_\perp}, \; \overline{\chi} = \frac{\chi_\parallel + \chi_\perp}{2}, \quad (5)$$

where σ_i and χ_i (i = || and ⊥) are the principal values of the electrical and thermal conductivity tensors.

The value of $\sigma_\parallel = 1/\rho_\parallel = 1/\rho_\infty$ was measured directly on *n*-Si strongly deformed along the [001] crystallographic direction. Here, $\rho_\parallel$ is the resistivity along the long axis of isoenergetic ellipsoid, ρ_∞ is the resistivity at $X \geq 0.6$ GPa, $\vec{X} \parallel \vec{J} \parallel [001]$, $\vec{J}$ is the density of current passed through the sample when measuring tensoresistance and electrical conductivity σ. The value of $\sigma_\perp$ was calculated by the formula

$$\sigma_\perp = \frac{1}{2} \left(3\sigma_0 - \sigma_\parallel \right), \quad (6)$$

where σ_0 is the resistivity of crystal at $X = 0$.

The sensitivity of conventional thermoelements is directly proportional to thermo-EMF, and of anisotropic thermoelements – to thermo-EMF anisotropy of thermoelectric materials employed.

Silicon has a high thermal conductivity that only grows with a decrease in temperature to 20 ÷ 40 K [16], which inhibits the application of *n-Si* as a thermoelectric material for low temperatures. Along with this, *n-Si* crystals also offer a number of advantages which include the following: 1) growth (due to electron-phonon drag) of thermo-EMF with a decrease in temperature to 20 ÷ 40 K; 2) multiple (3 ÷ 4 times) growth of thermo-EMF and the appearance of high thermo-EMF anisotropy [17] (in the case of almost constant thermal conductivity [18]) on application of a directional mechanical deformation stress

$X \geq 0.6$ GPa to the crystal. These advantages of silicon allowed us to hope that in the experiments with it (even in the temperature range of 77 ÷ 85 K), it will be possible to obtain satisfactory values of Z and thermoelectric sensitivity, which was verified experimentally.

Measurements were conducted on *n-Si* single crystals with phosphorus impurity in the range of charge carrier concentrations from $1.9 \cdot 10^{13}$ to $2.6 \cdot 10^{16}$ cm^{-3}. Mechanical stress $0 \leq X \leq 1.2$ GPa was applied in $\vec{X} \parallel [001] \parallel \nabla T$ (or $\vec{J}$) crystallographic direction, where ∇T is temperature gradient which was used during the study of thermo-EMF (at $T = 85$ K). The tensoresistance of the crystals was measured under conditions of $\vec{X} \parallel [001] \parallel \vec{J}$ at $T = 77$ K. The temperature differences in the determination of thermo-EMF and thermal conductivity were measured using copper-constantan thermocouples. The thermal conductivity was determined by the results of measurements of heat flow through the sample. The heat flow through the sample was obtained using heat flow sensors. The electrical conductivity σ, mobility μ and charge carrier concentration n_e were determined by the generally accepted method. The value of thermo-EMF anisotropy $\Delta\alpha = \alpha_{\parallel} - \alpha_{\perp}$ (where $\alpha_{\parallel}$ and $\alpha_{\perp}$ is thermo-EMF along and across the long axis of the isoenergetic ellipsoid) was calculated by the method described in [19].

The principal characteristics of samples under study are given in Table 2 and in Figs. 1 and 2, where σ_0 and σ_∞, α_0 and α_∞, Z_0 and Z_∞ are the values of conductivity, thermo-EMF and figure of merit of strongly deformed *n-Si* crystals; $\Delta\alpha$ and Z_a is thermo-EMF anisotropy and figure of merit of anisotropic thermoelement (based on strongly deformed *n-Si*).

Table 2

Characteristics of the investigated n-Si samples

Sample №	$n_e \cdot 10^{-14}$, cm^{-3}	$\mu_{77\,K}$, cm^2/V·s	$\sigma_{0\,77\,K}$, $\Omega^{-1}\cdot$cm^{-1}	$\sigma_{\infty\,77\,K}$, $\Omega^{-1}\cdot$cm^{-1}
1	0.19	19250	$6.28 \cdot 10^{-2}$	$1.59 \cdot 10^{-2}$
2	1.29	18700	$4.35 \cdot 10^{-1}$	$1.15 \cdot 10^{-1}$
3	6.55	14550	1.71	$5.48 \cdot 10^{-1}$
4	20.0	9300	3.23	1.24
5	62.1	6400	6.45	2.58
6	260	1800	7.14	3

On the right scale of Fig. 2, for the purpose of comparison, the Z_a value of the most common materials with anisotropic thermo-EMF is plotted (for instance, for Bi $Z_a = 0.9 \cdot 10^{-4}$ K^{-1}, however, thermo-EMF anisotropy is only $\Delta\alpha = 0.054$ μV/K [12]). Index (0) is used to denote the values that were measured in the absence of mechanical stress on the sample (at $X = 0$), and index (∞) – the values that were measured at such values of $X \to \infty$ ($X \geq 0.6$ GPa) which bring these values to saturation.

The values of Z_0 and Z_∞ were calculated by means of expressions of the type (2), and Z_a – using expressions (4) and (5). The values of electrical conductivity along ($\sigma_{\parallel}$) and across ($\sigma_{\perp}$) of the long axis of isoenergetic ellipsoid were obtained from the data on tensoresistance. Changes in the tensoresistance of *n-Si* crystals were measured at 77 K. Typical appearance of the dependences of the tensoresistance $\rho_X = f(X)$ and tenso-thermo-EMF $\alpha_X = \varphi(X)$, obtained on *n-Si* crystals under conditions $\vec{X} \parallel \vec{J} \parallel [001]$ and $\vec{X} \parallel \nabla T \parallel [001]$, respectively, is represented for one of silicon samples under study in Fig. 3.

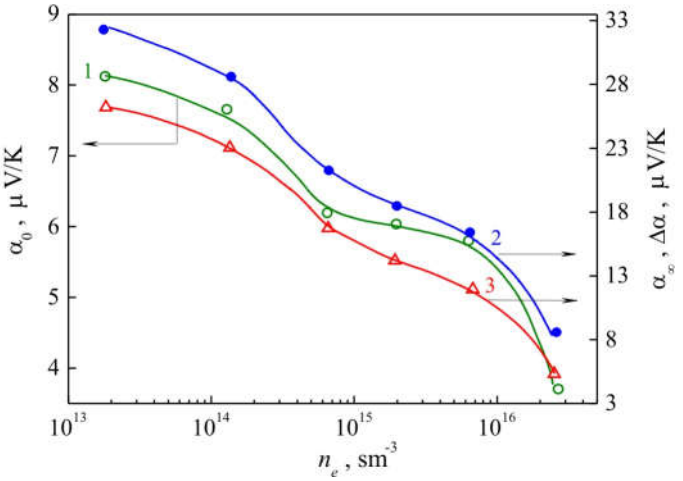

Fig. 1. Concentration dependences of thermo-EMF α_0 (1), tenso-thermo-EMF α_∞ (2) and thermo-EMF anisotropy $\Delta\alpha$ (3) in n-Si single crystals at T = 85 K.

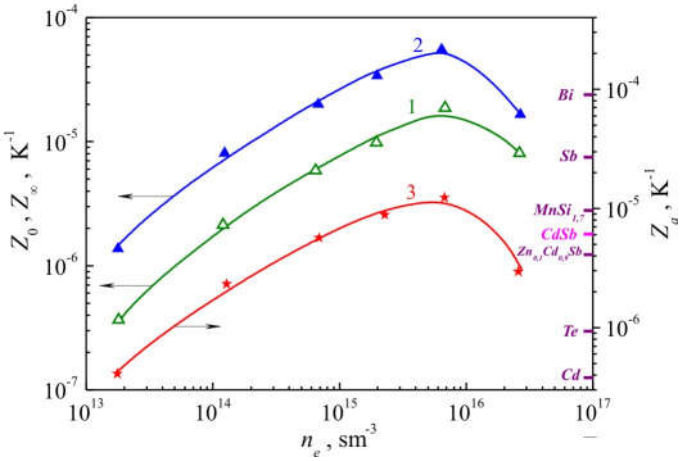

Fig. 2. Concentration dependences of thermoelectric figure of merit at T = 85 K of n-Si single crystals: in the absence of Z_0 (1) and in the presence of strong uniaxial elastic deformation Z_∞ (2) and Z_a (3). On the right scale, the data for Z_a for known thermoelectrically anisotropic materials are plotted (see Table 1 [12]).

According to [16], the thermal conductivity χ of pure Si at $T = 85$ K is 11.5 ± 1 W/cm·K. In the case of increasing n_e from $1.9 \cdot 10^{13}$ to $2.6 \cdot 10^{16}$ cm^{-3}, only a slight decrease of χ from 11.5 W/cm·K is possible due to some increase in the efficiency of phonon impurity scattering, which can only positively affect the values of Z and Z_a.

From Fig. 1 it is seen that the dependence $\alpha_0(n_e)$ (curve *1*) in the region of charge carrier concentration $6 \cdot 10^{14} \le n_e \le 6 \cdot 10^{15}$ cm^{-3} has a weakly expressed "plateau", due to a combined manifestation of conventional mechanism of formation of thermo-EMF with electron-phonon drag effect.

In the investigated range of concentrations n_e, on application of a deformation stress $X \ge 0.6$GPa to *n-Si,* both thermo-EMF α_∞ (Fig. 1) and thermoelectric figure of merit Z_∞ (Fig. 2) increase considerably as compared to α_0 and the figure of merit Z_0 in the absence of mechanical stress (at $X = 0$). The decrease in the figure of merit Z_0, Z_∞ and Z_a (Fig. 2) with increasing carrier concentration n_e over $7 \cdot 10^{15}$ cm^{-3} is due to a drastic decrease in the thermo-EMF α in the range of concentration values $n_e > 7 \cdot 10^{15}$ cm^{-3} (see Fig. 1).

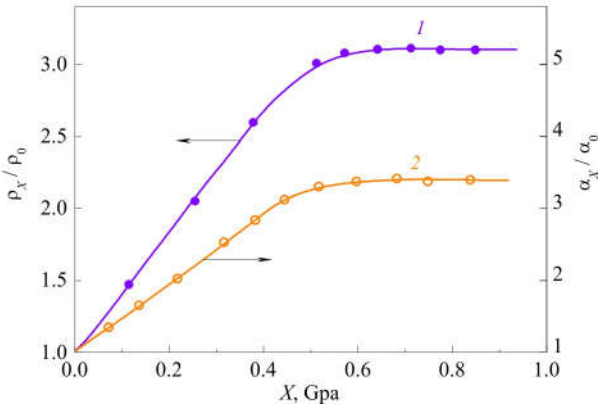

Fig. 3. Typical view of the dependences of tensoresistance ρ_X / ρ_0 *(1) and thermo-EMF and tenso-thermo-EMF* α_X / α_0 *(2) on mechanical stress X for n-Si.*

The values of thermo-EMF anisotropy $\Delta\alpha = \alpha_{\parallel} - \alpha_{\perp}$ arising in the region of electron-phonon drag in the case of elastic deformation of *n-Si* crystals ($\vec{X} \parallel \nabla T \parallel [001]$), by about two-three orders (see Table 1 [12]) exceed the thermo-EMF anisotropy of other (most common) thermoelectric materials.

Thus, the experiments performed allow us to state that on the basis of uniaxially elastically deformed *n-Si* single crystals at T = 85 K, it is possible to create anisotropic thermoelements with efficiencies not worse than the efficiency of thermoelements created on the basis of other known materials, but with sensitivity, which is approximately two to three orders of magnitude greater than the sensitivity of the latter.

Temperature dependences of thermoelectric characteristics in the elastically deformed *n-Si* crystals

Silicon of electron conductivity type even in the region of effective manifestation of electron-phonon drag is a thermoelectrically isotropic material. However, if by means of strong elastic deformation in crystallographic direction it is transferred from “six-” to “two-valley” state, it will not cause the appearance of thermo-EMF anisotropy in the case of electron-phonon drag. In this case the value of $\Delta\alpha$ at $T = 85$ K can reach $20 \div 30$ μV/K, which is factor of $100 \div 200$ higher than the respective values of thermo-EMF anisotropy of the most common materials characterized by natural thermoelectric anisotropy.

To solve a number of applied problems (in particular, when creating anisotropic thermoelements based on "two-valley" *n-Si* that operate in a wide temperature range), it is necessary to have information on the temperature dependences of thermoelectric characteristics, the study of which was the purpose of this work.

On *n-Si* crystals with phosphorus impurity concentration $N_P \equiv n_e = 1.75 \cdot 10^{14}$ cm^{-3}, the peculiarities of changes in thermoelectric parameters as a function of temperature were studied in the range of 85 to 355 K. The thermo-EMF α_∞ was measured on application of mechanical stresses which assured complete transfer of carriers from the six valleys rising in the energy scale due to deformation, into two descending valleys over the entire investigated temperature range: $X \geq 0.6$ GPa, $\vec{X} \parallel [001] \parallel \nabla T$. The thermo-EMF α_0 was measured in the absence of deformation ($X = 0$). Since under the experimental conditions the thermal conductivity was almost independent of the magnitude of the uniaxial elastic deformation [18], this coefficient was determined only for the case $X = 0$. The main initial data used in further calculations are given in Table. 3

Table 3

Characteristics of n-Si samples investigated at different temperatures

T, K	α_0, $\mu V \cdot K^{-1}$	$\alpha_\infty \equiv \alpha_\parallel$, $\mu V \cdot K^{-1}$	σ_0, $\Omega^{-1} \cdot cm^{-1}$	σ_∞, $\Omega^{-1} \cdot cm^{-1}$	χ, $W \cdot cm^{-1} \cdot K^{-1}$
85	7.7	29.5	$4.17 \cdot 10^{-1}$	$1.11 \cdot 10^{-1}$	11.2
100	6	21	$3.33 \cdot 10^{-1}$	$8.93 \cdot 10^{-2}$	9.0
120	4.3	13.5	$2.5 \cdot 10^{-1}$	$6.9 \cdot 10^{-2}$	6.8
140	3.4	9	$1.92 \cdot 10^{-1}$	$5.49 \cdot 10^{-2}$	5.3
160	2.75	6.3	$1.47 \cdot 10^{-1}$	$4.44 \cdot 10^{-2}$	4.2
180	2.45	4.9	$1.15 \cdot 10^{-1}$	$3.7 \cdot 10^{-2}$	3.4
200	2.25	4.1	$9.10 \cdot 10^{-2}$	$3.16 \cdot 10^{-2}$	2.8
220	2.15	3.6	$7.14 \cdot 10^{-2}$	$2.72 \cdot 10^{-2}$	2.4
240	2.05	3.2	$5.71 \cdot 10^{-2}$	$2.38 \cdot 10^{-2}$	2.2
260	1.95	2.85	$4.72 \cdot 10^{-2}$	$2.08 \cdot 10^{-2}$	2.0
280	1.85	2.65	$3.91 \cdot 10^{-2}$	$1.84 \cdot 10^{-2}$	1.9
300	1.84	2.5	$3.28 \cdot 10^{-2}$	$1.61 \cdot 10^{-2}$	1.8
320	1.82	2.45	$2.74 \cdot 10^{-2}$	$1.42 \cdot 10^{-2}$	1.8

It is known that in the region of low concentrations of charge carriers ($n_e \le 10^{15}$ cm^{-3}) the phonon and electron (diffusion) parts of thermo-EMF are additive [20], and thermo-EMF anisotropy in the region of impurity conduction (i.e. under conditions of one sort of carriers even in the case of strongly expressed anisotropy of their effective mass) is determined only by the anisotropy of phonon component [17] $\alpha^\phi = \alpha - \alpha^e$, where α is experimentally measured thermo-EMF; α^e is electronic (diffusion) component of thermo-EMF; α^ϕ is thermo-EMF component related to electron phonon drag. The thermo-EMF drag anisotropy in cubic crystals is determined by the difference in components of the phonon component of thermo-EMF along and across the long axis of isoenergetic ellipsoid. i.e. $\Delta\alpha = \alpha_\parallel - \alpha_\perp \equiv \alpha_\parallel^\phi - \alpha_\perp^\phi$. The electronic component of thermo-EMF is calculated by the Pisarenko formula [21] $\alpha^e = \frac{k}{e}\left[2 + \ln\frac{2\left(2\pi m^* kT\right)^{3/2}}{n_e h^3}\right]$, where n_e is charge carrier concentration; e is electron charge; k is the Boltzmann constant; T is temperature; h is the Planck constant; $m^* = N^{2/3}\sqrt[3]{m_\parallel m_\perp^2}$; $N = \begin{cases} 6 & \text{при } X = 0 \\ 2 & \text{при } X \ge 0.6\ \text{ГПа}, \quad \vec{X} \parallel [001] \end{cases}$ is the number of isoenergetic ellipsoids; m^* is density-of-state effective mass; $m_\parallel$ and $m_\perp$ is longitudinal and transverse effective masses of electron in the isoenergetic ellipsoid, respectively.

In order for the difference in thermo-EMF components along $\alpha_\parallel$ and across $\alpha_\perp$ of the long axis of isoenergetic ellipsoid to be different from zero ($\Delta\alpha = \alpha_\parallel - \alpha_\perp \ne 0$), it is sufficient that there was inequality $m_\parallel - m_\perp \ne 0$. However, even at $m_\parallel \ne m_\perp$, thermo-EMF anisotropy in silicon may appear ($\Delta\alpha \ne 0$) only under the conditions of the manifestation of the electron-phonon drag effect.

The value of thermo-EMF anisotropy $\Delta\alpha$ was determined by the results of measuring thermo-EMF, tenso-thermo-EMF and tensoresistance according to the following formula

$$\Delta\alpha = \left(\alpha_{\infty}^{\phi} - \alpha_{0}^{\phi}\right)\left(1 + \frac{1}{2K}\right), \qquad (7)$$

where $K = \frac{\mu_{\perp}}{\mu_{\parallel}} = \frac{3}{2}\frac{\rho_{\infty}^{[001]}}{\rho_0} - \frac{1}{2}$ is mobility anisotropy parameter; ρ_0 and ρ_∞ is the resistivity of undeformed crystal (at $X = 0$) and in saturation (at $X \geq 0.6$ GPa, $\vec{X} \parallel \vec{J} \parallel [001]$); $\alpha_0^{\phi} = \alpha_0 - \alpha^e$ and $\alpha_{\infty}^{\phi} = \alpha_{\infty} - \alpha^e$ are phonon components of thermo-EMF and tenso-thermo-EMF in the undeformed and deformed samples, respectively.

Fig. 4 represents the temperature dependences of thermo-EMF, tenso-thermo-EMF and thermo-EMF anisotropy of *n-Si* ⟨*P*⟩ crystals ($n_e = 1.75 \cdot 10^{14}$ cm^{-3}). For comparison, it also shows the dependence of thermo-EMF anisotropy $\Delta\alpha = \alpha_{22} - \alpha_{33}$ on the temperature of thermoelectrically anisotropic CdSb materials. In CdSb, at $T \geq 300$ K, according to [12], thermo-EMF anisotropy occurs due to the presence of several types of carriers (with one scattering mechanism) [22], whereas in the low-temperature range thermo-EMF anisotropy for CdSb is caused by the presence of several scattering mechanisms. In the elastically deformed *n-Si* over the entire investigated temperature range ($85 \leq T \leq 355$ K) thermo-EMF anisotropy is due to the action of the only mechanism related to phonon drag of electrons with anisotropic effective mass. With decreasing temperature, the decisive role of electron phonon drag effect assures the increase of thermo-EMF anisotropy in *n-Si*.

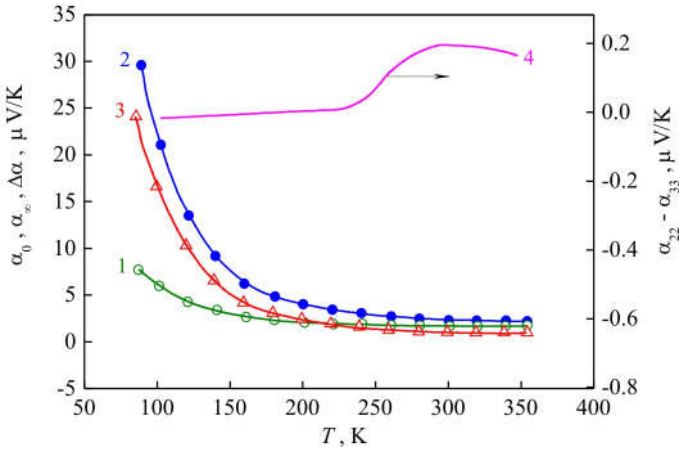

Fig. 4. Temperature dependences of thermo-EMF α_0 (1), tenso-thermo-EMF α_∞ (2) and thermo-EMF anisotropy $\Delta\alpha$ (3) of n-Si single crystals ⟨P⟩ ($n_e = 1.75 \cdot 10^{14}$ cm^{-3}) in the absence and in the presence of strong uniaxial elastic deformation. Curve 4 – dependence of thermo-EMF anisotropy $\Delta\alpha$ (T) for thermoelectrically anisotropic material CdSb [12].

Over the entire investigated temperature range, the values of $\Delta\alpha$, characteristic of deformed *n-Si*, are much in excess of the same values typical of known thermoelectrically anisotropic materials. Even under the most unfavourable conditions (i.e. at the highest $T \approx 300 \div 355$ K) the anisotropy of drag thermo-EMF of elastically deformed *n-Si* is 3 ÷ 3.5 times higher than the maximum values of $\Delta\alpha$ which characterize the best thermoelectric materials in the absence of deformation (Fig. 4, curve *4*). Whereas in the low-temperature range (~ 80 K) the thermo-EMF anisotropy $\Delta\alpha$ of elastically deformed *n-Si* reaches gigantic values (~ 24 μV/K) as compared to 0.2 μV/K for higher class conventional materials in the absence of deformation (i.e. exceeds the anisotropy of the aforementioned materials by more than two orders of magnitude).

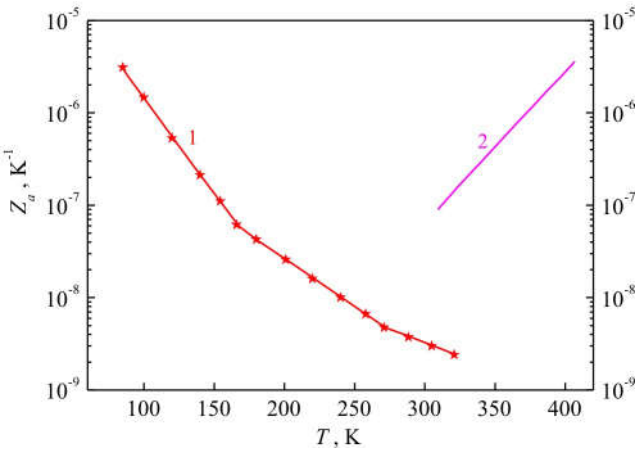

Fig. 5. Temperature dependences of thermoelectric figure of merit Z_a for n-Si ⟨P⟩ ($n_e = 1.75 \cdot 10^{14}$ cm^{-3}) (1) and CdSb (2).

According to the results of measuring the temperature dependences of the corresponding parameters, the dependence $Z_a = Z_a(T)$ (formula 5, curve *1*) is calculated according to formula (4). In the same segment of line 2, the dependence of the thermoelectric figure of merit $Z_a(T)$ for CdSb is given, calculated for two temperatures (300 and 400 K) according to the data of [23].

The results of investigations carried out showed that the uniaxially deformed *n-Si* is a good low-temperature thermoelectrically anisotropic material. In the studied temperature range, it has a fairly high thermoelectric figure of merit Z_a, which increases significantly with decreasing temperature (due to the growth of $\Delta\alpha$ (Fig. 4, curve 3) and the conductivity σ (Table 3)). The thermo-EMF anisotropy $\Delta\alpha = \alpha_{\parallel} - \alpha_{\perp}$, which determines the sensitivity of anisotropic thermoelements to the temperature gradient of deformed *n-Si* in the temperature range of 85 ÷ 355 K, is many times greater than the values of $\Delta\alpha$ typical of traditional thermoelectrically anisotropic materials.

Conclusion

As a result of the experiments, the following conclusions can be made.

1. The concentration and temperature dependences of thermo-EMF α_0, tenso-thermo-EMF α_∞ (under conditions of $\vec{X} \parallel \nabla T \parallel [001]$, $X \geq 0.6$ GPa), thermo-EMF anisotropy $\Delta\alpha$ and thermoelectric figure of merit Z_a for *n-Si* ⟨*P*⟩ crystals have been studied. It has been shown that despite the high thermal conductivity which grows in *n-Si* with decreasing temperature, these crystals (in the elastically deformed state) can have a thermoelectric figure of merit comparable to that of the most common thermoelectrically anisotropic materials.

2. The thermo-EMF anisotropy $\Delta\alpha$ of elastically deformed *n-Si* even at room temperature exceeds considerably the thermo-EMF anisotropy of traditional thermoelectrically anisotropic materials, while the thermo-EMF anisotropy $\Delta\alpha$ and the thermoelectric figure of merit Z_a of these materials decrease with decreasing temperature, $\Delta\alpha$ and Z_a of deformed *n-Si* in case of decreasing temperature are growing rapidly.

3. The results can be useful both for calculating various effects based on the theory of anisotropic scattering in a wide range of concentrations, and for determining the temperature range in which the use of anisotropic thermoelements based on elastically deformed *n-Si* will be more effective than anisotropic thermoelements based on traditional thermoelectrically anisotropic materials.

References

1. Anatychuk L.I., Vikhor L.N. (2012). *Termoelektrichestvo. T. IV. Funktsionalno-gradientnye termoelektricheskie materialy [Thermoelectricity. T. IV. Functionally-graded thermoelectric materials]*. Kyiv, Chernivtsi: Institute of Thermoelectricity [in Russian].
2. Dresselhaus M.S., Chen G., Tang M.Y., Yang R.G., Lee H., Wang D.Z., Ren Z.F., Fleurial J.P., Gogna P. (2007). New directions for low-dimensional thermoelectric materials. *Advanced Materials*, 19, 8, 1043 – 1053.
3. Harman T.C., Taylor P.J., Walsh M.P., LaForge B.E. (2002). Quantum dot superlattice thermoelectric materials and devices. *Science*, 297, 5590, 2229 – 2232.
4. Tritt T.M., Subramanian M.A. (2006). Thermoelectric materials, phenomena, and applications: A bird's eye view. *MRS Bull.*, 31, 03, 188 – 198.
5. Zhu T.J., Liu Y.Q., Zhao X.B. (2008). Synthesis of PbTe thermoelectric materials by alkaline reducing chemical routes. *Mater. Res. Bull.*, 43, 11, 2850 – 2854.
6. Martin J., Nolas G.S., Zhang W., Chen L. (2007). PbTe nanocomposites synthesized from PbTe nanocrystals. *Appl. Phys. Lett.*, 90, 22, 222112 (3).
7. Mori M., Shimotsuma Y., Sei T., Sakakura M., Miura K., Udono H. (2015). Tailoring thermoelectric properties of nanostructured crystal silicon fabricated by infrared femtosecond laser direct writing. *Phys. Status Solidi A*, 212, 4, 715 – 721.
8. Markussen T., Jauho A.-P., Brandbyge M. (2009). Electron and phonon transport in silicon nanowires: atomistic approach to thermoelectric properties. *Phys. Rev. B*, 79, 3, 035415 (7).
9. Hochbaum A.I., Chen R., Delgado R.D., Liang W., Garnett E.C., Najarian M., Majumdar A., Yang P. (2008). Enhanced thermoelectric performance of rough silicon nanowires. *Nature*, 451, 7175, 163 – 167.
10. Boukai A.I., Bunimovich Y., Tahir-Kheli J., Yu J.K., Goddard W.A. 3rd, Heath J.R. (2008). Silicon nanowires as efficient thermoelectric materials. *Nature*, 451, 7175, 168 – 171.
11. Gaidar G.P. (2017). Termoelektropreobrazovateli novogo pokoleniya: tendentsii razvitiya [Thermoelectroconverters of the new generation: The development trends]. *Scientific Research: Perspectives of Innovative Development of Society and Technologies*: *Proceedings of the II International Scientific and Practical Conference*, Kyiv, January 20–21, 2017, pp. 137 – 140 [in Russian].
12. Anatychuk L.I. (1979). *Termoelementy i termoelektricheskie ustroystva. Spravochnik [Thermoelements and thermoelectric devices. Handbook]*. Kyiv: Naukova Dumka [in Russian].
13. Buda I.S., Pilat I.M., Soliychuk K.D. (1973). Anizotropiya termoEDS monokristallov tverdykh rastvorov $Zn_xCd_{1-x}Sb$ [Thermo-emf anisotropy of single crystals of solid solutions $Zn_xCd_{1-x}Sb$]. *Fizika i tekhnika poluprovodnikov – Semiconductors*, 7, 10, 1925 – 1928 [in Russian].
14. Ioffe A.F. (1956). *Poluprovodnikovye termoelementy [Semiconductor thermoelements]*. Moscow, Leningrad: Izd-vo AN SSSR [in Russian].
15. Anatychuk L.I., Luste O.Ya. (1976). Vikhrevye termoelektricheskie toki i vikhrevye termoelementy [Vortex thermoelectric currents and vortex thermoelements]. *Fizika i tekhnika poluprovodnikov – Semiconductors*, 10, 5, 817 – 831 [in Russian].
16. Baranskiy P.I., Klochkov V.P., Potykevich I.V. *Poluprovodnikovaya elektronika. Spravochnik [Semiconductor Electronics. Handbook]*. Kyiv: Naukova Dumka [in Russian].
17. Baranskiy P.I., Savyak V.V., Shcherbina L.A. (1979). Uglovaya zavisimost pezotermoEDS odnoosno deformirovannogo *n-Si* v oblasti elektron-fononnogo uvlecheniya [Angular dependence of

piezo-termo-emf of the uniaxially deformed *n-Si* in the region of electron-phonon drag]. *Fizika i tekhnika poluprovodnikov – Semiconductors*, 13, 11, 2274 – 2276 [in Russian].

18. Baranskiy P.I., Kogutyuk P.P., Savyak V.V. (1981). Teploprovodnost *Ge* i *Si n*-tipa pri silnoi odnoosnoi uprugoi deformatsii [Thermal conductivity of *Ge* and *Si n*-type under strong uniaxial elastic deformation]. *Fizika i tekhnika poluprovodnikov – Semiconductors*, 15, 9, 1826 – 1828 [in Russian].
19. Gaidar G.P., Baranskii P.I. (2014). Thermoelectric properties of transmutation doped silicon crystals. *Physica B: Condensed Matter*, 441, 80 – 88.
20. Buda I.S., Samoylovich A.G. (1972). O fonon-fononnom vzaimodeystvii v germanii i kremnii [About the phonon-phonon interaction in germanium and silicon]. *Ukrainskyi Fizychnyi Zhurnal – Ukrainian Journal of Physics*, 17, 10, 1730 – 1736.
21. Baranskii P.I., Gaidar G.P. (2012). Anizotropiia termoERS zakhoplennia elektroniv fononamy v *n-Ge* [Anisotropy of electron-phonon drag thermo-emf in *n-Ge*]. *Termoelektrichestvo – Journal of Thermoelectricity*, 2, 29 – 38.
22. Gaidar G.P. (2013). Mekhanizmy formuvannia anizotropii termoelektrychnykh i termomahnitnykh yavyshch u bahatodolynnykh napivprovidnykakh [Mechanisms of the anisotropy formation of thermoelectric and thermomagnetic phenomena in the multivalley semiconductors]. *Fizyka i khimiia tverdoho tila – Physics and Chemistry of Solid State*, 14, 1, 7 – 20 [in Ukrainian].
23. Baranskiy P.I., Savyak V.V., Shcherbina L.A. (1980). Issledovanie fonon-fononnoy relaksatsii v neytronno-legirovannykh i obychnykh kristallakh kremniya [Investigation of the phonon-phonon relaxation in the neutron-doped and ordinary silicon crystals]. *Fizika i tekhnika poluprovodnikov – Semiconductors*, 14, 2, 302 – 305 [in Russian].

Submitted 18.07.2018

Гайдар Г.П. *доктор фіз.-мат. наук, ст. н. с.*[1],
Баранський П.І. *доктор фіз.-мат. наук, професор*[2]

[1]Інститут ядерних досліджень НАН України
просп. Науки, 47, Київ, 03680, Україна;
e-mail: gaydar@Kinr.Kiev.ua
[2]Інститут фізики напівпровідників
ім. В.Є. Лашкарьова НАН України,
просп. Науки, 45, Київ, 03028, Україна

КОНЦЕНТРАЦІЙНІ І ТЕМПЕРАТУРНІ ЗАЛЕЖНОСТІ ТЕРМОЕЛЕКТРИЧНИХ ХАРАКТЕРИСТИК ПРУЖНО ДЕФОРМОВАНОГО КРЕМНІЮ

Досліджено концентраційні і температурні залежності термоЕРС, тензотермоЕРС, анізотропії термоЕРС і термоелектричної добротності недеформованих і одновісно пружно деформованих кристалів n-Si. Встановлено, що, незважаючи на велику теплопровідність, яка зростає в n-Si зі зниженням температури, ці кристали (в пружно деформованому стані) можуть мати термоелектричну добротність, порівнянну з добротністю найбільш використовуваних термоелектрично-анізотропних матеріалів. Показано, що анізотропія термоЕРС деформованого n-Si, яка визначає чутливість анізотропного термоелемента,

перевищує Δα традиційних термоелектрично-анізотропних матеріалів на два-три порядки. Бібл. 23, рис. 5, табл. 3.
Ключові слова: кремній, одновісна пружна деформація, термоЕРС, тензотермоЕРС, анізотропія термоЕРС, термоелектрична добротність.

Гайдар Г. П., *доктор физ.-мат. наук*, *ст. н. с.*[1]
Баранский П. И., *доктор физ.-мат. наук, профессор*[2]

[1]Институт ядерных исследований НАН Украины,
просп. Науки, 47, Киев, 03028, Украина*e-mail: gaydar@kinr.kiev.ua*
[2]Институт физики полупроводников им. В. Е. Лашкарева НАН Украины,
просп. Науки, 45, Киев, 03028, Украина

Исследованы концентрационные и температурные зависимости термоЭДС, тензотермоЭДС, анизотропии термоЭДС и термоэлектрической добротности недеформируемых и одноосно упруго деформированных кристаллов n-Si. Установлено, что, несмотря на большую теплопроводность, которая в n-Si растет с понижением температуры, эти кристаллы (в упруго деформированном состоянии) могут иметь термоэлектрическую добротность, сравнимую с добротностью наиболее широко применяемых термоэлектрически анизотропных материалов. Показано, что анизотропия термоЭДС деформированного n-Si, определяющая чувствительность анизотропного термоэлемента, превышает Δα традиционных термоэлектрически анизотропных материалов на два-три порядка. Библ. 23, рис. 5, табл. 3
Ключевые слова: кремний, одноосная упругая деформация, термоЭДС, тензотермоЭДС, анизотропия термоЭДС, термоэлектрическая добротность.

References

1. Anatychuk L.I., Vikhor L.N. (2012). *Termoelektrichestvo. T. IV. Funktsionalno-gradientnye termoelektricheskie materialy [Thermoelectricity. T. IV. Functionally-graded thermoelectric materials]*. Kyiv, Chernivtsi: Institute of Thermoelectricity [in Russian].
2. Dresselhaus M.S., Chen G., Tang M.Y., Yang R.G., Lee H., Wang D.Z., Ren Z.F., Fleurial J.P., Gogna P. (2007). New directions for low-dimensional thermoelectric materials. *Advanced Materials*, 19, 8, 1043 – 1053.
3. Harman T.C., Taylor P.J., Walsh M.P., LaForge B.E. (2002). Quantum dot superlattice thermoelectric materials and devices. *Science*, 297, 5590, 2229 – 2232.
4. Tritt T.M., Subramanian M.A. (2006). Thermoelectric materials, phenomena, and applications: A bird's eye view. *MRS Bull.*, 31, 03, 188 – 198.
5. Zhu T.J., Liu Y.Q., Zhao X.B. (2008). Synthesis of PbTe thermoelectric materials by alkaline reducing chemical routes. *Mater. Res. Bull.*, 43, 11, 2850 – 2854.
6. Martin J., Nolas G.S., Zhang W., Chen L. (2007). PbTe nanocomposites synthesized from PbTe nanocrystals. *Appl. Phys. Lett.*, 90, 22, 222112 (3).
7. Mori M., Shimotsuma Y., Sei T., Sakakura M., Miura K., Udono H. (2015). Tailoring thermoelectric properties of nanostructured crystal silicon fabricated by infrared femtosecond laser direct writing. *Phys. Status Solidi A*, 212, 4, 715 – 721.
8. Markussen T., Jauho A.-P., Brandbyge M. (2009). Electron and phonon transport in silicon nanowires: atomistic approach to thermoelectric properties. *Phys. Rev. B*, 79, 3, 035415 (7).

9. Hochbaum A.I., Chen R., Delgado R.D., Liang W., Garnett E.C., Najarian M., Majumdar A., Yang P. (2008). Enhanced thermoelectric performance of rough silicon nanowires. *Nature*, 451, 7175, 163 – 167.
10. Boukai A.I., Bunimovich Y., Tahir-Kheli J., Yu J.K., Goddard W.A. 3rd, Heath J.R. (2008). Silicon nanowires as efficient thermoelectric materials. *Nature*, 451, 7175, 168 – 171.
11. Gaidar G.P. (2017). Termoelektropreobrazovateli novogo pokoleniya: tendentsii razvitiya [Thermoelectroconverters of the new generation: The development trends]. *Scientific Research: Perspectives of Innovative Development of Society and Technologies*: *Proceedings of the II International Scientific and Practical Conference*, Kyiv, January 20–21, 2017, pp. 137 – 140 [in Russian].
12. Anatychuk L.I. (1979). *Termoelementy i termoelektricheskie ustroystva. Spravochnik [Thermoelements and thermoelectric devices. Handbook]*. Kyiv: Naukova Dumka [in Russian].
13. Buda I.S., Pilat I.M., Soliychuk K.D. (1973). Anizotropiya termoEDS monokristallov tverdykh rastvorov $Zn_xCd_{1-x}Sb$ [Thermo-emf anisotropy of single crystals of solid solutions $Zn_xCd_{1-x}Sb$]. *Fizika i tekhnika poluprovodnikov – Semiconductors*, 7, 10, 1925 – 1928 [in Russian].
14. Ioffe A.F. (1956). *Poluprovodnikovye termoelementy [Semiconductor thermoelements]*. Moscow, Leningrad: Izd-vo AN SSSR [in Russian].
15. Anatychuk L.I., Luste O.Ya. (1976). Vikhrevye termoelektricheskie toki i vikhrevye termoelementy [Vortex thermoelectric currents and vortex thermoelements]. *Fizika i tekhnika poluprovodnikov – Semiconductors*, 10, 5, 817 – 831 [in Russian].
16. Baranskiy P.I., Klochkov V.P., Potykevich I.V. *Poluprovodnikovaya elektronika. Spravochnik [Semiconductor Electronics. Handbook]*. Kyiv: Naukova Dumka [in Russian].
17. Baranskiy P.I., Savyak V.V., Shcherbina L.A. (1979). Uglovaya zavisimost pezotermoEDS odnoosno deformirovannogo *n-Si* v oblasti elektron-fononnogo uvlecheniya [Angular dependence of piezo-termo-emf of the uniaxially deformed *n-Si* in the region of electron-phonon drag]. *Fizika i tekhnika poluprovodnikov – Semiconductors*, 13, 11, 2274 – 2276 [in Russian].
18. Baranskiy P.I., Kogutyuk P.P., Savyak V.V. (1981). Teploprovodnost *Ge* i *Si n*-tipa pri silnoi odnoosnoi uprugoi deformatsii [Thermal conductivity of *Ge* and *Si n*-type under strong uniaxial elastic deformation]. *Fizika i tekhnika poluprovodnikov – Semiconductors*, 15, 9, 1826 – 1828 [in Russian].
19. Gaidar G.P., Baranskii P.I. (2014). Thermoelectric properties of transmutation doped silicon crystals. *Physica B: Condensed Matter*, 441, 80 – 88.
20. Buda I.S., Samoylovich A.G. (1972). O fonon-fononnom vzaimodeystvii v germanii i kremnii [About the phonon-phonon interaction in germanium and silicon]. *Ukrainskyi Fizychnyi Zhurnal – Ukrainian Journal of Physics*, 17, 10, 1730 – 1736.
21. Baranskii P.I., Gaidar G.P. (2012). Anizotropiia termoERS zakhoplennia elektroniv fononamy v *n-Ge* [Anisotropy of electron-phonon drag thermo-emf in *n-Ge*]. *Termoelektrichestvo – Journal of Thermoelectricity*, 2, 29 – 38.
22. Gaidar G.P. (2013). Mekhanizmy formuvannia anizotropii termoelektrychnykh i termomahnitnykh yavyshch u bahatodolynnykh napivprovidnykakh [Mechanisms of the anisotropy formation of thermoelectric and thermomagnetic phenomena in the multivalley semiconductors]. *Fizyka i khimiia tverdoho tila – Physics and Chemistry of Solid State*, 14, 1, 7 – 20 [in Ukrainian].
23. Baranskiy P.I., Savyak V.V., Shcherbina L.A. (1980). Issledovanie fonon-fononnoy relaksatsii v neytronno-legirovannykh i obychnykh kristallakh kremniya [Investigation of the phonon-phonon relaxation in the neutron-doped and ordinary silicon crystals]. *Fizika i tekhnika poluprovodnikov – Semiconductors*, 14, 2, 302 – 305 [in Russian].

Submitted 18.07.2018

L.I. Anatychuk[1,2] *Acad. National Academy of Sciences of Ukraine*,
Vikhor L.M.[1] **,** *Doctor Phys.-math. Science*
A.V.Prybyla [1,2]*Cand. Phys.-math. Science*

[1]Institute of Thermoelectricity of the NAS and MES of Ukraine,
1, Nauky str, Chernivtsi, 58029, Ukraine;
[2]Yu.Fedkovych Chernivtsi National University, 2, Kotsiubynskyi str.,
Chernivtsi, 58000, Ukraine*, e-mail: anatych@gmail.com*

EFFECT OF MINIATURIZATION ON THE EFFICIENCY OF THERMOELECTRIC MODULES IN HEATING MODE

The paper presents the results of calculations of the effect of miniaturization on the maximum heating coefficient of a thermoelectric module for various temperature conditions of its operation. The possibilities of reducing the mass and size parameters of the thermoelectric module in the heating mode with minimal heating coefficient losses are analyzed. Bibl. 12, Fig. 5.
Key words: thermoelectric heat pump, efficiency, miniaturization, simulation.

Introduction

General characterization of the problem. Today, thermoelectric cooling and heating are increasingly used due to their attractive properties - the absence of harmful refrigerants, quiet operation, the ability to work with an arbitrary orientation in space and to maintain the specified temperature modes with a high degree of accuracy. Thermoelectric converters are used to stabilize the temperature of various elements of electronics, in everyday life and medicine, for air conditioning in vehicles, etc. [1-3]. Their use is especially important in space technology, in particular, in water purification devices [4-10], where, thanks to thermoelectricity, the coefficient of conversion of electrical into thermal energy K≈3 is achieved.

In [6-10], optimization of the design and power supply system of the thermoelectric heat pump of the water purification device for space purposes was carried out in order to achieve the maximum values of the energy conversion coefficient. However, the issue of reducing the mass and volume of thermoelectric converters in the heating mode for water purification devices was not considered. Meanwhile, this is especially important when using them in space programs at the International Space Stations and in the preparation of missions for the exploration of distant planets of the solar system. In addition, the need for miniaturization is also dictated by the considerations of reducing the cost of thermoelectric material, which is the most expensive part of these converters.

The purpose of the work is to study the effect of miniaturization of thermoelement legs on the efficiency of thermoelectric heat pumps used to heat the liquid and gas flows.

Physical model

The studies were carried out using a physical model of a thermoelectric module in the heating mode (Fig. 1). It consists of ceramic insulating plates *1*, which play the role of electrical insulation and conduct heat flow *Qh*. Electric current *I* passes through interconnect plates 2 and legs of thermoelectric material based on bismuth telluride *(BiTe)* of *n*- and *p*-type conductivity 3. At the contacts of thermoelectric material and interconnect plates there are contact layers 4, leading to additional contact electrical and thermal resistances.

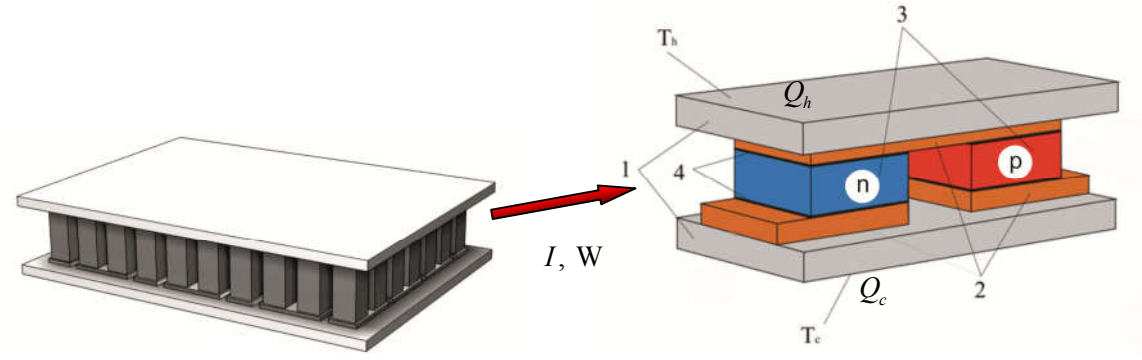

A *B*

Fig.1. Thermoelectric module: A – schematic image; B – fragment of the elementary module section; 1 – insulating plates, 2 –interconnect plates, 3 –thermoelement legs, 4 –contact layers.

To calculate the thermoelectric module in the heating mode and determine the effect of miniaturization on its efficiency, methods of optimal control theory were used [11, 12]. Below is a detailed description of the mathematical model that was used in the calculations.

Optimal control method for calculation of maximum heating coefficient of thermoelectric module

There is an obvious **r**equirement that the design parameters and the supply current of the thermoelectric module of the heat pump meet the condition of the maximum heating coefficient K, which is determined by the formula

$$K = \frac{Q_h}{W} = \frac{Q_h}{Q_h - Q_c} \ , \tag{1}$$

where $W = Q_h - Q_c$ is consumed electric power, Q_c, Q_h are external heat flows on the cold and hot surfaces of thermoelectric module, respectively. This will ensure the heating of heat carrier in the working circuit of the heat pump with minimal losses of electric energy.

Optimal control theory is successfully used to optimize thermoelectric modules in cooling and power generation modes [11, 12]. This method is easily generalized to calculate the maximum heating coefficient, which characterizes the heat pump mode.

According to optimal control methods [11,12], the operating efficiency of thermoelectric module in heating mode can be estimated by the functional

$$J = \ln \frac{Q_h}{Q_c} = \ln \frac{q_h}{q_c} = \ln q_h - \ln q_c \ , \tag{2}$$

where

$$q_h = \frac{Q_h}{n\, I}, \qquad q_c = \frac{Q_c}{n\, I} \tag{3}$$

are the specific (related to current strength I) heat flows on the hot and cold junctions of thermocouples, respectively, n is the number of thermocouples in the thermopile. The minimum functional J corresponds to the maximum value of the heating coefficient K.

To calculate the heat flow densities *qc, qh,* a system of equations of non-equilibrium thermodynamics [11, 12] is used, which for the legs of thermoelements of *n*- and *p*-type conductivity is given by

$$\left.\begin{aligned}\frac{dT}{dx} &= -\frac{\alpha j}{\kappa}T - \frac{q}{\kappa} \\ \frac{dq}{dx} &= \frac{\alpha^2 j^2}{\kappa}T + \frac{\alpha j}{\kappa}q + \frac{j^2}{\sigma}\end{aligned}\right\}_{n,p}, \tag{4}$$

where $j = \frac{I}{S}$ – is the specific density of current in the legs, *S* is cross-sectional area of the legs, *I* is the value of supply current. The Seebeck coefficient, the electric and thermal conductivities of legs materials are functions of temperature: $\alpha_{n,p} = \alpha_{n,p}(T)$; $\sigma_{n,p} = \sigma_{n,p}(T)$; $\kappa_{n,p} = \kappa_{n,p}(T)$ and can be assigned on the basis of approximation of experimental results of measuring thermoelectric material characteristics.

Solution of system (4) for the boundary conditions

$$T_n(0) = T_p(0) = T_h, \qquad T_n(l) = T_p(l) = T_c \tag{5}$$

will give an opportunity to calculate heat flows q_c, q_h, using the ratios

$$\begin{aligned} q_c &= -\sum_{n,p}\left[q(l) + j^2 r_0\right], \\ q_h &= -\sum_{n,p}\left[q(0) - j^2 r_0\right], \end{aligned} \tag{6}$$

where l is the height of thermoelement legs, r_0 is the value of contact resistance on thermoelement junctions.

From ratios (6) it follows that *qc, qh* depend on the parameters of the current density in the legs of thermoelements *j,* and on the magnitude of the contact resistance. According to the optimal control theory, the values of *jn, p*, ensuring the minimum of the functional *J* (2), must satisfy the following optimality conditions

$$-\frac{\partial J}{\partial j} + \int_0^l \frac{\partial H\ (\psi, T, q, j)}{\partial j} dx = 0, \tag{7}$$

where the Hamiltonian function *H* is given by

$$H = \sum_{n,p}(\psi_1 f_1 + \psi_2 f_2), \tag{8}$$

$(f_1, f_2)_{n,p}$ are right-hand sides of equations (4), $\psi = \left(\psi_1, \psi_2\right)_{n,p}$ is pulse vector, the method for determining which is described in [1,2].

The ratios (1) – (7) are the basis for computer design of optimal constructions and the calculation of optimal parameters of thermoelectric modules in the heating mode for heat pumps.

The algorithm of calculation of maximum heating coefficient is implemented by numerical methods by means of computer simulation tools. In so doing, the optimal current density in thermoelement legs *j*

and their respective heat flows q_c, q_h are calculated, and maximum value of heating coefficient $K = \dfrac{\exp J}{(\exp J - 1)}$ is determined.

The developed computer tool allows one to determine the maximum value of the heating coefficient, taking into account electrical losses in the contacts of thermoelements.

Computer simulation results

Thus, the dependences of the maximum heating coefficient of the thermoelectric module on the height of thermoelement legs for various temperature differences and temperatures of the heat-absorbing surface were calculated. The operating temperatures were chosen from the actual thermal conditions of operation of the thermoelectric heat pump of the water purification device for space use [6, 7]. The magnitude of the contact resistance is $r_0 = 5 \cdot 10^{-6}$ Ohm cm^2.

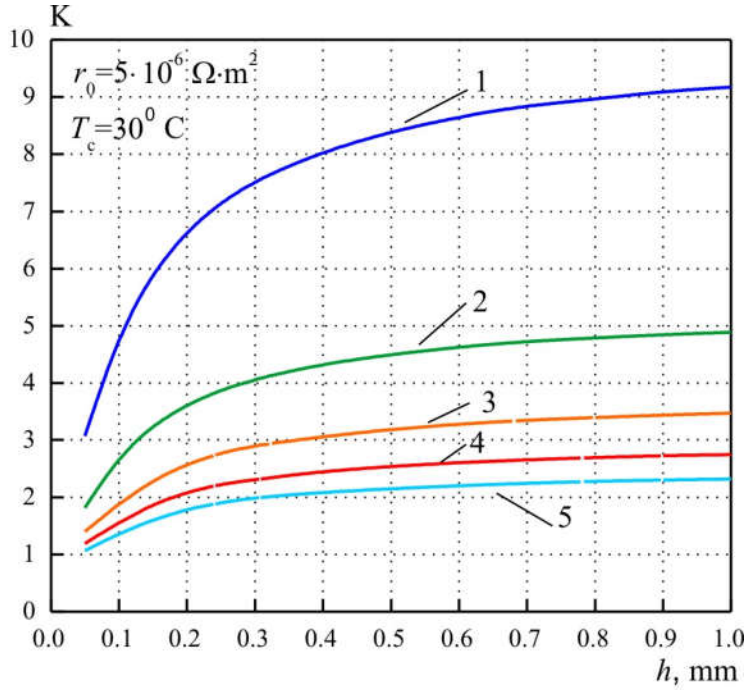

Fig.2. Dependences of heating coefficient K of thermoelectric module on the height of thermoelement legs for temperature differences 1 – ΔT=5 K, 2 - ΔT=10 K, 3 – ΔT=15 K, 4 – ΔT=20 K, 5 – ΔT=25 K. Temperature of the heat-absorbing surface T_c*=30ºC*

Fig. 2 shows the dependence of the heating coefficient of a thermoelectric module on the height of thermoelement legs for temperature differences ΔT = 5 - 25 K at a temperature of the heat-absorbing surface T_c = 30ºC. As can be seen from the figure, the value of the heating coefficient of a thermoelectric module in the range of heights of thermoelement legs from 1 to 0.5 mm decreases gradually by ~ 7–8%, and from 0.5 to 0.05 mm, the relative decrease in the heating coefficient is already ~ 50–63% depending on values of temperature differences.

Fig. 3 shows a similar dependence of the heating coefficient of a thermoelectric module on the height of thermoelement legs for temperature differences ΔT = 5 - 25 K at a temperature of heat-absorbing surface Tc = 27.5ºC. As can be seen from the figure, the qualitative picture of the change in the heating coefficient value repeats the dependence shown in Fig. 2, however, the heating coefficient value is slightly lower (by 1 - 2%), which is due to the temperature dependence of the thermoelectric material parameters.

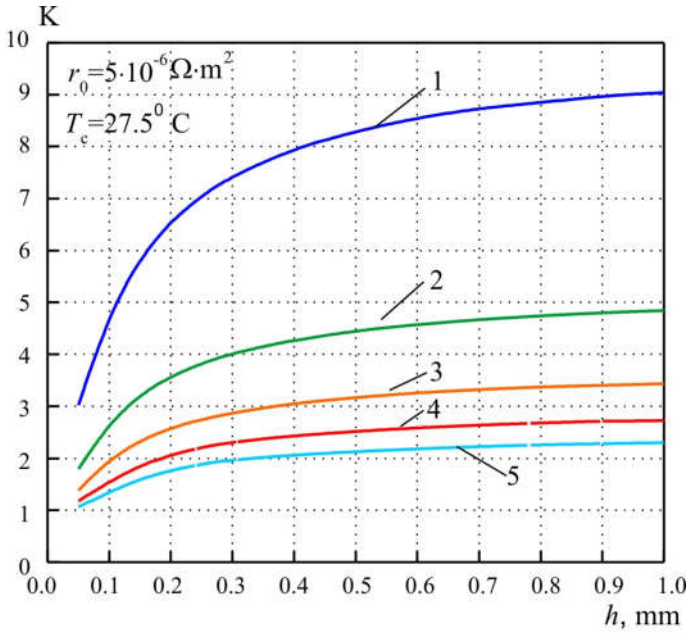

*Fig.3. Dependences of the heating coefficient K of thermoelectric module on the height of thermoelement legs for temperature differences 1 – Δ*T*=5 K, 2 - Δ*T*=10 K, 3 – Δ*T*=15 K, 4 – Δ*T*=20 K, 5 – Δ*T*=25 K. Temperature of the heat-absorbing surface* T_c*=27.5°C*

At the temperature of the heat-absorbing surface *Tc = 25°C* (Fig. 4), the relative decrease in the heating coefficient is already 2 - 3%, and at *Tc = 22.5°C* (Fig. 5) - 4 - 5%.

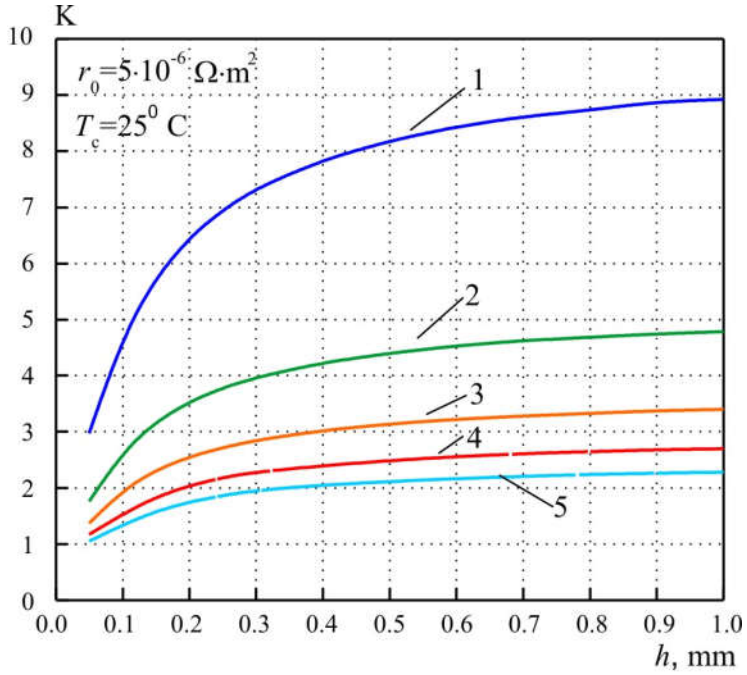

*Fig.4. Dependences of the heating coefficient K of thermoelectric module on the height of thermoelement legs for temperature differences 1 – Δ*T*=5 K, 2 - Δ*T*=10 K, 3 – Δ*T*=15 K, 4 – Δ*T*=20 K, 5 – Δ*T*=25 K. Temperature of the heat-absorbing surface* T_c*=25°C*

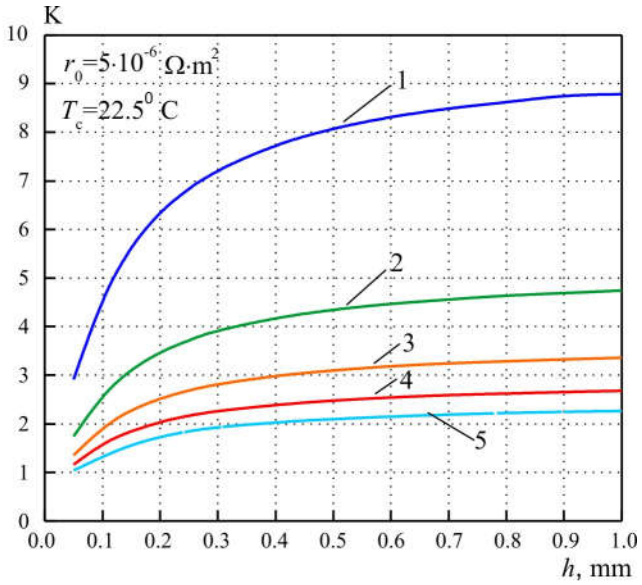

Fig.5. Dependences of the heating coefficient K of thermoelectric module on the height of thermoelement legs for temperature differences 1 – ΔT=5 K, 2 - ΔT=10 K, 3 – ΔT=15 K, 4 – ΔT=20 K, 5 – ΔT=25 K. Temperature of the heat-absorbing surface T_c=22.5°C

So, as a result of the calculations, it has been established that in a given temperature range the heating coefficient of the thermoelectric module mainly depends on the temperature difference ΔT and weakly depends on the absolute temperature value of its heat-absorbing surface T_c. When miniaturizing a thermoelectric module, the value of its heating coefficient in the range of heights of thermoelement legs from 1 to 0.5 mm gradually decreases by ~ 7–8%, and from 0.5 to 0.05 mm, the relative decrease in the heating coefficient is already ~ 50–63%. This allows us to determine the optimal height of the legs of the thermoelectric module h = 0.5 mm, whereby miniaturization will have the least effect on its efficiency.

Conclusion

1. It has been established that in a given temperature range the heating coefficient of the thermoelectric module mainly depends on the temperature difference ΔT and weakly depends on the absolute temperature value of its heat-absorbing surface.
2. It has been calculated that the value of the heating coefficient of thermoelectric module in the range of heights of thermoelement legs from 1 to 0.5 mm decreases gradually by ~ 7 - 8%, and from 0.5 to 0.05 mm the relative reduction of the heating coefficient is already ~ 50 - 63%.
3. The optimal height of thermoelectric module legs h = 0.5 mm has been determined, whereby miniaturization will have the least effect on its efficiency.

References

1. Anatychuk L.I., Vikhor L.M. (2013). The limits of thermoelectric cooling for photodetectors. *J. Thermoelectricity,* 5, 54-58.
2. Rozver Yu.Yu. (2003). Thermoelectric air-conditioner for vehicles. *J.Thermoelectricity*, 2, 52-56.
3. Anatychuk L.I., Vikhor L.N., Rozver Yu.Yu. (2004). Investigation on performance of thermoelectric cooler of liquid or gas flows. *J.Thermoelectricity*, 1, 73 – 80.
4. Rifert V.G., Usenko V.I., Barabash P.A., et al. (2011). Razrabotka i ispytaniie sistemy regeneratsii vody iz zhidkikh othodov zhiznedeiatelnosti na bortu pilotiruemykh kosmicheskikh apparatov s ispolzovaniiem termoelektricheskogo teplovogo nasosa [Development and test of water regeneration

system from liquid biowaste on board of manned spacecrafts with the use of thermoelectric heat pump]. *Termoelektrichestvo – J.Thermoelectricity*, 2, 63-74 [in Russian].
5. Anatychuk L.I., Barabash P.A., Rifert V.G., Rozver Yu.Yu., Usenko V.I., Cherkez V.G. (2013). Thermoelectric heat pump as a means of improving efficiency of water purification system on space missions. *J.Thermoelectricity*, 6, 78 – 83.
6. Anatychuk L.I., Prybyla A.V. (2015). Optimization of thermal connections in liquid-liquid thermoelectric heat pumps for water purification devices of space application. *J.Thermoelectricity*. 4, 45 – 51.
7. Anatychuk L.I., Prybyla A.V. (2015). Optimization of power supply system of thermoelectric liquid-liquid heat pump. *J.Thermoelectricity*, 6, 53 – 58.
8. Anatychuk L.I., Prybyla A.V. (2017). Limiting possibilities of thermoelectric liquid-liquid heat pump. *J. Thermoelectricity,* 4, 33 – 39.
9. Anatychuk L.I., Prybyla A.V. (2017). The influence of quality of heat exchangers on the properties of thermoelectric liquid-liquid heat pumps. *J.Thermoelectricity*, 5, 27 – 33.
10. Anatychuk L.I., Prybyla A.V. (2017). On the coefficient of performance of thermoelectric liquid-liquid heat pumps with regard to energy loss for heat carrier transfer. *J.Thermoelectricity*, 6, 30– 36.
11. Anatychuk L.I., Semeniuk V.A. (1992). *Optimalnoie upravleniie svoistvami termoelektricheskikh materialovi i priborov [Optimal control of the properties of thermoelectric materials and devices]*. Chernivtsi: Prut [in Russian].
12. Strutynskyi M.M. (2009). Computer technologies in thermoelectricity. *J. Thermoelectricity*, 4, 31-47.

Submitted 11.07.2018

Анатичук Л.І. *ак. НАН України*,[1.2]
Вихор Л.М.[1] *докт. фіз.-мат. наук*
Прибила А.В.[1,2] *канд. фіз.-мат. наук*

[1]Інститут термоелектрики, вул. Науки, 1;Чернівці, 58029, Україна;
[2]Чернівецький національний університет імені Юрія Федьковича,
вул. Коцюбинського 2, Чернівці, 58012, Україна;

ВПЛИВ МІНІАТЮРИЗАЦІЇ НА ЕФЕКТИВНІСТЬ ТЕРМОЕЛЕКТРИЧНИХ МОДУЛІВ У РЕЖИМІ НАГРІВУ

У роботі наводяться результати розрахунків впливу мінітюаризації на максимальний опалювальний коефіцієнт термоелектричного модуля для різних температурних умов його роботи. Проаналізовані можливості зменшення масогабаритних показників термоелектричного модуля в режимі нагріву за умови мінімальних втрат опалювального коефіцієнту. . Бібл. 12, Рис. 5.
Ключові слова: термоелектричний тепловий насос, ефективність, мініатюризація, моделювання.

Анатычук Л.И.[1,2] *ак. НАН Украины*,
Вихор Л.М.[1] *докт. физ.-мат. наук*
Прибила А.В.[1,2] *канд. физ.-мат. наук*

[1]Институт термоэлектричества, ул. Науки, 1;Черновцы, 58029, Украина;
[2]Черновицкий национальный университет имени Юрия Федьковича,
ул. Коцюбинского 2, Черновцы, 58012, Украина;

ВЛИЯНИЕ МИНИАТЮРИЗАЦИИ НА ЭФФЕКТИВНОСТЬ ТЕРМОЭЛЕКТРИЧЕСКИХ МОДУЛЕЙ В РЕЖИМЕ НАГРЕВА

В работе приводятся результаты расчетов влияния минитюаризации на максимальный отопительный коэффициент термоэлектрического модуля для различных температурных условий его работы. Проанализированные возможности уменьшения масогабаритних показателей термоэлектрического модуля в режиме нагрева при условии минимальных потерь отопительного коэффициента. . Библ. 12, Рис. 5.

Ключевые слова: термоэлектрический тепловой насос, эффективность, миниатюризация, моделирование.

References

1. Anatychuk L.I., Vikhor L.M. (2013). The limits of thermoelectric cooling for photodetectors. *J. Thermoelectricity,* 5, 54-58.
2. Rozver Yu.Yu. (2003). Thermoelectric air-conditioner for vehicles. *J.Thermoelectricity*, 2, 52-56.
3. Anatychuk L.I., Vikhor L.N., Rozver Yu.Yu. (2004). Investigation on performance of thermoelectric cooler of liquid or gas flows. *J.Thermoelectricity*, 1, 73 – 80.
4. Rifert V.G., Usenko V.I., Barabash P.A., et al. (2011). Razrabotka i ispytaniie sistemy regeneratsii vody iz zhidkikh othodov zhiznedeiatelnosti na bortu pilotiruemykh kosmicheskikh apparatov s ispolzovaniiem termoelektricheskogo teplovogo nasosa [Development and test of water regeneration system from liquid biowaste on board of manned spacecrafts with the use of thermoelectric heat pump]. *Termoelektrichestvo – J.Thermoelectricity*, 2, 63-74 [in Russian].
5. Anatychuk L.I., Barabash P.A., Rifert V.G., Rozver Yu.Yu., Usenko V.I., Cherkez V.G. (2013). Thermoelectric heat pump as a means of improving efficiency of water purification system on space missions. *J.Thermoelectricity*, 6, 78 – 83.
6. Anatychuk L.I., Prybyla A.V. (2015). Optimization of thermal connections in liquid-liquid thermoelectric heat pumps for water purification devices of space application. *J.Thermoelectricity*. 4, 45 – 51.
7. Anatychuk L.I., Prybyla A.V. (2015). Optimization of power supply system of thermoelectric liquid-liquid heat pump. *J.Thermoelectricity*, 6, 53 – 58.
8. Anatychuk L.I., Prybyla A.V. (2017). Limiting possibilities of thermoelectric liquid-liquid heat pump. *J. Thermoelectricity,* 4, 33 – 39.
9. Anatychuk L.I., Prybyla A.V. (2017). The influence of quality of heat exchangers on the properties of thermoelectric liquid-liquid heat pumps. *J.Thermoelectricity*, 5, 27 – 33.
10. Anatychuk L.I., Prybyla A.V. (2017). On the coefficient of performance of thermoelectric liquid-liquid heat pumps with regard to energy loss for heat carrier transfer. *J.Thermoelectricity*, 6, 30– 36.
11. Anatychuk L.I., Semeniuk V.A. (1992). *Optimalnoie upravleniie svoistvami termoelektricheskikh materialovi i priborov [Optimal control of the properties of thermoelectric materials and devices]*. Chernivtsi: Prut [in Russian].
12. Strutynskyi M.M. (2009). Computer technologies in thermoelectricity. *J. Thermoelectricity*, 4, 31-47.

Submitted 11.07.2018

L.I. Anatychuk[1,2] *acad. National Academy of Sciences of Ukraine*,
O.I. Denisenko *doctor med. science, proffessor*[3],
O.V.Shulenina *cand. med. sciencer*[3],
O.P.Mykytiuk *cand. med. sciencer*[3],
R.R.Kobylianskyi *cand. Phys.-math. sciences*[1,2]

[1]Institute of Thermoelectricity of the NAS and MES of Ukraine, 1, Nauky str, Chernivtsi, 58029, Ukraine;
[2]Yu.Fedkovych Chernivtsi National University, 2, Kotsiubynskyi str.,
Chernivtsi, 58000, Ukraine*, e-mail: anatych@gmail.com*
[3]Higher State Educational Institution of Ukraine "Bukovinian State Medical University",
2 Theatre Square, Chernivtsi, 58002, Ukraine.

RESULTS OF CLINICAL APPLICATION OF THERMOELECTRIC DEVICE FOR THE TREATMENT OF SKIN DISEASES

The paper presents the design and technical characteristics of an upgraded thermoelectric device for the treatment of skin diseases. The mechanism of action and the method of temperature influence on the surface of human skin are analyzed. The results of clinical application of the thermoelectric device in medical practice, in particular in dermatology and cosmetology, are presented. Bibl. 39, Fig. 1, Tables 2.

Key words: thermoelectric cooling, dermatology, cosmetology.

Introduction

General characterization of the problem. It is well known that temperature exposure is an important factor in the treatment of many diseases of the human body, including the skin. Cryotherapy methods have found particularly widespread use in dermatology and cosmetology — the use of low temperatures for therapeutic purposes [1–8]. However, devices that are used for this purpose in most cases are cumbersome, without proper possibilities of temperature control and reproduction of thermal modes. Therefore, the use of temperature effects on the patient's body has certain difficulties, and to obtain low temperatures, in most cases, chilled solutions, chloroethyl or systems with liquid nitrogen are used, but their use does not allow for the necessary controlled temperatures and significantly reduces the effectiveness of treatment as a whole.

The use of thermoelectric cooling devices [9-11] allows solving this problem. Studies on the use of thermoelectric cooling in medicine, carried out over many years, confirm its successful practical application in many fields of medicine, in particular, in dermatology and cosmetology. It is relevant to create new modern thermoelectric medical equipment designed to reproduce with high accuracy the necessary temperature regimes in order to increase the efficiency of complex treatment of various diseases of the human body [12-15].

The use of cold in dermatology and cosmetology for cryomassage (stimulation of metabolic processes, smoothing wrinkles, accelerating the regression of skin rash elements with various dermatoses) and cryodestruction (freezing of warts, skin neoplasms, etc.) is promising [16-21]. It should be noted that there is still no complete information on the methods of using thermoelectric devices for complex treatment of skin diseases.

Therefore*, the purpose of this work* is to determine the clinical effectiveness of the use of an upgraded thermoelectric device in the complex treatment of skin diseases and the removal of cosmetic defects.

Design and technical characteristics of an upgraded thermoelectric device for treatment of skin diseases and solution of cosmetology problems

The Institute of Thermoelectricity of the National Academy of Sciences and the Ministry of Education and Science of Ukraine has developed an upgraded thermoelectric device designed for cryomassage and complex treatment of skin diseases. The design feature of such a device is the ability to conduct therapeutic procedures in the outpatient (non-stationary) treatment conditions. The mechanism of action of the device is the temperature effect on the nerve endings of the skin and the vascular bed, resulting in improved metabolic and reparative processes and accelerated regression of inflammatory processes in cases of acute and chronic dermatoses. Due to the positive effect on human skin, the cryomassage method is used in the complex treatment of such skin diseases as pink and acne vulgaris, patchy alopecia, limited neurodermatitis, pruritus, chronic eczema, lichen planus, flat wart, annular granuloma, etc. The appearance of the device is shown in Fig.1.

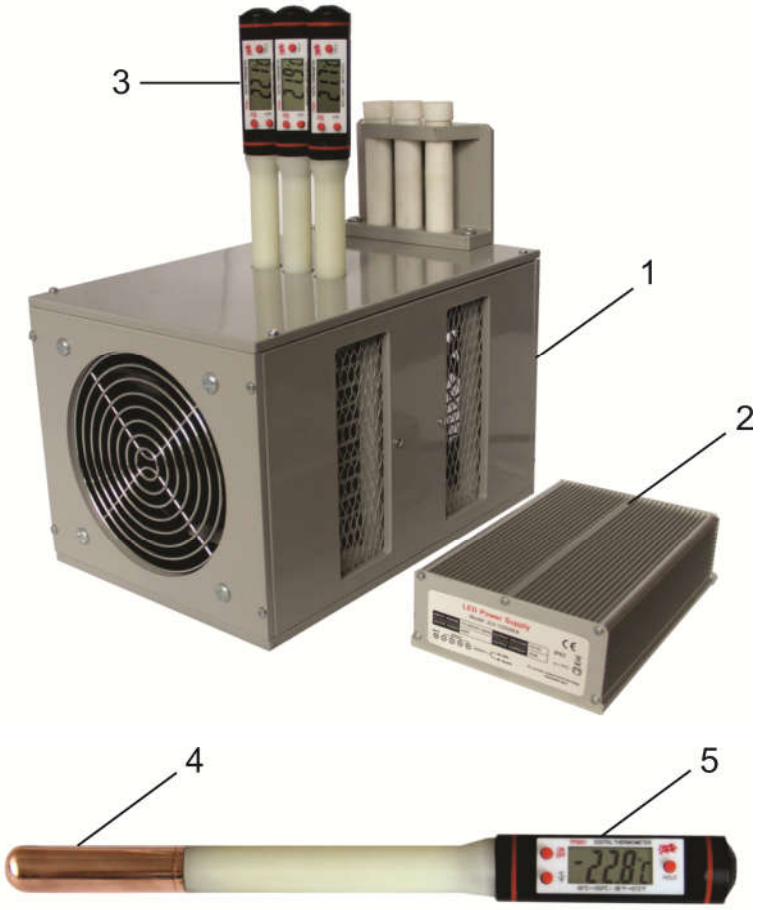

Fig.1 Upgraded thermoelectric device for the treatment of skin diseases:
1 - thermoelectric cooling unit, 2 - power supply unit,
3 - a set of working tools, 4 - cylindrical container filled with high heat capacity liquid,
5 – built-in electronic thermometer.

The device consists of three main functional units: a thermoelectric cooling unit (1), a power supply unit (2) and a set of working tools (3) (Fig. 1). In turn, the thermoelectric cooling unit includes a housing, a cooling chamber for working tools, high-performance two-stage thermoelectric modules "Altec-11" and air radiators with powerful axial fans to cool the hot sides of thermoelectric modules. The instrument's working tools contain cylindrical nozzles (4) filled with a cold storage battery in the form of high heat capacity liquid, as well as stand-alone electronic thermometers (5) with a digital display for visual control of the tip temperature (Fig. 1). The main advantages of such a thermoelectric device for the treatment of skin diseases is that its working tools are galvanically disconnected from the electrical grid and provide a controlled temperature of the working tools, which in general creates a safe and effective use of the device in dermatological and cosmetic practice.

The operating principle of the proposed device is to cool the working tools with the help of thermoelectric Peltier modules. A cooled working tool has a temperature effect on the corresponding areas of the human skin. The technical advantages of such a device include: the presence of electronic thermometers of working tools, the lack of connection of working tools with the cooling unit and small overall dimensions of the device working tools. The technical characteristics of such a device are shown in Table 1.

Table 1.

Technical specifications of thermoelectric device for treatment of skin diseases

№	Technical specifications of device	Parameters values
1.	The operating temperature range of device	(–50 ÷ +5) °C
2.	Time required for the device to reach the temperature mode	10 min.
3.	Temperature measurement accuracy	±1 ºC
4.	AC power supply voltage	(220 ± 10) V
5.	Device power consumption	250 W
6.	Overall dimensions of thermoelectric cooling unit	(240×160×150) mm
7.	Overall dimensions of operating instrument	(250×23×20) mm
8.	Operating instrument weight	0.08 kg
9.	Device weight	7 kg
10.	Time of continuous operation of the device	8 h

Of the known analogs, the thermoelectric device for the treatment of skin diseases is the closest to the technical characteristics [12-13, 22 – 23]. Such a device makes it possible to carry out therapeutic procedures in outpatient (non-stationary) conditions while simultaneously visualizing the temperature of working instruments. On the basis of the instrument proposed in this work, the medical methods of complex treatment of skin diseases [24 – 29] were developed, the mechanism of action of which is given below.

Mechanism of action and methods of conducting cryoimpact

Cooling of biological tissue is accompanied by a decrease in metabolic rate, consumption of oxygen

and nutrients, a decrease in the rate of transport of nutrients through the cell membrane, etc. These processes are dose-dependent and occur predominantly in the surface layers of biological tissue and are reversible in the case of cryomassage. After increasing the temperature of the cooled areas of the skin, there is an increase in the metabolic processes and acceleration of the regression of skin rash elements. At the same time, the phenomena occurring in deep tissues of the skin are not associated with the direct influence of cold stimulus and have a secondary reflex and neurohumoral origin. Thus, in acute and chronic dermatoses, cryotherapy has anti-inflammatory, analgesic, anti-edema, trophicoregenerative, immunostimulating action, normalizes the tone of the venous and lymphatic vessels and the like.

The mechanism of destruction of biological tissue by cryogen in the case of cryodestruction is due to the destructive effect of ultralow temperatures on cellular elements due to the formation of crystals of ice inside cells. During thawing, in the cells the concentration of the electrolytes increases, which is accompanied by repeated crystallization and accelerated destruction of cells. Under the influence of ultralow temperatures, microcirculatory disturbances arise in the form of a vascular stasis (termination of circulation of blood in vessels for a short time). Repeated freezing cycles are accompanied by maximum cell destruction. It retains the structural composition of tissue, collagen fibers and the ability to regenerate nerve fibers. This ensures normal healing of the wound after cryodestruction [30 – 32].

When conducting cryosurgery it is important to take into account three main factors [33 – 35]:

- freezing and thawing time of the fabric;
- the spread of freezing on the periphery of the tumor;
- number of freezing-thaw cycles.

The freezing time depends on the type of tumor and the method of cryo impact. When treating benign neoplasms of the skin, such as common warts, the time of contact with cryogen should be relatively short, since in this case it is only necessary to freeze the epidermal layer of the tumor in order to separate it from the dermis of the peripheral surface. When freezing tumors, the time of contact of cryogen with the neoplasm increases in connection with the need to destroy the entire volume of the tumor. To destruct the malignant neoplasms of the skin, it is necessary to reach the temperature inside the biological tissue up to -50 ° C, with the time of the temperature effect about 30 seconds. The thawing time is also an important parameter for monitoring cryosurgery and should be about 2-3 times greater than that of freezing.

The spread of freezing beyond the skin neoplasm is permissible both in the case of the removal of benign neoplasms and during the cryodestruction of malignant tumors. In the first case, freezing can extend beyond the neoplasm by 2-3 mm, in the second - by 10 30 mm. The number of freeze-thaw cycles is important for high-quality cryo-effects. To achieve the desired result when removing benign neoplasms, one cycle is sufficient, while 2-3 such cycles are necessary when removing malignant neoplasms [33 – 35].

Results of clinical application of the device

62 patients (43 women, 19 men) aged 19 to 67 were under observation - patients with chronic skin diseases, including rosacea (acne pink), acne vulgaris (acne) and patchy alopecia, as well as 36 patients (24 women, 12 men) aged 23 to 69 years with complaints about the presence of cosmetic skin defects (post-acne, facial skin wrinkles). In the course of treatment, all patients were divided into 2 groups: the first (comparative) - 49 people who received standardized therapy for dermatoses or cosmetic skin defects, and the second (main) - 49 people who used a cryomassage method in a complex therapy using the upgraded thermoelectric device for the treatment of skin diseases. Clinical application of the upgraded thermoelectric device in the complex therapy of dermatoses was carried out on the basis of the Department of Dermatovenereology of the Higher State Educational Institution of Ukraine "Bukovinian State Medical University." Examples of clinical application of the thermoelectric device are given below.

Rosacea (pink acne). Among the patients examined, 26 were diagnosed with rosacea (pink acne). Rosacea (pink acne) is a chronic dermatosis with polyfactor etiopathogenesis, which occurs as a result of a

number of external factors (alimentary, meteo- and occupational factors, excessive proliferation of demodex mites) against endogenous mechanisms of the development of dermatoses (hormonal, microcirculatory, immune, metabolic disorders etc). Dermatosis is localized on the skin of the face, is manifested by redness (erythema), dilatation of superficial vessels (telangiectasia), small densely packed nodules (papules), pustules, and occasionally nodules (rinofima). According to the well-known classification [36, 37], in 14 patients, the stage (form) of rosacea was erythematous-papulo-pustularosis, in the remaining 12 patients - the erythematous-papulosis stage (form) of dermatosis. All patients were prescribed standard therapy of dermatoses, which included systemic and external (topical) actions, and in the combination therapy of 13 patients (the main group) - additionally used the method of cryomassage using a thermoelectric device: 6 patients with erythematous and papular stage (form) of dermatosis - from the first days of treatment, and 7 patients with erythematous-papulo-pustular stage (form) - only after recurrence of pustular rashes (on 6-8 days after the start of treatment).

Cryomassage sessions were prescribed to patients with rosacea of the main group for 30-40 seconds, 2-3 times in each field (with a total exposure - up to 10 minutes) daily - for 5 days and every other day for the next 10-12 days (total for the course - 10- 12 procedures).

To assess the dermatological status of patients with rosacea before and after their treatment, the diagnostic assessment scale for rosacea (DASR) was used, which included the sum of points of severity of clinical manifestations of dermatoses: erythema (0 - no erythema, 1 - light, 2 - moderate, 3 - expressive erythema); determination of the number of papules and pustules (0 - up to 10 elements, 1 - from 11 to 20, 2 - from 21 to 30, 3 - more than 30 elements); presence of telangiectasia (0 - absence; 1 - occupy less than 10% of the face; 2 - from 11% to 30%; 3 - more than 30%); skin dryness and peeling (0 - no dryness, 1 - weak, 2 - moderate with slight peeling, 3 - strong with distinct peeling); burning sensation and tingling (0 - lack of, 1 - light, 2 - moderate, 3 - strong); presence of edema of the face (0 - absent, 1 - weak, 2 - moderate, 3 - expressive) [38].

The statistical processing of the obtained research results was performed using the licensed Microsoft Excel and STATISTICA 6.0 software packages of StatSoft Inc, using Student's t-test to assess the probability of difference in the indicators which was considered probable at $p < 0.05$. In order to evaluate the relationship between the indicators, a non-parametric Friedman dispersion analysis was used with the definition of χ-square (χ^2), the dependence between the indicators was considered probable if the value of the χ-square exceeded the critical one [39].

The dynamics of the regression of elements of the rash in patients of rosacea of various groups - comparative (received standardized treatment) and the main one, which in the complex therapy additionally used cryomassage sessions using a thermoelectric device, is presented in Table 2 and in the form of photo illustrations in Fig.2.

According to the results of the research (Table 2), the positive dynamics of clinical manifestations of rosacea after treatment was noted in patients of both groups, however, a more significant decrease in the DASR indicator was determined in patients of the main group as compared to its initial values before treatment (2.43 times, $p < 0.001$, including: in patients with erythematous-telangiective stage of dermatosis – 2.31 times, $p = 0.005$, with papulo-pustular stage – 2.50 times, $p = 0.001$), and with respect to the values of the SHDOR indicator after treatment in patients of a comparative group (1.66 times, $p = 0.004$, including: in patients with erythematous-telangiectal stage of dermatosis - 1.56 times, $p = 0.017$, with the papulo-pustular stage - 1.72 times, $p = 0.013$)

Table 2

Dynamics of clinical manifestations of rosacea in patients of different groups *

The value of DASR in patients with different stages of rosacea		Patients with rosacea (n=26)		Probability of difference of indicators
		I (comparative group) (n_1=13)	II (main group (n_2=13)	
Patients with erythematous-telangiectal stage (n_1=6, n_2=6)	Before treatment	5.83 ± 0.54	6.17 ± 0.87	p_{1-2} = 0.75
	After treatment	4.17 ± 0.31	2.67 ± 0.42	p_{1-2} = 0.017
	P	*P* = 0.024	*P* = 0.005	
Patients with papulo-pustular stage (n_1=7, n_2=7)	Before treatment	9.71 ± 0.99	10.01 ± 1.31	p_{1-2} = 0.86
	After treatment	6.86 ± 0.80	4.00 ± 0.58	p_{1-2} = 0.013
	P	*P* = 0.045	*P* = 0.001	
Average value of the indicator in the group (n_1=13, n_2=13)	Before treatment	7.92 ± 0.79	8.23 ± 0.96	p_{1-2} = 0.81
	After treatment	5.62 ± 0.58	3.38 ± 0.41	p_{1-2} = 0.004
	P	*P* = 0.028	*P* < 0.001	

*Note. P_{1-2} - probability of difference of indicators in patients of different groups; P - probability of the difference before and after treatment.

a) *b)*

Fig.2 Patient K., 49 years old. Diagnosis: Rosacea, erythematous-papular stage (form), to (a) and after the course of treatment (b) with the use of cryomassage (the disappearance of the majority of venous lakes, decrease in size or recurrence of papular rashes).

Acne vulgaris (acne). Among the examined patients acne vulgaris was diagnosed in 25 people. Acne vulgaris (acne) is a multifactorial chronic skin disease whose etiological factor is certain microorganisms (Propionibacterium acnes, Staphylococcus epidermidis and other cocci) that develop on the background of neuroendocrinal, immune, metabolic disorders, and the like. Dermatosis is localized on the skin of the face, shoulders and trunk, manifested by comedones, inflammatory nodules (papular acne), pustules (pustular acne), nodules (indurative, conglobate acne). By degree of severity distinguish mild forms of acne, moderate severity and severe forms of dermatosis [37]. Of the 25 examine patients with acne, 21 were diagnosed with acne of moderate severity, and 4 - with acute forms of acne. All patients were prescribed standard therapy for dermatosis, which included systemic and external effects, and for 12 patients (the main group), of which 10 were diagnosed

acne vulgaris of moderate severity, 2 – with acute forms of acne, a cryomassage method using thermoelectric device was additionally applied (Fig. 3).

Fig. 3. Patient N., 19 years. Diagnosis: Acne vulgaris (acne), of moderate severity.

Sessions of cryomassage to patients with common acne were prescribed after regressing pustular acne for 30-40 sec 3-4 times in each field (with a total exposure of up to 10 min) daily for 5-8 days and the next 10-12 days every day (total course - 11-14 procedures). According to the analysis of the dynamics of the regression of elements of the rash, probably the best results of treatment were observed in patients with acne vulgaris from the main group, who were assessed 3 months after the end of the course of treatment (Fig. 4).

a) *b)*

Fig. 4. Patient S., 4 years. Diagnosis: Acne vulgaris (acne), of moderate severity before (a) and 3 months after treatment (b).

Thus, among 12 patients with acne of the main group, the state of clinical recovery or mild manifestations of acne was observed in 9 people, moderate in 3 patients (in the comparison group, respectively, in 4 and 9). When performing non-parametric Friedman dispersion analysis, it was established that between the number of patients with achieving clinical recovery or mild acne and the number of patients with moderate acne 3 months after standard treatment and combination therapy using cryo massage by thermoelectric device there is a statistically significant dependence (calculated value $\chi^2 = 4.89$ for its critical value - 3.84).

Patchy alopecia (circular, circumscribed) was diagnosed in 11 patients. Dermatosis has polyfactor etiopathogenesis and usually occurs after acute infectious diseases, stresses, intoxications and other

influences in the context of concomitant, often combined, pathology of internal organs, chronic foci of focal infection, metabolic disorders, etc. Treatment of this disease involves complex examination of the patient and correction of the detected comorbidity. The method of cryomassage has long been an important component of the treatment of this dermatosis. In the course of treatment, patients were divided into two groups: 5 patients (comparison group) who received standardized dermatologic therapy; for the other 6 patients (main group), the cryomassage method was used in the complex therapy using a modernized thermoelectric device for the treatment of skin diseases.

Cryomassage sessions for patients with patchy alopecia were prescribed for 40-50 seconds in 2-3 stages for 5 minutes daily (15-20 procedures in total). One month after the completion of the treatment, a repeated course of cryomassage was prescribed according to the same scheme. It was established that in the patients of the main group, complete hair overgrowth of alopecia cells occurred on average 1.5-2 months earlier than in the patients from the comparison group. The results of treatment of a patient with focal alopecia after 5 months of complex therapy are presented in Fig.5.

a) *b)*

Fig. 5. Patient N., 28 years. Diagnosis: patchy alopecia of the hair part of the head before (a) and 5 months after treatment (b).

Treatment of post-acne (cryomassagey in cosmetology). Patients with post-acne complaints (19 people) were also monitored. Post-acne is a symptom complex that develops after resolution (spontaneous or as a result of treatment) of acne rash elements and includes: secondary spots of vascular (pink, purple) and pigment (hyper-, depigmented) character, hypotrophic scars, enlarged pores of the skin. Correction of such deficiencies is carried out in a complex way and involves a combination of methods with positive (mesotherapy, biorevitalization) and negative (chemical peelings of various depths, microdermabrasion, laser skin resurfacing, scar subcision) stimulation. In the course of treatment, patients were divided into two groups: the first (comparative) - 9 people who were prescribed a course of cosmetic procedures with 5 sessions with positive and 5 sessions with negative stimulation, and 10 (main group), which, in addition to the specified set of procedures, used the method cryomassage using the upgraded thermoelectric instrument for treatment of skin diseases.

Sessions of cryomassage to patients in the main group were prescribed for 30-50 seconds 3-4 times for each field - forehead, cheeks, chin (for a total exposure - up to 10 minutes) daily - within 5-8 days and the next day for the next 10-12 days (total for the course - 11-14 procedures). It was found that in patients of the main group, the complete correction of post-acne elements (regression of stains, leveling of skin relief, narrowing of pores) occurred on average by 1-1.5 months faster than in patients from the comparison group. Results of treatment of a patient with post-acne after 3 months of integrated therapy with the use of the upgraded thermoelectric device are presented in Fig. 6.

a) *b)*

Fig. 6 Patient Yu, 28 years old. Reduced depth of atrophic scars, narrowing of pores, regression of venous lakes before (a) and after cryomassage (b).

Treatment (correction) of age-related changes in the face skin (cryomassage in cosmetology).

Age-related changes in the skin of the face associated with broken trophism, lymph drainage system, slowing metabolic processes, etc., are manifested primarily by the presence of facial skin swelling, edema in the area of the eyelids, small static wrinkles in the face, decreased elasticity and tone of the skin. Under supervision were 17 patients with these complaints. In the course of treatment, patients were divided into two groups: the first (comparative) - 9 persons, who were prescribed a course of mesotherapy with lymphatic drainage, peptide components, non-reticulated hyaluronic acid, vitamins of 5-10 sessions performed weekly, and 8 subjects (main group), in which the proposed course included cryomassage with the use of the upgraded thermoelectric device for the treatment of skin diseases.

Sessions of cryomassage patients were prescribed for 40-50 seconds 3-4 times for each field (for a total exposure - up to 10 minutes) three times a week for 5-7 weeks (only for the course - 15-20 procedures). A more significant improvement of the skin quality parameters (improvement of turgor, elasticity, decrease in the depth of static wrinkles, edema of the periorbital area and general pastosity) was established in the patients of the main group.

The results of cryomassage using the upgraded thermoelectric device to the patient with complaints of reduced skin tone of the face and nasolabial wrinkles of the skin are shown in Fig.7.

a) *b)*

Fig.7 Patient M., 54 years old. Reducing the depth of nasolabial folds and facial swelling before (a) and after the course of cryomassage (b).

So, as evidenced by the results of using the upgraded thermoelectric device for treatment of skin diseases in cosmetology, the use of a hardware cryomassage method with the possibility of controlled cooling of problem areas of the skin significantly increases the efficiency of correcting cosmetic skin defects, in particular post-acne, and such age-related changes of the skin as static wrinkles, a decrease in turgor and elasticity, as well as swelling and edema of the skin, predominate in the deformation-edematous type skin.

It is important to note that all patients have tolerated the hardware cryomassage method using the upgraded thermoelectric device well, without side effects or complications.

Conclusion

1. It is confirmed that the upgraded thermoelectric device for treatment of skin diseases provides the opportunity to conduct cryomassage in the complex treatment of chronic dermatoses and cosmetic skin defects with the ability to accurately control the temperature of cooling the local area of patient's skin.
2. Clinical efficiency and safety of using the upgraded thermoelectric device in dermatology is established for treatment of the following skin diseases: acne rosacea, acne vulgaris, patchy allopecia (circumscribed, circular), as well as in cosmetology for correction of cosmetic skin defects (post-acne, wrinkles of the face skin), which makes it possible to significantly improve the efficiency of treatment of such patients.

References

1. Hryshchenko V.I., Sandomyrskyi B.P., Kolontai Yu.Yu. (1987). *Prakticheskaia kriomeditsina*
2. *[Practical cryomedicine]*. Kyiv: Zdorovie [in Russian].
3. Zadorozhnyi B.A. (1985). *Krioterapiia v dermatologii (Biblioteka practicheskogo vracha). [Cryotherapy in dermatology (Library of practicing physician)]*. Kyiv: Zdorovie [in Russian].
4. Burenina I.A. (2014). Sovremennyie metodiki krioterapii v klinicheskoi praktike [Modern cryotherapy methods in clinical practice]. *Vestnik sovremennoi klinicheskoi meditsiny – Bulletin of Modern Clinical Medicine*, 7, 1, 57 – 61 [in Russian]
5. Mashkilleison A.L. (2000). *Lecheniie kozhnykh boleznei [Treatment of skin diseases]*. Moscow: Kron-Pres [in Russian].
6. Zemskov V.S., Gasanov L.I. (1988). *Nizkiie temperatury v meditsine [Low temperatures in medicine]*. Kyiv: Naukova dumka [in Russian].
7. Albrova V.K. (1968*). Lecheniie borodavok, vesnushek s keloidnykh rubtsov zhidkim azotom. V knige: Voprosy vrachebnoi kosmetiki [Treatment of warts, freckles, keloid scars with liquid nitrogen. In: Medical cosmetcs issues]*. Moscow: Medicine [in Russian].
8. Rozentul M.A. (1964). *Spravochnik po kosmetike [Handbook on cosmetics]*. Moscow: Medicine [in Russian].
9. Klymyshina S.O., Tsysnetska A.V., Rachkevych L.V. (2009). Farmatsevtychna kosmetologiia: Posibnyk [Pharmaceutical cosmetology: Manual]. Ternopil: Volia [in Ukrainian].
10. Anatychuk L.I. (1979). *Termoelementy i termoelektricheskiie ustroistva [Thermoelements and thermoelectric devices]*. Kyiv: Naukova dumka [in Russian].
11. Anatychuk L.I. (2003). *Termoelektrichestvo. T.2. Termoelektricheskiie preobrazovateli energii [Thermoelectricity. Vol.2. Thermoelectric power converters]*. Kyiv, Chernivtsi: Institute of Thermoelectricity [in Russian].

12. Kolenko E.A. (1967). *Termoelektricheskiie okhlazhdaiushchiie pribory [Thermoelectric cooling devices]*. Leningrad: Nauka [in Russian].
13. Anatychuk L.I., Kobylianskyi R.R., Mocherniuk Yu.M. (2009). Thermoelectric device for skin treatment. *J.Thermoelectricty*, 4, 90-96.
14. Anatychuk L.I., Denisenko O.I., Kobylianskyi R.R., Kadeniuk T.Ya. (2015). On the use of thermoelectric cooling in dermatology and cosmetology. *J.Thermoelectricity*, 3, Anatychuk L.I. (1979). *Termoelementy i termoelektricheskiie ustroistva [Thermoelements and thermoelectric devices]*. Kyiv: Naukova dumka [in Russian].
15. Anatychuk L.I., Vikhor L.M., Kobylianskyi R.R., Kadeniuk T.Ya. (2017). Computer simulation and optimization of the dynamic operating modes of thermoelectric device for treatment of skin diseases. *J.Thermoelectricity,* 2, 44-57.
16. Anatychuk L., Vikhor L., Kotsur M., Kobylianskyi R., Kadeniuk T. (2018). Optimal control of time dependence of temperature in thermoelectric devices for medical purposes. *International Journal of Thermophysics*, 39:108. https://doi.org/10.1007/s10765-018-2430-z.
17. Kobylianskyi R.R., Kadeniuk T.Ya. (2016). Pro perspektyvy vykorystannia termoelektryky dlia likuvannia zakhvoriuvan shkiry kholodom [On the prospects of using thermoelectricity for treatment of skin diseases with cold]. *Naukovy visnyk Chernivetskoho Universitetu: Zbirnyk naukovykh prats. Fizyka. Elektronika – Scientific Herald of Chernivtsi University: Collection of Scientific Papers. Physics. Electronics*, 5, 1, 67-72 [in Ukrainian].
18. Anatychuk L.I., Denisenko O.I., Kobylianskyi R.R., Kadeniuk T.Ya., Perepichka M.P. (2017). Suchasni metody kriovpluvu u dermatologichnii practytsi [Modern cryotherapy methods in dermatology practice]. *Klinichna ta eksperymentalna patologia – Clinical and Experimental Pathology,* XVI, 1(59), 150 –156 [in Ukrainian].
19. Anatychuk L.I., Kobylianskyi R.R., Kadeniuk T.Ya. (2017). Computer simulation of local thermal effect on human skin. *J.Thermoelectricity*, 1, 69-79.
20. Anatychuk L.I., Vikhor L.M., Kobylianskyi R.R., Kadeniuk T.Ya. (2017). Kompiuterne modeliuvannia lokalnoho temperaturnoho vplyvu na shkiru liudyny u dynamichnomu rezhymi [Computer simulation of local temperature effect on human skin in dynamic mode]. *Visnyk Natsionalnoho Universytetu "Lvivska Polytechnika" (fizyko-matematychni nauky) – Herald of National University "Lvivska Politechnica" (physico-mathematical sciences)*, 4, CTP. ?. (In Ukrainian).
21. Kobylianskyi R.R., Bezpalchuk O.O., Vyhonnyi V.Yu. (2018). Pro zastosuvannia termoelektrychnoho okholodzhennia u kosmetolohii [On the use of thermoelectric cooling in cosmetology]. *Fizyka i Khimiia Tverdoho Tila – Physics and Chemistry of the Solid State*, 19, CTP?
22. Anatychuk L.I., Kobylianskyi R.R. (2018). Computer simulation of the unsteady temperature effect on human skin. *J.Thermoelectricity*, 2, CTP ?
23. *Patent of Ukraine № 104682.* (2016). Anatychuk L.I., Kobylianskyi R.R., Kadeniuk T.Ya. Thermoelectric device for treatment of skin diseases [in Ukrainian].
24. *Patent of Ukraine № 106790.* (2016). Anatychuk L.I., Kobylianskyi R.R., Kadeniuk T.Ya. Thermoelectric device for treatment of skin diseases [in Ukrainian].
25. *Patent of Ukraine № 107918.* (2016). Anatychuk L.I., Denisenko O.I., Kobylianskyi R.R., Kadeniuk T.Ya. Method for complex treatment of psoriasis in stationary and regressive stage [in Ukrainian] .
26. Patent of Ukraine № 107922. (2016). Anatychuk L.I., Denisenko O.I., Kobylianskyi R.R., Kadeniuk T.Ya.Method for complex treatment of acne rosacea [in Ukrainian].

27. Patent of Ukraine № 108563. (2016). Anatychuk L.I., Denisenko O.I., Kobylianskyi R.R., Kadeniuk T.Ya.Method for complex treatment of acne vulgaris [in Ukrainian].
28. Patent of Ukraine № 108580. (2016). Anatychuk L.I., Denisenko O.I., Kobylianskyi R.R., Kadeniuk T.Ya. Method for complex treatment of limited forms of neurodermatitis [in Ukrainian].
29. Patent of Ukraine № 108581. (2016). Anatychuk L.I., Denisenko O.I., Kobylianskyi R.R., Kadeniuk T.Ya.Method for complex treatment of prurigo [in Ukrainian].
30. Patent of Ukraine № 108582. (2016). Anatychuk L.I., Denisenko O.I., Kobylianskyi R.R., Kadeniuk T.Ya. Method for complex treatment of verrucose forms of lichen ruber planus [in Ukrainian].
31. *Dermatologiia, venerologiia. Uchebnik [Dermatology, venerology. Textbook]*. Stepanenko V.I. (Ed). (2012). Kyiv: KIM [in Ukrainian].
32. Butova Yu.S., Skripkina Yu.K., Ivanova O.L. (2013). *Dermatovenerologiia. Natsionalnoie rukovodstvo. Kratkoie izdanie. [Dermatovenerology. National manual. Brief edition]*. Moscow: GEOTAR-Media [in Russian].
33. Chebotarev V.V., Tamrazova O.B., Chebotareva N.V., Odinets A.V. (2013). *Dermatovenerologiia: uchebnik dlia studentov vuzov [Deramatovenerology: textbook for students of higher educational institutions]* [in Russian].
34. Korpan N. N. (2001). *Basics of cryosurgery*. Wien : Springer – Veriag.
35. Mourot L. Cluzeau C., Regnard J. (2007). Hyperbaric gaseous cryotherapy: effects on skin temperature and systemic vasoconstriction. *Archives of physical medicine and rehabilitation, November* 2007, 1339 – 1343.
36. Pasquali P. (2015). *Cryosurgery: a practical manual*. Heidelberg: Springer.
37. Adaskevich V.P. (2004*).* *Diagnosticheskiie indeksy v dermatologii [Diagnostic indices in dermatology]*. Moscow: Med.Kniga [in Russian].
38. Bolotnaya L.A. (2017). Topicheskii metronidazole v kompleksnom lechenii rosacea [Topical metrodinazole in complex treatment of rosacea]. Ukrainskyi zhurnal dermatologii, venerologii, cosmetologii – Ukrainian Journal of Dermatology, Venerology, Cosmetology, 4(67), 34-41 [in Russian].
39. Lapach S.N., Chubenko A.V., Babich P.N. (2002). *Osnovnyie printsipy primeneniia statisticheskikh metodov v klinicheskikh ispytaniiakh [Basic principles of using statistical methods in clinical tests]*. Kyiv: Morion [in Russian].

Submitted 28.06.2018

Анатичук Л.І. *ак. НАН України*,[1,2]
Денисенко О.І. *доктор мед. наук, професор*[3],
Шуленіна О.В. *канд. мед. наук*[3],
Микитюк О.П. *канд. мед. наук*[3],
Кобилянський Р.Р. *канд. фіз.-мат. наук*[1,2]

[1]Інститут термоелектрики НАН і МОН України,
вул. Науки, 1, Чернівці, 58029, Україна;
[2]Чернівецький національний університет
ім. Юрія Федьковича, вул. Коцюбинського 2,
Чернівці, 58000, Україна, *e-mail: anatych@gmail.com*;
[3]Вищий державний навчальний заклад України
"Буковинський державний медичний університет",
Театральна площа, 2, Чернівці, 58002, Україна

РЕЗУЛЬТАТИ КЛІНІЧНОГО ЗАСТОСУВАННЯ ТЕРМОЕЛЕКТИРИЧНОГО ПРИЛАДУ ДЛЯ ЛІКУВАННЯ ЗАХВОРЮВАНЬ ШКІРИ

У роботі наведено конструкцію та технічні характеристики модернізованого термоелектричного приладу для лікування захворювань шкіри. Проаналізовано механізм дії та методику проведення температурного впливу на поверхню шкіри людини. Представлено результати клінічного застосування термоелектричного приладу у медичній практиці, зокрема у дерматології та косметології. Бібл. 39, рис. 7, табл. 2.
Ключові слова: термоелектричне охолодження, дерматологія, косметологія.

Анатычук Л.И. *ак. НАН Украины*,[1,2]
Денисенко О.И. *доктор мед. наук, професор*[3],
Шуленина О.В. *канд. мед. наук*[3],
Микитюк О.П. *канд. мед. наук*[3],
Кобылянський Р.Р. *канд. физ.-мат. наук*[1,2]

[1]Институт термоэлектричества НАН и МОН Украины,
вул. Науки, 1, Черновцы, 58029, Украина;
[2]Чернивецький национальный университет
им. Юрия Федьковича, ул. Коцюбинского 2,
Черновцы, 58000, Украина, *e-mail: anatych@gmail.com*;
[3]Вищий государственное учебное заведение Украины
"Буковинский государственный медицинский университет»,
Театральная площадь, 2, Черновцы, 58002, Украина

РЕЗУЛЬТАТЫ КЛИНИЧЕСКОГО ПРИМЕНЕНИЯ ТЕРМОЭЛЕКТРИЧЕСКОГО ПРИБОРА ДЛЯ ЛЕЧЕНИЯ ЗАБОЛЕВАНИЙ КОЖИ

В работе описаны конструкция и технические характеристики модернизированного термоэлектрического прибора для лечения заболеваний кожи. Проанализирован механизм действия и методика осуществления температурного воздействия на поверхность кожи человека. Представлены результаты клинического приложения термоэлектрического прибора в медицинской практике, в частности в дерматологии и косметологии. Библ. 39, рис. 7, табл. 2.
Ключевые слова: термоэлектрическое охлаждение, дерматология, косметология.

References

1. Hryshchenko V.I., Sandomyrskyi B.P., Kolontai Yu.Yu. (1987). *Prakticheskaia kriomeditsina*
2. *[Practical cryomedicine]*. Kyiv: Zdorovie [in Russian].
3. Zadorozhnyi B.A. (1985). *Krioterapiia v dermatologii (Biblioteka practicheskogo vracha). [Cryotherapy in dermatology (Library of practicing physician)]*. Kyiv: Zdorovie [in Russian].
4. Burenina I.A. (2014). Sovremennyie metodiki krioterapii v klinicheskoi praktike [Modern cryotherapy methods in clinical practice]. *Vestnik sovremennoi klinicheskoi meditsiny – Bulletin of Modern Clinical Medicine*, 7, 1, 57 – 61 [in Russian]

5. Mashkilleison A.L. (2000). *Lecheniie kozhnykh boleznei [Treatment of skin diseases]*. Moscow: Kron-Pres [in Russian].
6. Zemskov V.S., Gasanov L.I. (1988). *Nizkiie temperatury v meditsine [Low temperatures in medicine]*. Kyiv: Naukova dumka [in Russian].
7. Albrova V.K. (1968*). Lecheniie borodavok, vesnushek s keloidnykh rubtsov zhidkim azotom. V knige: Voprosy vrachebnoi kosmetiki [Treatment of warts, freckles, keloid scars with liquid nitrogen. In: Medical cosmetcs issues]*. Moscow: Medicine [in Russian].
8. Rozentul M.A. (1964). *Spravochnik po kosmetike [Handbook on cosmetics]*. Moscow: Medicine [in Russian].
9. Klymyshina S.O., Tsysnetska A.V., Rachkevych L.V. (2009). Farmatsevtychna kosmetologiia: Posibnyk [Pharmaceutical cosmetology: Manual]. Ternopil: Volia [in Ukrainian].
10. Anatychuk L.I. (1979). *Termoelementy i termoelektricheskiie ustroistva [Thermoelements and thermoelectric devices]*. Kyiv: Naukova dumka [in Russian].
11. Anatychuk L.I. (2003). *Termoelektrichestvo. T.2. Termoelektricheskiie preobrazovateli energii [Thermoelectricity. Vol.2. Thermoelectric power converters]*. Kyiv, Chernivtsi: Institute of Thermoelectricity [in Russian].
12. Kolenko E.A. (1967). *Termoelektricheskiie okhlazhdaiushchiie pribory [Thermoelectric cooling devices]*. Leningrad: Nauka [in Russian].
13. Anatychuk L.I., Kobylianskyi R.R., Mocherniuk Yu.M. (2009). Thermoelectric device for skin treatment. *J.Thermoelectricty*, 4, 90-96.
14. Anatychuk L.I., Denisenko O.I., Kobylianskyi R.R., Kadeniuk T.Ya. (2015). On the use of thermoelectric cooling in dermatology and cosmetology. *J.Thermoelectricity*, 3, Anatychuk L.I. (1979). *Termoelementy i termoelektricheskiie ustroistva [Thermoelements and thermoelectric devices]*. Kyiv: Naukova dumka [in Russian].
15. Anatychuk L.I., Vikhor L.M., Kobylianskyi R.R., Kadeniuk T.Ya. (2017). Computer simulation and optimization of the dynamic operating modes of thermoelectric device for treatment of skin diseases. *J.Thermoelectricity,* 2, 44-57.
16. Anatychuk L., Vikhor L., Kotsur M., Kobylianskyi R., Kadeniuk T. (2018). Optimal control of time dependence of temperature in thermoelectric devices for medical purposes. *International Journal of Thermophysics*, 39:108. https://doi.org/10.1007/s10765-018-2430-z.
17. Kobylianskyi R.R., Kadeniuk T.Ya. (2016). Pro perspektyvy vykorystannia termoelektryky dlia likuvannia zakhvoriuvan shkiry kholodom [On the prospects of using thermoelectricity for treatment of skin diseases with cold]. *Naukovy visnyk Chernivetskoho Universitetu: Zbirnyk naukovykh prats. Fizyka. Elektronika – Scientific Herald of Chernivtsi University: Collection of Scientific Papers. Physics. Electronics*, 5, 1, 67-72 [in Ukrainian].
18. Anatychuk L.I., Denisenko O.I., Kobylianskyi R.R., Kadeniuk T.Ya., Perepichka M.P. (2017). Suchasni metody kriovpluvu u dermatologichnii practytsi [Modern cryotherapy methods in dermatology practice]. *Klinichna ta eksperymentalna patologia – Clinical and Experimental Pathology,* XVI, 1(59), 150 –156 [in Ukrainian].
19. Anatychuk L.I., Kobylianskyi R.R., Kadeniuk T.Ya. (2017). Computer simulation of local thermal effect on human skin. *J.Thermoelectricity*, 1, 69-79.
20. Anatychuk L.I., Vikhor L.M., Kobylianskyi R.R., Kadeniuk T.Ya. (2017). Kompiuterne modeliuvannia lokalnoho temperaturnoho vplyvu na shkiru liudyny u dynamichnomu rezhymi [Computer simulation of local temperature effect on human skin in dynamic mode]. *Visnyk Natsionalnoho Universytetu "Lvivska Polytechnika" (fizyko-matematychni nauky) – Herald of National University "Lvivska Politechnica" (physico-mathematical sciences)*, 4, (In Ukrainian).

21. Kobylianskyi R.R., Bezpalchuk O.O., Vyhonnyi V.Yu. (2018). Pro zastosuvannia termoelektrychnoho okholodzhennia u kosmetolohii [On the use of thermoelectric cooling in cosmetology]. *Fizyka i Khimiia Tverdoho Tila – Physics and Chemistry of the Solid State*, 19, CTP?
22. Anatychuk L.I., Kobylianskyi R.R. (2018). Computer simulation of the unsteady temperature effect on human skin. *J.Thermoelectricity*, 2, CTP ?
23. *Patent of Ukraine № 104682*. (2016). Anatychuk L.I., Kobylianskyi R.R., Kadeniuk T.Ya. Thermoelectric device for treatment of skin diseases [in Ukrainian].
24. *Patent of Ukraine № 106790*. (2016). Anatychuk L.I., Kobylianskyi R.R., Kadeniuk T.Ya. Thermoelectric device for treatment of skin diseases [in Ukrainian].
25. *Patent of Ukraine № 107918*. (2016). Anatychuk L.I., Denisenko O.I., Kobylianskyi R.R., Kadeniuk T.Ya. Method for complex treatment of psoriasis in stationary and regressive stage [in Ukrainian] .
26. Patent of Ukraine № 107922. (2016). Anatychuk L.I., Denisenko O.I., Kobylianskyi R.R., Kadeniuk T.Ya.Method for complex treatment of acne rosacea [in Ukrainian].
27. Patent of Ukraine № 108563. (2016). Anatychuk L.I., Denisenko O.I., Kobylianskyi R.R., Kadeniuk T.Ya.Method for complex treatment of acne vulgaris [in Ukrainian].
28. Patent of Ukraine № 108580. (2016). Anatychuk L.I., Denisenko O.I., Kobylianskyi R.R., Kadeniuk T.Ya. Method for complex treatment of limited forms of neurodermatitis [in Ukrainian].
29. Patent of Ukraine № 108581. (2016). Anatychuk L.I., Denisenko O.I., Kobylianskyi R.R., Kadeniuk T.Ya.Method for complex treatment of prurigo [in Ukrainian].
30. Patent of Ukraine № 108582. (2016). Anatychuk L.I., Denisenko O.I., Kobylianskyi R.R., Kadeniuk T.Ya. Method for complex treatment of verrucose forms of lichen ruber planus [in Ukrainian].
31. *Dermatologiia, venerologiia. Uchebnik [Dermatology, venerology. Textbook]*. Stepanenko V.I. (Ed). (2012). Kyiv: KIM [in Ukrainian].
32. Butova Yu.S., Skripkina Yu.K., Ivanova O.L. (2013). *Dermatovenerologiia. Natsionalnoie rukovodstvo. Kratkoie izdanie. [Dermatovenerology. National manual. Brief edition]*. Moscow: GEOTAR-Media [in Russian].
33. Chebotarev V.V., Tamrazova O.B., Chebotareva N.V., Odinets A.V. (2013). *Dermatovenerologiia: uchebnik dlia studentov vuzov [Deramatovenerology: textbook for students of higher educational institutions]* [in Russian].
34. Korpan N. N. (2001). *Basics of cryosurgery*. Wien : Springer – Veriag.
35. Mourot L. Cluzeau C., Regnard J. (2007). Hyperbaric gaseous cryotherapy: effects on skin temperature and systemic vasoconstriction. *Archives of physical medicine and rehabilitation, November* 2007, 1339 – 1343.
36. Pasquali P. (2015). *Cryosurgery: a practical manual*. Heidelberg: Springer.
37. Adaskevich V.P. (2004*). Diagnosticheskiie indeksy v dermatologii [Diagnostic indices in dermatology]*. Moscow: Med.Kniga [in Russian].
38. Bolotnaya L.A. (2017). Topicheskii metronidazole v kompleksnom lechenii rosacea [Topical metrodinazole in complex treatment of rosacea]. Ukrainskyi zhurnal dermatologii, venerologii, cosmetologii – Ukrainian Journal of Dermatology, Venerology, Cosmetology, 4(67), 34-41 [in Russian].
39. Lapach S.N., Chubenko A.V., Babich P.N. (2002). *Osnovnyie printsipy primeneniia statisticheskikh metodov v klinicheskikh ispytaniiakh [Basic principles of using statistical methods in clinical tests]*. Kyiv: Morion [in Russian].

Submitted 28.06.2018


L.I. Anatychuk

L.I. Anatychuk *acad. National Academy of Sciences of Ukraine*[1,2], **M.V. Maksimuk**[1]

[1]Institute of Thermoelectricity of the NAS and MES of Ukraine, 1 Nauky str., Chernivtsi, 58029, Ukraine;
[2]Yu. Fedkovych Chernivtsi National University, 2, Kotsyubinsky str., Chernivtsi, 58012, Ukraine;
e-mail: anatych@gmail.com


M.V.Maksimuk

EFFICENCY OF STARTING PREHEATERS WITH THERMOELECTRIC POWER SOURCES

This paper presents the results of research on the thermodynamic features of systems for start heating of the internal combustion engine, with thermoelectric generators as sources of electrical power. The physical models of the "starting preheater - thermogenerator" systems are considered and their energy characteristics are evaluated. On the basis of the calculations, the most effective variants of using thermoelectric power sources for start preparation of vehicle engines for operation are determined.. Bibl. 15, Fig. 3.

Key words: starting preheater, thermoelectric generator, physical model.

Introduction

To overcome the difficulties associated with the operation of vehicles at low temperatures, various facilities of thermal start preparation of internal combustion engines are increasingly being used [1, 2]. The most effective among such facilities are starting preheaters - flame sources of heat that are powered by motor vehicles and carry out heating of the engine coolant. In addition to a reliable start of the internal combustion engine, the use of preheaters creates conditions for saving an average of about 90-150 liters of fuel per season, reduces exhaust emissions by up to 5 times during engine warming up and allows you to increase the engine service life by 200-300 km per start when warming up from temperature (-20 ÷ -30) ° C [3, 4].

The determining factor limiting the possibility of mass use of starting preheaters is the discharge of the battery during the operation of the pre-start equipment [5].

One of the promising methods for solving the problem of discharge of batteries during the thermal preparation of motor vehicles for start-up is the use of thermoelectric generators as sources of electrical power for starting preheaters [6 – 11].

Creation of such a system for start heating of engines poses a number of tasks, which consist in the search for a rational scheme of using starting pre-heaters with thermoelectric power sources, both in terms of their energy characteristics and taking into account its cost indicators.

The purpose of this work is to analyze models of starting preheaters with thermoelectric power sources and determine the most effective option for using thermoelectric generators in systems of start heating of vehicle engines.

Physical models and thermodynamic peculiarities of starting preheaters with thermoelectric power sources

We first introduce the efficiency η for "starting preheater-thermoelectric generator" system as the ratio of the obtained useful energy to the spent thermal energy Q. Useful energy will be considered the obtained

thermal energy Q, which is directly used for start heating of the engine, and electrical energy W, which is necessary for the functioning of the system:

$$\eta = \frac{Q' + \sum_i W_i}{Q}, \tag{1}$$

where W_i are power consumers of electrical energy system.

The consumed thermal energy of the system is assumed to be equal to the total thermal energy of the burners of the starting preheater and the thermoelectric generator (TEG):

$$Q = Q_1 + Q_2, \tag{2}$$

where Q_1 and Q_2 are thermal energies of the burners of starting preheater and thermogenerator which can be expressed by the following relations:

$$Q_1 = \eta_{A1} \cdot A \cdot m_1 \tag{3}$$

$$Q_2 = \eta_{A2} \cdot A \cdot m_2 \tag{4}$$

where ηA1, ηA2 are the efficiencies of burners of starting preheater and TEG; A is the calorific value of the fuel, which is used to operate the system; m1, m2 is the fuel consumption of starting preheater and thermogenerator, respectively.

Variants of using thermoelectric generators for preheating the engines can be reduced to the three main physical models, which are listed below.

Physical model of "starting preheater- thermoelectric generator" system with individual heat sources.

Fig.1 shows a physical model of engine start heating system which comprises liquid starting preheater and thermoelectric generator, the heat supply to which is carried out individually, with the use of separate heat sources.

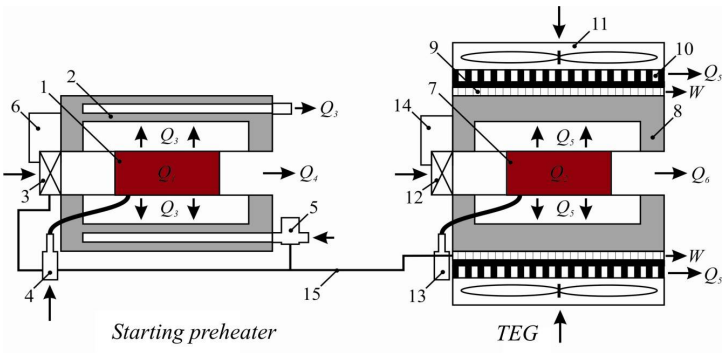

Fig.1 – Physical model of "starting preheater—thermoelectric generator" system with individual heat sources: 1 – starting preheater burner; 2 – heat exchanger; 3 – starting preheater air fan; 4 – starting preheater fuel pump; 5 – circulation pump; 6 – starting preheater electronic unit; 7 –thermogenerator burner; 8 – hot heat exchanger; 9 – thermopile; 10 – air radiator; 11 – fan for heat removal; 12 – thermogenerator air fan; 13 – thermogenerator fuel pump; 14 – thermogenerator electronic unit; 15 – electrical switching facilities.

Liquid starting preheater consists of heat source 1 which is in the internal space of heat exchanger 2. A flame burner is used as a heat source, to which air and fuel are supplied by fan 3 and pump 4. In the heat exchanger of the heater, channels are made in which the heat carrier heats up, after which, by pumping with the circulation pump 5, it flows to the car engine. The starting and operation control of starting preheater components (air fan, fuel pump, circulation pump) is carried out by the electronic unit 6.

The thermoelectric generator contains an individual flame burner 7, a hot heat exchanger 8 for supplying heat to the thermopile 9 and a heat removal system, which consists of air radiators 10 and fans 11.

The supply of fuel and air to the heat source of the thermal generator is carried out by the fan 12 and the fuel pump 13. To stabilize the output voltage of the thermogenerator and control its operation, an electronic unit 14 is provided in the TEG model.

The thermoelectric generator works as follows. Thermal energy resulting from the combustion of fuel heats the hot heat exchanger, passes through a thermopile and is discharged into the environment. Due to the temperature difference between the hot and cold sides of the thermopile, an electric current is generated that is used to power the preheater.

Thus, the system in question provides the starting heater with the necessary electrical energy, practically without using a battery. At the same time, such a system can also perform additional functions, in particular, a thermogenerator can be used as an additional source of electrical energy on a vehicle. This energy can be directed, if necessary, to charge the battery or other energy supply needs, for example, to power various additional electrical devices - anti-theft tools for long-term work, laptops, TV sets, communication systems, and a refrigerator for storing products, when the engine is not running.

Consider the energy performance of such a system. The heat energy Q_1 and Q_2, which is produced for its operation, is provided by a starting preheater burner and a thermoelectric generator burner. Part of heat Q_1 is used to heat the circulating fluid Q_3,, the other part Q_4 is delivered by combustion products into surrounding space. A similar heat distribution takes place also in a thermoelectric generator, namely, the heat Q_5 from the burner 7 through the thermopiles 9 is transferred to the air radiators 10 and is discharged into the environment by the fans 11. Another part of heat Q_6 is discharged from the heat generator by combustion products.

Therefore, total thermal energy of system Q is equal to:

$$Q = Q_1 + Q_2 = Q_3 + Q_4 + Q_5 + Q_6 \tag{5}$$

The electrical energy W, produced by a thermoelectric generator, is used to supply pumps 4, 5, 13 and fans 3, 11, 12. Then, the relation (1) for this system will be written as:

$$\eta = \frac{Q_3 + W}{Q_1 + Q_2}, \tag{6}$$

We will evaluate the efficiency for the above system using the example of a Webasto Thermo Top EVO liquid starting preheater (gasoline version, A = 44 MJ / kg) with a thermal power Q_3 = 4 kW and fuel consumption m_1 = 0.56 l / h [12].

The initial electric power of the thermogenerator is assumed to be W = 50 W: 35 W - to power the components of the starting preheater [12] and 15 W for the power supply of the pumps and fans of the TEG [13].

The value of thermal energy Q_2 can be estimated by the following relation:

$$\eta_{TEG} = \frac{W}{Q_2}, \tag{7}$$

where η_{TEG} is the efficiency of thermoelectric generator.

If we take into account that the maximum efficiency of modern TEG, where single-stage modules based on bismuth telluride are applied, is 3.5% [14], it is necessary to spend approximately Q_2 = 1.4 kW of heat to provide the set initial electric power.

Thus, substituting the calculated values of heat and electric power into equation (6), we obtain that the efficiency of the "starting preheater - thermoelectric generator" system with individual heat sources is ~ 60%.

Physical model of "starting preheater-thermoelectric generator" system with individual heat sources and a common hydraulic circuit.

As compared to the previous system, this system combines starting preheater and thermoelectric generator by a single hydraulic circuit (Fig.2). In this connection, in thermogenerator cooling system, air

radiators and fans for the removal of heat from the thermopile are replaced by liquid heat exchangers 10 in which heat carrier circulates.

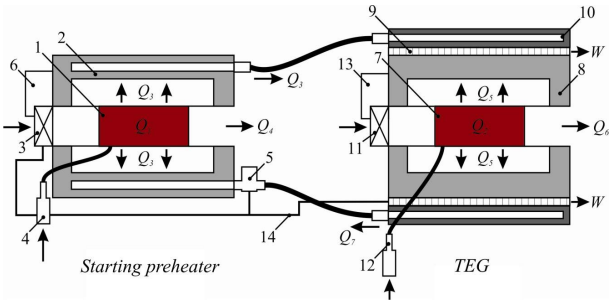

Fig.2 – Physical model of "starting preheater-thermoelectric generator" system with individual heat sources and a common hydraulic circuit: 1 – starting preheater burner; 2 – heat exchanger; 3 – starting preheater air fan; 4 – starting preheater fuel pump; 5 – circulation pump; 6 – starting preheater electronic unit; 7 – thermogenerator burner; 8 – hot heat exchanger; 9 – thermopile; 10 – cold liquid heat exchanger; 11 – thermogenerator air fan; 12 – thermogenerator fuel pump; 13 – thermogenerator electronic unit; 14 – electrical switching facilities

Since the heat flow Q7, which is removed from the thermopile, is spent on heating the heat carrier, this system allows the engine to be preheated both with a starting preheater and using a thermoelectric generator. Therefore, the expression (1) for the efficiency of the system will be rewritten as follows:

$$\eta = \frac{Q_3 + Q_7 + W}{Q_1 + Q_2}, \tag{8}$$

where useful heat Q_7 can be found from the equality of heat fluxes of TEG:

$$Q_2 = W + Q_7 + Q_6 \tag{9}$$

Using the previously found values of electric power W and thermal power Q2 and taking into account that the amount of heat Q6 that is lost with combustion products in thermoelectric generator designs is 25% on average of the thermal power Q2 [15], we find the value of the thermal energy Q7 (Q7 = 1 kW) spent on heating the heat carrier and the approximate efficiency of this system (η ~ 75%).

Physical model of "thermoelectric generator-starting preheater" system with a common heat source.

Physical model of a system (Fig.3) with a common heat source comprises hot heat exchanger 1 with burner 2 arranged in its internal space. Fuel and air delivery to the burner is done by fan 3 and fuel pump 4. On the external surface of the hot heat exchanger there is a thermopile 5 the heat from which is removed by heating fluid circulating in the cold heat exchangers 6 due to pumping by liquid pump 7. Start-up and operation of the heater is carried out by the electronic unit 8.

Thus, in the above system, the thermoelectric generator and the starting preheater are combined into a single structure, which allows to obtain electrical energy and to warm up the engine with a single heat flow Q. In this case, part of the heat Q_1 is removed by the combustion products into the environment, and the heat Q_2, in the form of thermal Q_3, and electric power W, is used to warm up the engine and power the components of the heater, as well as, if necessary, to recharge the battery during start heating:

$$\begin{cases} Q = Q_1 + Q_2 \\ Q_2 = W + Q_3 \end{cases} \tag{10}$$

Therefore, the efficiency of "thermoelectric generator-starting preheater" system with a common heat source can be estimated by the following relationship:

$$\eta = W + Q_3 / Q \tag{11}$$

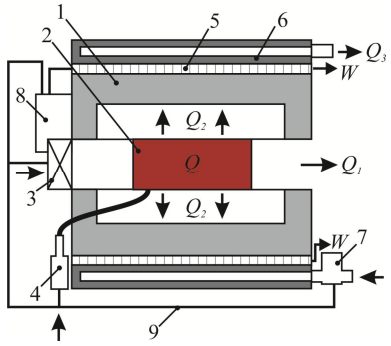

Fig.3 – Physical model of system "starting preheater-thermoelectric generator" with a common heat source: 1 – starting preheater burner; 2 – hot heat exchanger; 3 – starting preheater air fan; 4 – starting preheater fuel pump; 5 – thermopile; 6 – cold liquid heat exchanger; 7 – starting preheater circulation pump; 8 – electronic unit; 9 – electrical switching facilities.

Using the known values of the electrical and thermal characteristics of the Webasto Thermo Top EVO starting preheater (Q = 5.3 kW, W = 50 W), taking into account an approximate estimate of Q_1 ($Q_1 = 0.25Q$ = 1.3 kW), we determine that the efficiency of this engine start heating system is 75 %.

Thus, the highest values of efficiency are typical for "thermoelectric generator starting preheater" system with a common heat source and a system in which starting preheater and TEG are combined by a hydraulic circuit. Obviously, a system with a common heat source is cheaper, making it more efficient to use. However, this question requires separate studies, which will be presented in subsequent works.

Conclusion

1. Three variants of physical models of starting preheaters with thermoelectric power sources were considered. It has been established that the most rational for start heating of internal combustion engines is “starting preheater-thermoelectric generator" system with a common heat source and a system that combines starting preheater and thermogenerator with one hydraulic circuit. The use of such systems yields the highest total thermal and electrical efficiency of 75 %.
2. It is shown that the efficiency of the system with individual sources of heat is 60 %, therefore its application is less effective. However, such a system has several advantages, namely the possibility of using a thermoelectric generator as a standby power source in a car.

References

1. Kuznetsov E.S., Boldin A.P., Vlasov V.M. et al. (2001). *Tekhnicheskaia ekspluatatsiia avtomobilei: Uchebnik dlia vuzov. 4 izdaniie, pererabotannoie i dopolnennoie [Technical operation of cars: Textbook for high schools. 4th ed., revised and enlarged]*. Moscow: Nauka [in Russian].
2. Reznik L.G., Romalis G.M., Charkov S.T. (1989). *Efektivnost ispolzovaniia avtomobilei v razlichnykh usloviiakh ekspluatatsii [Efficiency of using automobiles in different operating conditions]*. Moscow: Transport [in Russian].
3. Matiukhin L.M. (2010). *Teplotekhnicheskiie ustroistva avtomobilei [Heat engineering devices of automobiles]*. Moscow: MADI [in Russian].
4. Naiman V.S. (2007). *Vse o predpuskovykh obogrevateliakh i otopiteliakh [All about starting preheaters]*. Moscow: ACT [in Russian].
5. Mykhailovsky V.Ya., Maksimuk M.V. (2014). Automobile operating conditions at low temperatures. The necessity of applying heaters and the rationality of using thermal generators for their work. *J.Thermoelectricity*, 3, 20-31.
6. *Patent of Ukraine № 102303* (2013). Anatychuk L.I., Mykhailovsky V.Ya. Thermoelectric power supply for automobile [in Ukrainian].
7. *Patent of Ukraine №72304* (2012). Anatychuk L.I., Mykhailovsky V.Ya. Automobile heater with thermoelectric power supply [in Ukrainian].
8. *Patent of Ukraine №124999* (2017). Maksimuk M.V. Automobile heater with thermoelectric power supply [in Ukrainian].

9. *Patent of US6527548B1* (2003). Aleksandr S. Kushch, Daniel Allen. Self powered electric generating space heater.
10. *Patent of US0115968A1* (2010). Jorn Budde, Jeans Baade, Michael Stelter. Heating apparatus comprising a thermoelectric device.
11. *Patent of Russia* 2268393 (2006). Prilepo Yu.P. A device to facilitate the start of internal combustion engine [in Russian].
12. Retrieved from: http://www.webasto.com//
13. *Patent of Ukraine №54900* (2010). Mykhailovsky V.Ya., Strutynska L.T., Gischuk V.S. Portable thermoelectric generator [in Ukrainian].
14. Anatychuk L.I., Mykhailovsky V.Ya. (2008). Two-sectional thermoelectric generator on gas fuel. *J. Thermoelectricity*, 1, 76-86.
15. Mykhailovsky Vilius Yaroslavovich. (2007). Termoelektrychni generatory na organichnomu palyvi [Thermoelectric generators on organic fuel]. *Doctor's thesis (Phys-Math)*. Chernivtsi [in Ukrainian].

Submitted 20.06.2018

Анатичук Л.І. *ак. НАН України*,[1,2], **Максимук М.В.**[1]

[1]Інститут термоелектрики НАН і МОН України,
вул. Науки, 1, Чернівці, 58029, Україна;
[2]Чернівецький національний університет
ім. Юрія Федьковича, вул. Коцюбинського 2,
Чернівці, 58000, Україна, *e-mail: anatych@gmail.com*

ЕФЕКТИВНІСТЬ ПЕРЕДПУСКОВИХ НАГРІВНИКІВ З ТЕРМОЕЛЕКТРИЧНИМИ ДЖЕРЕЛАМИ ЕЛЕКТРИКИ

Наведено результати досліджень термодинамічних особливостей систем передпускового розігріву двигуна внутрішнього згорання, в яких джерелами електричної енергії є термоелектричні генератори. Розглянуто фізичні моделі систем «передпусковий нагрівник–термогенератор» та проведено оцінку їхніх енергетичних характеристик. На основі проведених розрахунків визначено найефективніші варіанти застосування термоелектричних джерел електрики для передпускової підготовки двигунів транспортних засобів до експлуатації. Бібл.15, рис.3.
Ключові слова: передпусковий нагрівник, термоелектричний генератор, фізична модель.

Анатычук Л.И. *ак. НАН Украины*,[1,2], **Максимук М.В.**[1]

[1]Институт термоэлектричества НАН и МОН Украины, ул. Науки, 1,
Черновцы, 58029, Украина, *e-mail: anatych@gmail.com*;
[2]Черновицкий национальный университет им. Ю. Федьковича,
ул. Коцюбинского, 2, Черновцы, 58012, Украина,
e-mail: anatych@gmail.com

ЭФФЕКТИВНОСТЬ ПРЕДПУСКОВЫХ НАГРЕВАТЕЛЕЙС ТЕРМОЭЛЕКТРИЧЕСКИМИ ИСТОЧНИКАМИ ЭЛЕКТРИЧЕСТВА

Приведены результаты исследований термодинамических особенностей систем предпускового разогрева двигателя внутреннего сгорания, в которых источниками электрической энергии являются термоэлектрические генераторы. Рассмотрены физические модели систем «предпусковой нагреватель – термогенератор» и проведена оценка их энергетических характеристик. На основе проведенных расчетов определенно самые эффективные варианты приложения термоэлектрических источников электричества для предпусковой подготовки двигателей транспортных средств к эксплуатации. Библ.15, рис.3.
Ключевые слова: предпусковой нагреватель, термоэлектрический генератор, физическая модель.

References

1. Kuznetsov E.S., Boldin A.P., Vlasov V.M. et al. (2001). *Tekhnicheskaia ekspluatatsiia avtomobilei: Uchebnik dlia vuzov. 4 izdaniie, pererabotannoie i dopolnennoie [Technical operation of cars: Textbook for high schools. 4th ed., revised and enlarged]*. Moscow: Nauka [in Russian].
2. Reznik L.G., Romalis G.M., Charkov S.T. (1989). *Efektivnost ispolzovaniia avtomobilei v razlichnykh usloviiakh ekspluatatsii [Efficiency of using automobiles in different operating conditions]*. Moscow: Transport [in Russian].
3. Matiukhin L.M. (2010). *Teplotekhnicheskiie ustroistva avtomobilei [Heat engineering devices of automobiles]*. Moscow: MADI [in Russian].
4. Naiman V.S. (2007). *Vse o predpuskovykh obogrevateliakh i otopiteliakh [All about starting preheaters]*. Moscow: ACT [in Russian].
5. Mykhailovsky V.Ya., Maksimuk M.V. (2014). Automobile operating conditions at low temperatures. The necessity of applying heaters and the rationality of using thermal generators for their work. *J.Thermoelectricity*, 3, 20-31.
6. *Patent of Ukraine № 102303* (2013). Anatychuk L.I., Mykhailovsky V.Ya. Thermoelectric power supply for automobile [in Ukrainian].
7. *Patent of Ukraine №72304* (2012). Anatychuk L.I., Mykhailovsky V.Ya. Automobile heater with thermoelectric power supply [in Ukrainian].
8. *Patent of Ukraine №124999* (2017). Maksimuk M.V. Automobile heater with thermoelectric power supply [in Ukrainian].
9. *Patent of US6527548B1* (2003). Aleksandr S. Kushch, Daniel Allen. Self powered electric generating space heater.
10. *Patent of US0115968A1* (2010). Jorn Budde, Jeans Baade, Michael Stelter. Heating apparatus comprising a thermoelectric device.
11. *Patent of Russia* 2268393 (2006). Prilepo Yu.P. A device to facilitate the start of internal combustion engine [in Russian].
12. Retrieved from: http://www.webasto.com//
13. *Patent of Ukraine №54900* (2010). Mykhailovsky V.Ya., Strutynska L.T., Gischuk V.S. Portable thermoelectric generator [in Ukrainian].
14. Anatychuk L.I., Mykhailovsky V.Ya. (2008). Two-sectional thermoelectric generator on gas fuel. *J. Thermoelectricity*, 1, 76-86.
15. Mykhailovsky Vilius Yaroslavovich. (2007). Termoelektrychni generatory na organichnomu palyvi [Thermoelectric generators on organic fuel]. *Doctor's thesis (Phys-Math)*. Chernivtsi [in Ukrainian].

Submitted 20.06.2018

O.V.Nitsovych

O.V.Nitsovych[1,2], *Cand. Phys.-math. science*

[1]Institute of Thermoelectricity of the NAS and MES of Ukraine,
1 Nauky str., Chernivtsi, 58029, Ukraine,
e-mail: anatych@gmail.com;
[2]Yuriy Fedkovych Chernivtsi National University,
2 Kotsiubynsky str.,
Chernivtsi, 58012, Ukraine *e-mail: anatych@gmail.com*

RESEARCH ON THE CONDITIONS OF FORMING A FLAT CRYSTALLIZATION FRONT WHEN GROWING Bi_2Te_3 BASED THERMOELECTRIC MATERIAL BY VERTICAL ZONE MELTING METHOD

This paper presents the results of computer research on Bi_2Te_3 based thermoelectric materials grown by vertical zone melting method. The optimal height of the furnace and its temperature whereby the crystallization front will be as flat as possible, contributing to the formation of a single crystal, is determined. It is shown that simulation of such processes makes it possible to reduce considerably material costs and research time, while ensuring growth of crystals of the required quality. Bibl. 3, Fig. 7.

Key words: bismuth telluride, crystallization front, simulation.

Introduction

The unique properties of thermoelectricity ensure its wide application in telecommunications, optoelectronic, military and automotive equipment, microelectronics, space, everyday life, and medicine. Thus, according to experts, the number of used thermoelectric modules from 2020 will exceed 20 million units. The increase in thermoelectric applications is accompanied by an increase in the number of companies that employ thermoelectric generators and coolers in their products.

Creation of high-quality thermoelectric devices is possible only with the presence of appropriate materials possessing the necessary physical and mechanical properties, which depend on their chemical composition, purity, structural perfection, as well as the technology of their growing and processing.

Much attention is paid to the improvement of methods for producing Bi_2Te_3 based thermoelectric materials (TEM) due to the fact that there is practically no alternative to these materials in the manufacture of thermoelectric converters for the temperature range 200 to 400 K. The vertical zone melting method is one of the most common industrial methods of growing single crystals of Bi_2Te_3 –Sb_2Te_3 and Bi_2 Te_3 –Bi_2 Se_3 solid solutions. When TEM is obtained by this method, the curvature of the crystallization front, which is the main technological characteristic of growth, has a great influence on the stability of single-crystal growth and its homogeneity [1 – 2].

The crystallization front shape, which can be convex to the liquid phase, flat or concave to the solid phase, is determined by the magnitude of the radial and axial temperature gradients in the crystal during growth. The most favorable for growing single crystals with a small number of structural defects is a flat crystallization front, since on the convex to the melt or concave to the crystal crystallization front random

crystalline nuclei (impurity nuclei) will grow together with the main crystallization front, and on a flat crystallization front they will be pushed back to the periphery and degenerate (Fig. 1).

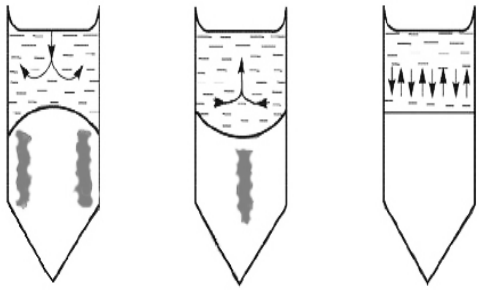

Fig. 1. Distribution of impurities in the crystal relative to crystallization front shape

So, it is relevant to simulate the process of TEM growth, which allows investigating the dependence of the crystallization front shape on the technological parameters of vertical zone melting while significantly reducing material costs and research time, ensuring the growth of crystals of the required quality.

The purpose of this work is to simulate the process of growing Bi_2Te_3 based thermoelectric materials using the method of vertical zone melting, as well as to analyze the influence of TEM growth conditions on the formation of a flat crystallization front in order to obtain a material with a uniform structure and composition.

Physical model of vertical zone melting process

Physical model of the process of growing Bi_2Te_3 based single crystals by vertical zone melting is represented in Fig.2.

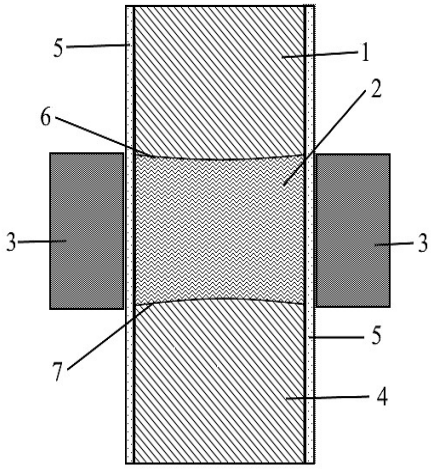

Fig.2. Physical model of installation for growing TEM by vertical zone melting method:
1 – material in solid phase (polycrystal), 2 –material in liquid phase (melt zone),
3- heaters, 4 – material in solid phase (single crystal), 5 – quartz ampoule,
6 – melting front boundary, 7 –crystallization front boundary.

The figure depicts a fragment of an ingot comprising polycrystalline material 1, a molten zone 2, and a single crystal 4. The ingot is placed in a quartz ampoule 5. Using a heater 3, a molten zone 2 is formed that moves together with the heater along the sample to provide melting of the polycrystal and crystallization of the melt below the boundary 7, which is called the crystallization front.

Mathematical and computer description of the model

When modeling the heat conduction process in a homogeneous medium with a phase transition in the COMSOL Multiphysics software package, the classical system of nonstationary differential heat conduction equations is solved, supplemented by the dependences of the physical properties of the solid under study as a function of the phase state at a given point at a specified temperature:

$$\rho C_p \frac{\partial t}{\partial t} + \rho C_p u \nabla T + \nabla q = Q \tag{1}$$

$$q = -\kappa \nabla T, \tag{2}$$

$$\rho = \theta \rho_{phase1} + (1-\theta)\rho_{phase2}, \tag{3}$$

$$C_p = \frac{1}{2}\left(\theta \rho_{phase1} C_{p\,phase1} + (1-\theta)\rho_{phase2} C_{p\,phase2}\right) + L\frac{d\alpha_m}{dT}, \tag{4}$$

$$\alpha_m = \frac{1}{2} \cdot \frac{(1-\theta)\rho_{phase2} - \theta\rho_{phase1}}{\theta\rho_{phase1} + (1-\theta)\rho_{phase2}}, \tag{5}$$

$$\kappa = \theta\kappa_{phase1} + (1-\theta)\kappa_{phase2}. \tag{6}$$

where ρ is the density; C_p is the heat capacity of material at constant pressure; κ is thermal conductivity; u is the velocity of the medium, in the problem under study is equal to zero; T is temperature; t is time; θ is phase ratio at a given temperature; α_m is mass ratio between phases; L is latent heat of phase transition; Q is external heat flux. The indices *phase*1 and *phase*2 indicate to which phase, solid or liquid, respectively, the properties are related.

Equations (1) are solved with the following boundary conditions:
thermally insulated heater

$$-n \cdot (-\kappa \nabla T) = 0 \tag{7}$$

heat exchange with the environment

$$-n \cdot (-\kappa \nabla T) = \varepsilon\sigma(T_1^4 - T^4) \tag{8}$$

ε is the coefficient of surface radiation (emissivity factor of the medium), T_1 is the temperature of the body surface (ampoules), T is the temperature of the medium, σ is the Stefan-Boltzmann constant, n is the normal vector to the heater face.

To construct a computer model, we set the geometric dimensions of the quartz ampoule in which the material is grown, the temperature dependences of the parameters of the polycrystalline material and the melt (the coefficient of thermal conductivity *κ(T)*, the heat capacity *C(T),* density *ρ(T)*), as well as the melting point of TEM and the phase transition heat *L*.

The model allows in a wide range to change the geometric and temperature parameters of the growth installation, as well as the characteristics of the material in the solid and molten states.

Results of computer simulation of the process of growing Bi_2Te_3 based thermoelectric material by vertical zone melting

The process of growing the synthesized material Bi_2Te_3-Sb_2Te_3, in a quartz ampoule, with a wall thickness of 3 mm, an ingot length of 250 mm, diameter d = 24 mm, was considered. The temperature of the heater varied within 680-950 ° C, height from 24 to 96 mm.

The dependence of the crystallization front shape on the width of the molten zone (height of the heater *h*) at different temperatures was investigated.

The computer model of the vertical zone melting process and the appearance of the crystallization front are shown in Fig.3.

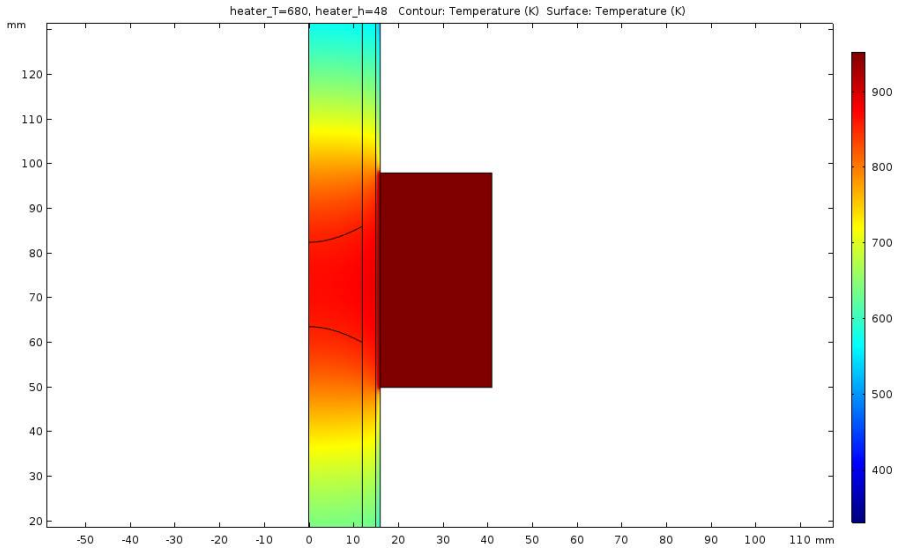

Fig. 3. Computer model and schematic of crystallization front in the process of vertical zone melting with the furnace height h=48mm, T= 680°C.

As is known [3], the crystallization front is an indicator of the thermal conditions that are created during the growing process. The crystallization front shape is determined by the kinetic and thermal conditions of the vertical zone melting process and characterizes the structure of the crystal grown. The coefficients of the distribution of impurities in the crystal and its mechanical properties depend on the crystallization front shape. Therefore, one of the most important tasks in obtaining crystals by the method of vertical zone melting is to maintain the optimal front shape throughout the entire process of growing TEM.

The results of simulation according to the described program showed that when growing, for example, an ingot with a diameter d = 24 mm with a heater height h = 24 mm (the height of the heater is equal to the diameter of the grown crystal $h = 1d$), the temperature at which the flat crystallization front is formed corresponds to the value T = 860 °C (Fig.4).

The crystallization front shape at a height of the heater from 2d to 4d for different temperatures is shown in Figs. 5 – 7.

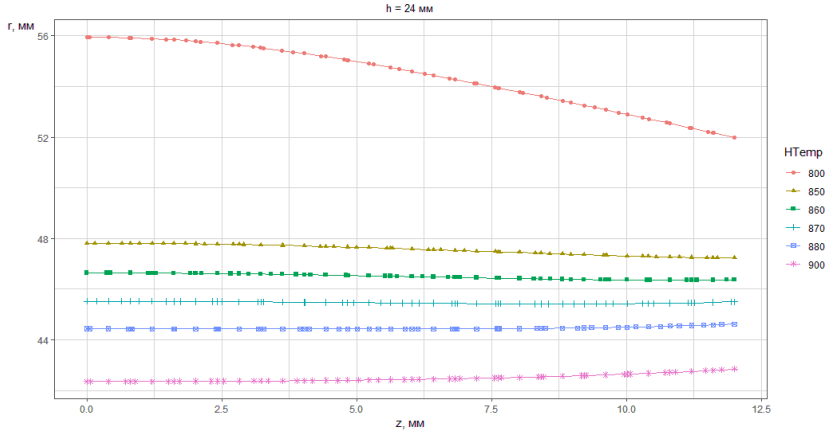

Fig. 4. Crystallization front shape with the furnace height h=1d for different temperatures.

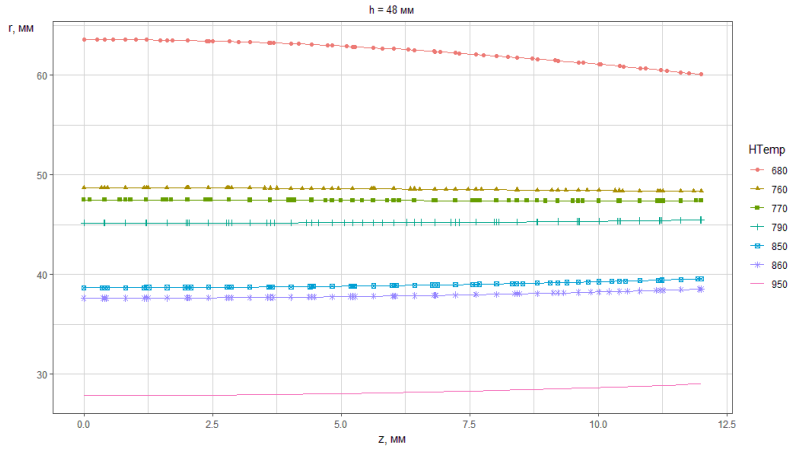

Fig. 5.Crystallization front shape with the furnace height h=2d for different temperatures.

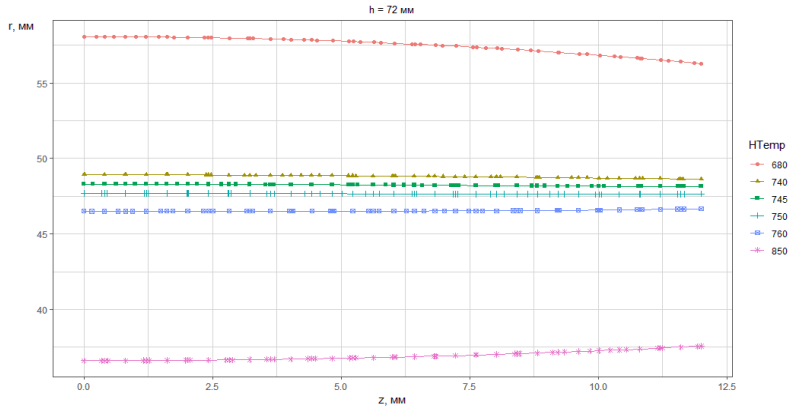

Fig. 6. Crystallization front shape with the furnace height h=3d for different temperatures.

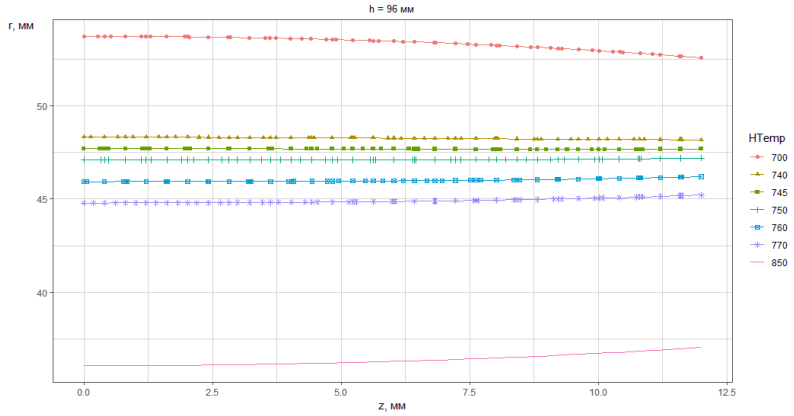

Fig. 7. Crystallization front shape with the furnace height h=4d for different temperatures.

As can be seen from the figures, with the increase in the height of the furnace, for a given temperature, the crystallization front is aligned. One can also notice that for h = 3d and 4d, the crystallization front is flat at the same heater temperatures from 745° C to 750° C, which are optimal for the growth of a given material, and conclude that h = 3d is the optimal heater parameter.

Conclusion

It is shown that the developed computer model of the vertical zone melting process makes it possible to investigate the crystallization front shape, which is the main technological characteristic of growth, as well as to determine the optimal growing conditions for multicomponent thermoelectric materials.

The crystallization front shape in the wide limits of the change in the geometric and temperature parameters of the heater is studied. It is determined that homogeneous monocrystal structures can be obtained at a height of the heater equal to three diameters of the grown ingot h = 3d and an optimum temperature of 745 – 750° C.

References

1. Goltsman B.M., Kudinov V.A., Smirnov I.A. (1972). *Poluprovodnikovyie termoelektricheskiie materialy na osnove Bi_2Te_3 [Semiconductor thermoelectric materials based on Bi_2Te_3]*. B.Ya.Moizhes (Ed.). Moscow: Nauka [in Russian].
2. Anatychuk L.I. (1979). *Termoelementy i termoelektricheskiie ustroistva [Thermoelements and thermoelectric devices]*. Kyiv: Naukova Dumka [in Russian].
3. Vilke K.T. (1977). *Metody vyrashchivaniia kristallov [Methods of crystal growth]*. Leningrad: Nedra [in Russian].

Submitted 19.07.2018

Ніцович О.В. *канд. фіз.-мат. наук*[1,2]

[1]Інститут термоелектрики НАН і МОН України,
вул. Науки, 1, Чернівці, 58029, Україна;
[2]Чернівецький національний університет
ім. Юрія Федьковича, вул. Коцюбинського 2,
Чернівці, 58000, Україна, *e-mail: anatych@gmail.com*;

ДОСЛІДЖЕННЯ УМОВ ФОРМУВАННЯ ПЛОСКОГО ФРОНТУ КРИСТАЛІЗАЦІЇ ПРИ ВИРОЩУВАННІ ТЕРМОЕЛЕКТРИЧНОГО МАТЕРІАЛУ НА ОСНОВІ Bi_2Te_3 МЕТОДОМ ВЕРТИКАЛЬНОЇ ЗОННОЇ ПЛАВКИ

У роботі представлено результати комп'ютерних досліджень термоелектричних матеріалів на основі Bi_2Te_3, вирощених методом вертикальної зонної плавки. Визначено оптимальну висоту пічки і її температуру, при яких фронт кристалізації буде максимально плоским, що сприяє формуванню монокристала. Показано, що моделювання таких процесів дає можливість суттєво знизити матеріальні витрати і час досліджень, при цьому забезпечивши вирощування кристалів необхідної якості. Бібл. 3, рис. 7.

Ключові слова: телурид вісмуту, фронт кристалізації, моделювання.

Ницович О.В. *канд. фіз.-мат. наук*[1,2]

[1]Институт термоэлектричества НАН и МОН Украины, ул. Науки, 1,
Черновцы, 58029, Украина, *e-mail: anatych@gmail.com*;
[2]Черновицкий национальный университет им. Ю. Федьковича,
ул. Коцюбинского, 2, Черновцы, 58012, Украина, *e-mail: anatych@gmail.com*

ИССЛЕДОВАНИЕ УСЛОВИЙ ФОРМИРОВАНИЯ ПЛОСКОГО ФРОНТА КРИСТАЛЛИЗАЦИИ ПРИ ВЫРАЩИВАНИИ ТЕРМОЭЛЕКТРИЧЕСКОГО МАТЕРИАЛА НА ОСНОВЕ Bi_2Te_3 МЕТОДОМ ВЕРТИКАЛЬНОЙ ЗОННОЙ ПЛАВКИ

В работе представлены результаты компьютерных исследований термоэлектрических материалов на основе Bi_2Te_3, выращенных методом вертикальной зонной плавки. Определенно оптимальную высоту печи и ее температуру, при которых фронт кристаллизации будет максимально плоским, что способствует формированию монокристалла. Показано, что моделирование таких процессов дает возможность существенно снизить материальные расходы и время исследований, при этом обеспечив выращивание кристаллов необходимого качества. Библ. 3, рис. 7.

Ключевые слова: теллурид висмута, фронт кристаллизации, моделирование.

References

1. Goltsman B.M., Kudinov V.A., Smirnov I.A. (1972). *Poluprovodnikovyie termoelektricheskiie materialy na osnove Bi_2Te_3 [Semiconductor thermoelectric materials based on Bi_2Te_3]*. B.Ya.Moizhes (Ed.). Moscow: Nauka [in Russian].
2. Anatychuk L.I. (1979). *Termoelementy i termoelektricheskiie ustroistva [Thermoelements and thermoelectric devices]*. Kyiv: Naukova Dumka [in Russian].
3. Vilke K.T. (1977). *Metody vyrashchivaniia kristallov [Methods of crystal growth]*. Leningrad: Nedra [in Russian].

Submitted 19.07.2018

L.I. Anatychuk, *acad. National Academy of Sciences of Ukraine*[1,2],
V.V. Lysko, *cand. Phys.-math. sciences*[1,2]
M.V. Havryliuk, V.A. Tiumentsev

Institute of Thermoelectricity of the NAS and MES of Ukraine,
1, Nauky str, Chernivtsi, 58029, Ukraine; *e-mail: anatych@gmail.com,*
[2]Yu.Fedkovych Chernivtsi National University, 2, Kotsiubynskyi str.,
Chernivtsi, 58000, Ukraine*, e-mail: anatych@gmail.com*

AUTOMATION AND COMPUTERIZATION OF MEASUREMENTS OF THERMOELECTRIC PARAMETERS OF MATERIALS

The results of development of the automation system for measuring the thermoelectric properties of materials and their data processing are presented. The measurement control unit is based on a multichannel analog-to-digital converter. Measurement process control, processing and display of results are carried out using a computer to which the measurement unit is connected via a standard USB channel. The results are displayed as graphs and tables. The developed automation system is universal and allows realizing both classic stationary methods of measuring thermoelectric properties of materials and complex measurement algorithms with increased speed. An example of using the developed system to determine the thermoelectric properties of a material by the complex absolute method is given. Bibl. 9, Fig. 5.
Key words: electrical conductivity, thermoEMF, thermal conductivity, thermoelectric material, automation, computerization.

Introduction

General characterization of the problem.

It is known that success in thermoelectricity to a large extent depends on the quality of thermoelectric material, which is determined by the figure of merit of material Z and which governs the efficiency of thermoelectric power converters, namely generator efficiency, maximum temperature difference and coefficient of performance of coolers, heating coefficient of heaters [1, 2]. To improve the figure of merit Z, experimental methods for optimizing materials are used, in which the correct measurement of their parameters plays a decisive role [3].

One of the best for determining the quality of materials is a complex absolute method. It has important advantages:

- measurement of electrical conductivity σ, thermoEMF α and thermal conductivity κ is carried out simultaneously on the same sample which reduces errors in determining the figure of merit Z;
- thermoelectric parameters are found from classical formulae without applying corrections;
- the method allows minimizing various errors.

In [4-8], the results of comprehensive studies conducted at the Institute of Thermoelectricity of the National Academy of Sciences of Ukraine and Ministry of Education and Science of Ukraine aimed at developing methods to minimize the errors of the absolute method are presented. The result of these studies is creation of measuring equipment, the accuracy of which in determining the figure of merit is 3-5 times higher than the accuracy of measurement using other methods.

In [9], methods are also given for increasing the speed with the use of the absolute method by applying alternating current pulses to accelerate the achievement of steady-state conditions in the samples

under study, as well as programmed forced heating of the sample and thermostat. The implementation of these complex algorithms requires complete automation of the measurement process. In addition, it will eliminate possible human errors when measuring electrical signals, processing them to determine σ, α, κ, Z, when building graphs and tables that determine the dependence of these parameters on the concentration of impurities, the composition and structure of the material and other factors.

Therefore, *the purpose* of the work was to create a computerized measurement control system for automation of the processes of determining thermoelectric properties, processing and displaying their results.

Requirements to automation of measurements

The scheme of the complex absolute method, taken as a basis for the creation of automated equipment, is shown in Fig. 1

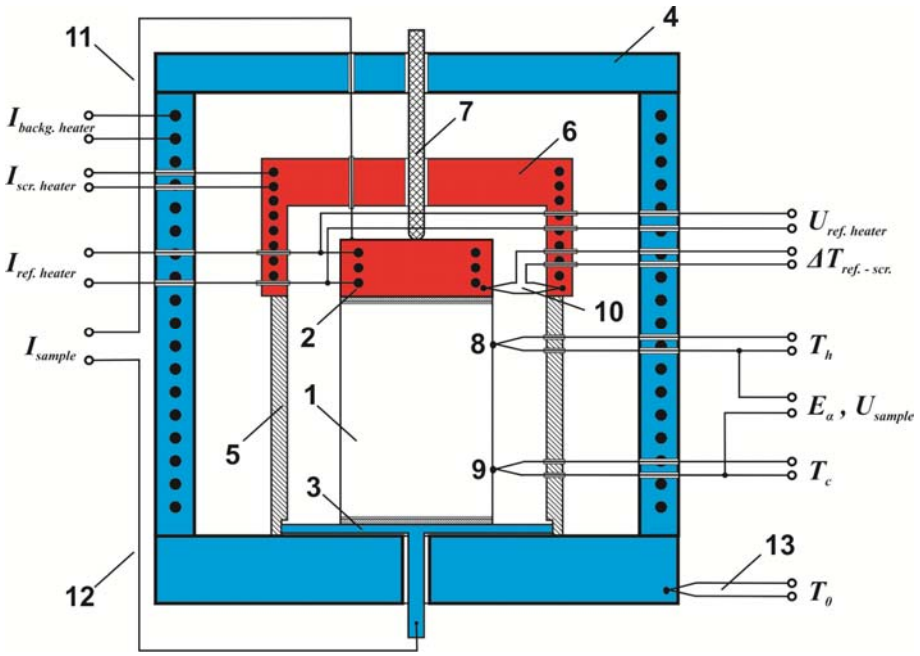

Fig. 1. Complex absolute method of measuring thermoelectric parameters of materials.
1 – sample under study; 2 – reference heater; 3 – mounting pad; 4 – thermostat;
5 – screen; 6 – screen heater; 7 – clamp; 8, 9 – measuring thermocouple probes;
10 – zero thermocouple; 11, 12 – sample conductors; 13 – thermostat thermocouple;
I_{sample}, U_{sample} – current through the sample and voltage drop between measuring thermocouple probes when measuring electrical conductivity; E_α – thermoEMF between identical legs of thermocouple probes; T_h and T_c – "hot" and "cold" temperature on the sample; $I_{ref.heater}$, $U_{ref.heater}$ – supply current and voltage of reference heater when measuring thermal conductivity; $I_{scr.heater}$ – supply current of screen heater;
$I_{backg.heater}$ – supply current of background heater.

Thermoelectric parameters of sample under study are determined by the formulae

$$\sigma = \frac{I_{sample}}{U_{sample}} \frac{l}{S}, \qquad (1)$$

$$\alpha = \frac{E_\alpha}{T_h - T_c}, \tag{2}$$

$$\kappa = \frac{I_{ref.heater} \cdot U_{ref.heater}}{T_h - T_c} \frac{l}{S}, \tag{3}$$

$$Z = \frac{\alpha^2 \sigma}{\kappa}, \tag{4}$$

where l is the distance between the probes, S is the cross-sectional area of the sample.

To implement such a method, the measurement control system should have:

- means for setting and maintaining the temperature of the measuring thermostat over a wide temperature range (thermostat, power supply, control thermocouple, etc.);
- adjustable power supply for passing current through the sample when measuring electrical conductivity, current switch;
- adjustable power supply of the reference heater;
- adjustable power supply of the screen heater;
- means for maintaining a zero temperature difference between the reference and screen heaters (thermostat, power supply, control zero-thermocouple, etc.);
- high-precision voltage meter with a resolution of not less than 1 μV;
- the ability to set the required cyclogram of switching on/off power supply units and the moments of recording the measurement results of all measuring channels (temperatures of "hot" and "cold" probes, voltage drop between the probes, current and voltage values through the sample, current and supply voltage of the reference heater);
- the ability to transfer measurement results to a computer for their further processing, plotting graphs and tables, forming a sample passport.

Description of the measurement control unit

Universal units have been developed that have discrete control inputs and corresponding analog outputs. By combining these units and controlling them according to the required cyclogram using a programmable controller, one can create various settings which make it possible to implement any method of measuring parameters of thermoelectric materials. A system for measuring automation has also been developed, the block diagram of which is shown in Fig. 2. It is based on a 24-bit 8-channel analog-to-digital converter (ADC) 4 with differential inputs, the range of measured voltages of which is ± (5 μV – 2.5 V). Differential inputs of the ADC allow high-precision measurements of voltages in the electrical circuits of various units, which may have different power sources.

The system also includes intelligent keys 6 and 7 with their short circuit and over-current protection circuitry. The use of such keys ensures high reliability of the installation, preventing its failure during malfunctions in power circles. The use of modern field-effect transistors manufactured using MOSFET technology with low resistance in the open state as an element base reduces heat generation on it, which eliminates the need for radiators. The keys are able to switch up to 600 watts of load.

An adjustable stable voltage source 8 is used to supply the reference heater with a stable voltage. It can provide a reference heater with power up to 10 W.

Electronic switch 9 allows one to enable or disable the current through the sample, change the direction of the current, and also supply it with alternating current. The switch is assembled according to the H-bridge scheme on the basis of powerful field-effect MOSFET transistors. The current of the electronic switch may be in the range from 0.01 to 8.0 A.

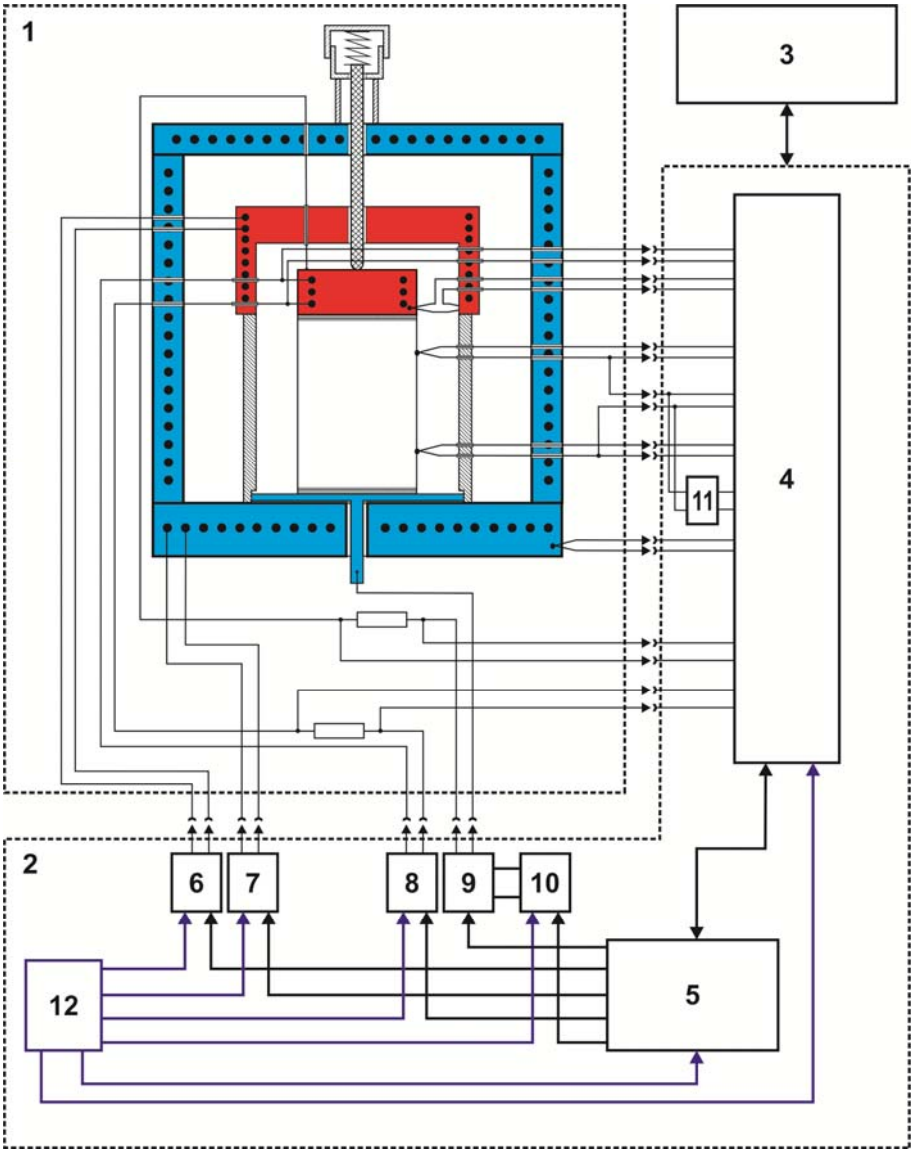

Fig. 2. Block-diagram of automation of measurement of thermoelectric parameters of materials by complex absolute method.
1 – measuring unit; 2 – measurement control unit; 3 – computer;
4 – analog to digital converter; 5 – controller; 6, 7 – switches;
8, 10 – regulated voltage sources; 9 – electronic switch;
11 – synchronous detector; 12 – power supply unit.

An adjustable source of stable current 10 provides current through the sample, which can be set between 0.05 A and 4.0 A. Synchronous detector 11 allows one to accurately detect alternating voltages, as well as to measure the pulse values of voltages on the sample. The synchronous detector is assembled according to a key scheme, with various discrete control inputs, by controlling which it is possible to realize various modes of operation with a pulsed power supply of the sample.

The system contains an actuator control unit. In this method, the sound buzzer as an actuator signals the end of the cycle or the completion of work. If the system is used in equipment to study the heterogeneity of samples, this unit can control the motors to create a programmable movement of probes over the surface of the sample under study.

Programmable controller 5 contains two PID-PWM temperature controllers, the discrete outputs of which provide automatic or manual operation of the installation in accordance with specified cyclograms

and algorithms of work and input for processing the signal coming from the ADC.

The power supply unit of installation 12 is assembled on the basis of a power toroidal transformer and linear voltage regulators without high-frequency noise inherent in pulsed power supplies, which improves the measurement accuracy.

The measuring unit is connected via USB to a personal computer 3, where cyclograms of measurements are set, necessary calculations are made, corresponding graphs are built and measurement protocols are formed.

When using a measuring unit designed for a temperature range of 30 - 500 ° C, the system is designed to work as follows.

One controller thermostat through a key controls the thermostat heater, which maintains the background temperature T0 with an error of no more than ± 0.1 ° C. The value of the background temperature is set at the controller input from the table specified on the computer. The second thermostat of the screen heater maintains zero temperature difference between the reference and screen heaters with an error of no more than ± 0.1 ° C. The electronic switch provides a direct, reverse and alternating current through the sample using a controlled current source. A synchronous detector rectifies alternating voltages on a sample, if the electrical conductivity is measured on alternating current. An analog-to-digital converter measures the background temperature, the temperature of thermocouple probes, the voltage drop between the probes, the current through the sample, the voltage and the current through the reference heater. All measured signals are sent to the controller, where they are normalized to specific physical quantities, and then enter a personal computer for calculations and plotting in a given temperature range. The sequence of measurements and time dwells between them are specified in the cyclogram, which the operator forms before starting the measurements.

The technical characteristics of the developed system make it possible to carry out measurements for a wide range of parameters of the materials studied: electrical conductivity - from 10 to 10.000 Ω^{-1} cm^{-1}; thermoEMF - from ± 10 to ± 500 μV / K; thermal conductivity - from 0.1 to 20 W/(m· K) (for samples with a diameter of 6-8 mm and a length of 8 – 13 mm).

The developed system is universal. The number and characteristics of control and measurement channels allows it to be used for other measurement methods – the comparative method, the Harman method, methods for studying the heterogeneity of ingots and discs of thermoelectric materials, and the like.

Software for computerization of measurements

The system is controlled by a computer with the SThEM software, developed jointly with Tereks Scientific Production Enterprise (Kyiv, Ukraine). The program allows one to perform real-time measurements, process the measurement result, display data on the screen in the form of graphs and tables, save them on a computer, export to MS Excel, print.

The "SThEM" measurement control program has a standard structure adopted in the Windows operating system (Fig. 3). It comprises measurement process control tools (experiment setup windows, indicators for switching on/off current through the sample, powering the hot probe heater, etc), the area for plotting measurement results, tables with the measured and calculated values of the sample properties.

The SThEM program also sets the parameters of the control unit — the settings of the measuring channels and temperature controllers.

Each of the eight measuring channels can be configured using the polynomial dependence of the 7th power between the measured signal X_i and the output signal Y_i

$$Y_i = a_0 + a_1 X_i + a_2 X_i^2 + a_3 X_i^2 + a_4 X_i^4 + a_5 X_i^5 + a_6 X_i^6 + a_7 X_i^7 , \quad (5)$$

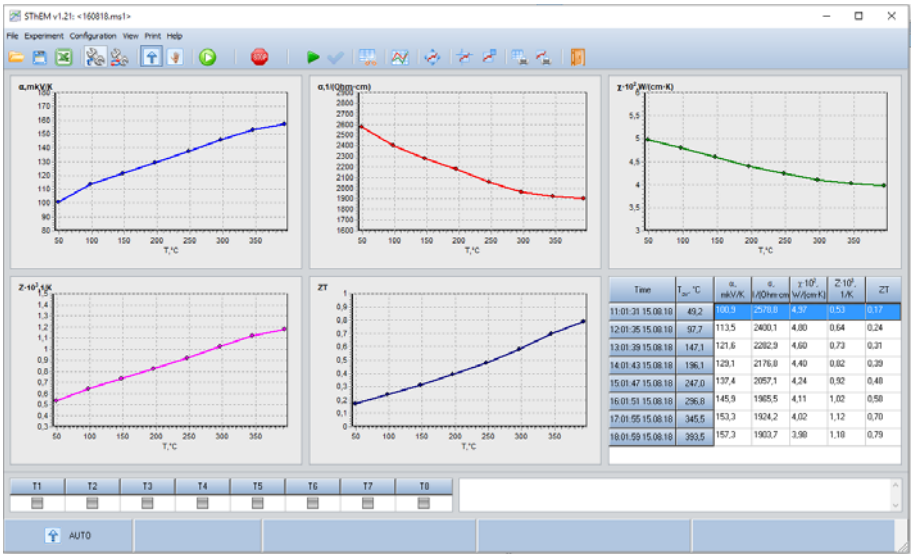

Fig. 3. Appearance of the main window of the STheM program for control of measurement process.

where a_0 - a_7 are polynomial coefficients of each channel assigned by the operator.

This makes it possible, with a high accuracy (up to 0.1 μV), to convert the thermopower of the measuring thermocouples into degrees in accordance with their calibration characteristics, as well as the coefficients of conversion of other signals in accordance with the reference resistance used, voltage dividers, and the like.

Before starting the measurements, the operator enters information about the sample under investigation into the window of setting the experiment parameters (Fig. 4) and selects the desired temperatures, whereby measurements will be carried out automatically.

The program also allows forming the cyclogram of measurements (Fig. 5) - the moments of recording the readings of the measuring channels, turning the current on and off through the sample, powering the reference heater and the like.

On the basis of the developed control system, the automation of measuring equipment "ALTEC-10001" and "ALTEC-10001M" was carried out for measuring the thermoelectric properties of materials in the temperature ranges of 30 – 500 ° C and 30 – 900 ° C, respectively.

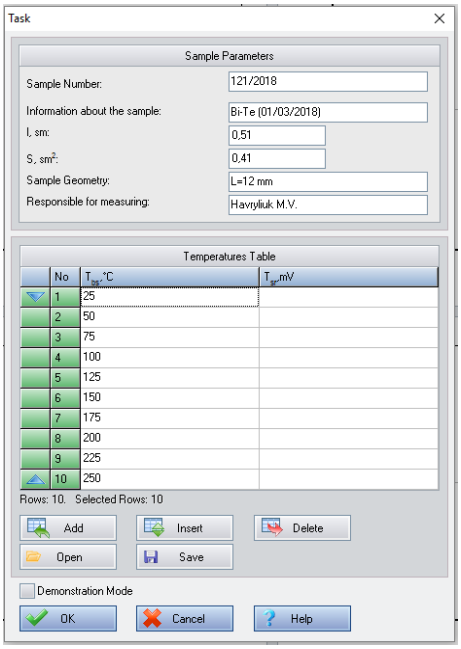

Fig. 4. The window of setting the experiment parameters in the STheM software

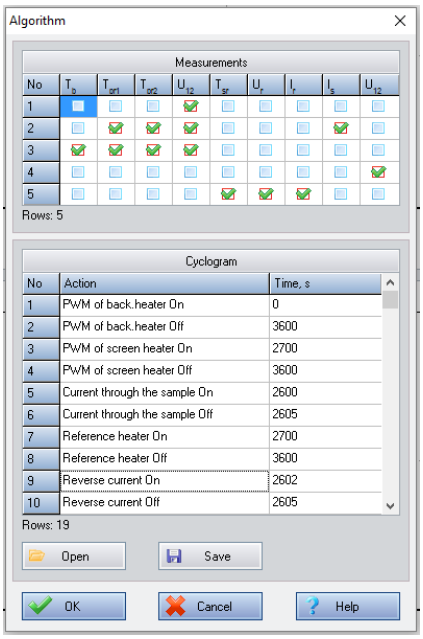

Fig. 5. The window of forming the cyclogram of measurements in the STheM software

Conclusion

1. A universal electronic control system has been developed that allows the implementation of automated measurements of thermoelectric properties by various methods, including the complex absolute method. Automated measuring equipment based on such a system allows measurements for a wide range of parameters of the materials under study: electrical conductivity - from 10 to 10.000 $\Omega^{-1}sm^{-1}$; thermoEMF - from ± 10 to ± 500 μV/ K; thermal conductivity - from 0.1 to 20 W/ (m ·K). A universal electronic control system has been developed that allows the implementation of automated measurements of thermoelectric properties by various methods, including the complex absolute method. Automated measuring equipment based on such a system allows measurements for a wide range of parameters of the materials under study: electrical conductivity - from 10 to 10.000 Ω^{-1} sm^{-1}; thermoelectric power - from ± 10 to ± 500 μV / K; thermal conductivity - from 0.1 to 20 W / (m· K).
2. Software for computerization of the measurement process has been created. The program allows one to perform real-time measurements, process their results, display the measurement results on the screen in the form of graphs and tables, save them on a computer, export to MS Excel and print the passport of the studied sample.

References

1. Ioffe A.F. (1960). *Poluprovodnikovyie termoelementy (Semiconductor thermoelements)*. Moscow-Leningrad: AN SSSR [in Russian].
2. Anatychuk L.I. (1978*). Termoelementy i termoelektricheskiie ustroistva (Thermoelements and thermoelectric devices)*. Kyiv: Naukova dumka [in Russian].
3. V. Lysko. (2015). Metrology of materials and its role in development of thermoelectricity. *Proc. of XVI International Forum on Thermoelectricity*. (Paris, France, 2015).
4. Anatychuk L.I., Lysko V.V. (2012). Investigation of the effect of radiation on the precision of thermal conductivity measurement by the absolute method. *J.Thermoelectricity*, 1, 67-76.

5. *Patent of Ukraine № 71614* (2012). Anatychuk L.I., Lysko V.V. Device for determining the electrical conductivity, thermal conductivity and thermoEMF of thermoelectric materials [in Ukrainian].
6. Anatychuk L.I., Lysko V.V. (2014). Methods for assuring high quality electric and thermal contacts when measuring parameters of thermoelectric materials. *J.Thermoelectricity*, 4, СТОР ?
7. Anatychuk L.I., Lysko V.V. (2014). On improvement of the accuracy and speed in the process of measuring characteristics of thermoelectric materials. *J. Electronic Materials*, 43(10), 3863-3869.
8. Lysko V.V. (2016). On the temperature dependences of errors in measuring thermal conductivity by the absolute method. *J.Thermoelectricity*, 2.
9. Anatychuk L.I., Lysko V.V. (2014). Increasing the rapidity of thermal conductivity measurement by the absolute method. *J.Thermoelectricity*, 5.

Submitted 10.07.2018

Анатичук Л.І., *ак. НАН України,*[1,2] **Гаврилюк М.В.,**[1,2]
Лисько В.В., *канд. фіз. – мат. наук,*[1,2] **Тюменцев В.А.**[1]

[1]Інститут термоелектрики НАН і МОН України,
вул. Науки, 1, Чернівці, 58029, Україна;
[2]Чернівецький національний університет
ім. Юрія Федьковича, вул. Коцюбинського 2,
Чернівці, 58000, Україна, *e-mail: anatych@gmail.com*

АВТОМАТИЗАЦІЯ ТА КОМП'ЮТЕРИЗАЦІЯ ВИМІРЮВАНЬ ТЕРМОЕЛЕКТРИЧНИХ ПАРАМЕТРІВ МАТЕРІАЛІВ

Представлено результати розробки системи автоматизації процесу вимірювань термоелектричних властивостей матеріалів і обробки їх результатів. Блок керування вимірюваннями побудовано на основі багатоканального аналогово-цифрового перетворювача. Управління процесом вимірювань, обробка та відображення результатів проводяться за допомогою комп'ютера, до якого блок вимірювань підключається по стандартному каналу USB. Результати відображаються у вигляді графіків і таблиць. Розроблена система автоматизації є універсальною та дозволяє реалізовувати як класичні стаціонарні методи вимірювань термоелектричних властивостей матеріалів, так і складні алгоритми вимірювань з підвищеною швидкодією. Наведено приклад використання розробленої системи для визначення термоелектричних властивостей матеріалу комплексним абсолютним методом. Бібл. 9, рис. 5.
Ключові слова: електропровідність, термоЕРС, теплопровідність, термоелектричний матеріал, автоматизація, комп'ютеризація.

Анатычук Л.И., *ак. НАН Украины,*[1,2] **Гаврилюк М.В.,**[1,2]
Лысько В.В., *канд. физ – мат. наук,*[1,2] **Тюменцев В.А.**[1]

[1]Институт термоэлектричества НАН и МОН Украины,
вул. Науки, 1, Черновцы, 58029, Украина;
[2]Чернивецький национальный университет
им. Юрия Федьковича, ул. Коцюбинского 2,
Черновцы, 58000, Украина, *e-mail: anatych@gmail.com*

Представлены результаты разработки системы автоматизации процесса измерений термоэлектрических свойств материалов и обработки их результатов. Блок управления измерениями построен на основе многоканального аналого-цифрового преобразователя. Управление процессом измерений, обработка и отображение результатов проводятся с помощью компьютера, к которому блок измерений подключается по стандартному каналу USB. Результаты отображаются в виде графиков и таблиц. Разработанная система автоматизации является универсальной и позволяет реализовывать как классические стационарные методы измерений термоэлектрических свойств материалов, так и сложные алгоритмы измерений с повышенным быстродействием. Приведен пример использования разработанной системы для определения термоэлектрических свойств материала комплексным абсолютным методом. Библ. 9, рис. 5.

Ключевые слова: электропроводимость, термоЕРС, теплопроводимость, термоэлектрический материал, автоматизация, компьютеризация.

References

1. Ioffe A.F. (1960). *Poluprovodnikovyie termoelementy (Semiconductor thermoelements)*. Moscow-Leningrad: AN SSSR [in Russian].
2. Anatychuk L.I. (1978*). Termoelementy i termoelektricheskiie ustroistva (Thermoelements and thermoelectric devices)*. Kyiv: Naukova dumka [in Russian].
3. V. Lysko. (2015). Metrology of materials and its role in development of thermoelectricity. *Proc. of XVI International Forum on Thermoelectricity*. (Paris, France, 2015).
4. Anatychuk L.I., Lysko V.V. (2012). Investigation of the effect of radiation on the precision of thermal conductivity measurement by the absolute method. *J.Thermoelectricity*, 1, 67-76.
5. *Patent of Ukraine № 71614* (2012). Anatychuk L.I., Lysko V.V. Device for determining the electrical conductivity, thermal conductivity and thermoEMF of thermoelectric materials [in Ukrainian].
6. Anatychuk L.I., Lysko V.V. (2014). Methods for assuring high quality electric and thermal contacts when measuring parameters of thermoelectric materials. *J.Thermoelectricity*, 4, СТОР ?
7. Anatychuk L.I., Lysko V.V. (2014). On improvement of the accuracy and speed in the process of measuring characteristics of thermoelectric materials. *J. Electronic Materials*, 43(10), 3863-3869.
8. Lysko V.V. (2016). On the temperature dependences of errors in measuring thermal conductivity by the absolute method. *J.Thermoelectricity*, 2.
9. Anatychuk L.I., Lysko V.V. (2014). Increasing the rapidity of thermal conductivity measurement by the absolute method. *J.Thermoelectricity*, 5.

Submitted 10.07.2018

ARTICLE SUBMISSION GUIDELINES

For publication in a specialized journal, scientific works are accepted that have never been printed before. The article should be written on an actual topic, contain the results of an in-depth scientific study, the novelty and justification of scientific conclusions for the purpose of the article (the task in view).

The materials published in the journal are subject to internal and external review which is carried out by members of the editorial board and international editorial board of the journal or experts of the relevant field. Reviewing is done on the basis of confidentiality. In the event of a negative review or substantial remarks, the article may be rejected or returned to the author(s) for revision. In the case when the author(s) disagrees with the opinion of the reviewer, an additional independent review may be done by the editorial board. After the author makes changes in accordance with the comments of the reviewer, the article is signed to print.

The editorial board has the right to refuse to publish manuscripts containing previously published data, as well as materials that do not fit the profile of the journal or materials of research pursued in violation of ethical norms (for instance, conflicts between authors or between authors and organization, plagiarism, etc.). The editorial board of the journal reserves the right to edit and reduce the manuscripts without violating the author's content. Rejected manuscripts are not returned to the authors.

Submission of manuscript to the journal

The manuscript is submitted to the editorial office of the journal in paper form in duplicate and in electronic form on an electronic medium (disc, memory stick). The electronic version of the article shall fully correspond to the paper version. The manuscript must be signed by all co-authors or a responsible representative.

In some cases it is allowed to send an article by e-mail instead of an electronic medium (disc, memory stick).

English-speaking authors submit their manuscripts in English. Russian-speaking and Ukrainian-speaking authors submit their manuscripts in English and in Russian or Ukrainian, respectively. Page format is A4. The number of pages shall not exceed 15 (together with References and extended abstracts). By agreement with the editorial board, the number of pages can be increased.

To the manuscript is added:

1. Official recommendation letter, signed by the head of the institution where the work was carried out.

2. License agreement on the transfer of copyright (the form of the agreement can be obtained from the editorial office of the journal or downloaded from the journal website – Dohovir.pdf). The license agreement comes into force after the acceptance of the article for publication. Signing of the license agreement by the author(s) means that they are acquainted and agree with the terms of the agreement.

3. Information about each of the authors – full name, position, place of work, academic title, academic degree, contact information (phone number, e-mail address), ORCID code (if available). Information about the authors is submitted as follows:

authors from Ukraine - in three languages, namely Ukrainian, Russian and English;

authors from the CIS countries - in two languages, namely Russian and English;

authors from foreign countries – in English.

4. Medium with the text of the article, figures, tables, information about the authors in electronic

form.

5. Colored photo of the author(s). Black-and-white photos are not accepted by the editorial staff. With the number of authors more than two, their photos are not shown.

Requirements for article design

The article should be structured according to the following sections:

- *Introduction*. Contains the problem statement, relevance of the chosen topic, analysis of recent research and publications, purpose and objectives.
- *Presentation of the main research material* and the results obtained.
- *Conclusions* summing up the work and the prospects for further research in this direction.
- *References*.

The first page of the article contains information:

1) in the upper left corner – UDC identifier (for authors from Ukraine and the CIS countries);

2) surname(s) and initials, academic degree and scientific title of the author(s);

3) the name of the institution where the author(s) work, the postal address, telephone number, e-mail address of the author(s);

4) article title;

5) abstract to the article – not more than 1 800 characters. The abstract should reflect the consistent logic of describing the results and describe the main objectives of the study, summarize the most significant results;

6) key words – not more than 8 words.

The text of the article is printed in Times New Roman, font size 11 pt, line spacing 1.2 on A4 size paper, justified alignment. There should be no hyphenation in the article.

Page setup: "mirror margins" – top margin – 2.5 cm, bottom margin – 2.0 cm, inside – 2.0 cm, outside – 3.0 cm, from the edge to page header and page footer – 1.27 cm.

Graphic materials, pictures shall be submitted in color or, as an exception, black and white, in .opj or .cdr formats, .jpg or .tif formats being also permissible. According to author's choice, the tables and partially the text can be also in color.

Figures are printed on separate pages. The text in the figures must be in the font size 10 pt. On the charts, the units of measure are separated by commas. Figures are numbered in the order of their arrangement in the text, parts of the figures are numbered with letters – a, b, .. On the back of the figure, the title of the article, the author (authors) and the figure number are written in pencil. Scanned images and graphs are not allowed to be inserted.

Tables are provided on separate pages and must be executed using the MSWord table editor. Using pseudo-graph characters to design tables is inadmissible.

Formulae shall be typed in Equation or MatType formula editors. Articles with formulae written by hand are not accepted for printing. It is necessary to give definitions of quantities that are first used in the text, and then use the appropriate term.

Captions to figures and tables are printed in the manuscript after the references.

Reference list shall appear at the end of the article. References are numbered consecutively in the order in which they are quoted in the text of the article. References to unpublished and unfinished works are inadmissible.

Attention! In connection with the inclusion of the journal in the international bibliographic abstract database, the reference list should consist of two blocks: CITED LITERATURE and REFERENCES (this requirement also applies to English articles):

CITED LITERATURE – sources in the original language, executed in accordance with the Ukrainian standard of bibliographic description DSTU 8302:2015. With the aid of VAK.in.ua

(http://vak.in.ua) you can automatically, quickly and easily execute your "Cited literature" list in conformity with the requirements of State Certification Commission of Ukraine and prepare references to scientific sources in Ukraine in understandable and unified manner. This portal facilitates the processing of scientific sources when writing your publications, dissertations and other scientific papers.

REFERENCES – the same cited literature list transliterated in Roman alphabet (recommendations according to international bibliographic standard APA-2010, guidelines for drawing up a transliterated reference list "References" are on the site http//www.dse.org.ua, section for authors).

To speed up the publication of the article, please adhere to the following rules:

- in the upper left corner of the first page of the article – the UDC identifier;
- family name and initials of the author(s);
- academic degree, scientific title;

begin a new line, Times New Roman font, size 12 pt, line spacing 1.2, center alignment;

- name of organization, address (street, city, zip code, country), e-mail of the author(s);

begin a new line 1 cm below the name and initials of the author(s), Times New Roman font, size 11 pt, line spacing 1.2, center alignment;

- the title of the article is arranged 1 cm below the name of organization, in capital letters, semi-bold, font Times New Roman, size 12 pt, line spacing 1.2, center alignment. The title of the article shall be concrete and possibly concise;
- the abstract is arranged 1 cm below the title of the article, font Times New Roman, size 10 pt, in italics, line spacing 1.2, justified alignment in Ukrainian or Russian (for Ukrainian-speaking and Russian-speaking authors, respectively);
- key words are arranged below the abstract, font Times New Roman, size 10 pt, line spacing 1.2, justified alignment. The language of the key words corresponds to that of the abstract. Heading "Key words" - font Times New Roman, size 10 pt, semi-bold;
- the main text of the article is arranged 1 cm below the abstract, indent 1 cm, font Times New Roman, size 11 pt, line space spacing 1.2, justified alignment;
- formulae are typed in formula editor, fonts Symbol, Times New Roman. Font size is "normal" – 12 pt, "large index" – 7 pt, "small index" – 5 pt, "large symbol" – 18 pt, "small symbol" – 12 pt. The formula is arranged in the text, center aligned and shall not occupy more than 5/6 of the line width, formulae are numbered in parentheses on the right;
- dimensions of all quantities used in the article are represented in the International System of Units (SI) with the explication of the symbols employed;
- figures are arranged in the text. The figures and pictures shall be clear and contrast; the plot axes – parallel to sheet edges, thus eliminating possible displacement of angles in scaling; figures are submitted in color, black-and-white figures are not accepted by the editorial staff of the journal;
- tables are arranged in the text. The width of the table shall be 1 cm less than the line width. Above the table its ordinary number is indicated, right alignment. Continuous table numbering throughout the text. The title of the table is arranged below its number, center alignment;
- references should appear at the end of the article. References within the text should be

enclosed in square brackets behind the text. References should be numbered in order of first appearance in the text. Examples of various reference types are given below.

Examples of LITERATURE CITED

Journal articles

Anatychuk L.I., Mykhailovsky V.Ya., Maksymuk M.V., Andrusiak I.S. Experimental research on thermoelectric automobile starting pre-heater operated with diesel fuel. *J.Thermoelectricity*. 2016. №4. P.84–94.

Books

Anatychuk L.I. *Thermoelements and thermoelectric devices. Handbook.* Kyiv, Naukova dumka, 1979. 768 p.

Patents

Patent of Ukraine № 85293. Anatychuk L.I., Luste O.J., Nitsovych O.V. Thermoelement.

Conference proceedings

Lysko V.V. *State of the art and expected progress in metrology of thermoelectric materials.* Proceedings of the XVII International Forum on Thermoelectricity (May 14-18, 2017, Belfast). Chernivtsi, 2017. 64 p.

Authors' abstracts

Kobylianskyi R.R. *Thermoelectric devices for treatment of skin diseases*: extended abstract of candidate's thesis. Chernivtsi, 2011. 20 p.

Examples of REFERENCES

Journal articles

Gorskiy P.V. (2015). Ob usloviakh vysokoi dobrotnosti i metodikakh poiska perspektivnykh sverhreshetochnykh termoelektricheskikh materialov [On the conditions of high figure of merit and methods of search for promising superlattice thermoelectric materials]. *Termoelektrichestvo - J.Thermoelectricity,* 3, 5 – 14 [in Russian].

Books

Anatychuk L.I. (2003). *Thermoelectricity. Vol.2. Thermoelectric power converters*. Kyiv, Chernivtsi: Institute of Thermoelectricity.

Patents

Patent of Ukraine № 85293. Anatychuk L. I., Luste O.Ya., Nitsovych O.V. Thermoelements [In Ukrainian].

Conference proceedings

Rifert V.G. Intensification of heat exchange at condensation and evaporation of liquid in 5 flowing-down films. In: *Proc. of the 9th International Conference Heat Transfer.* May 20-25, 1990, Israel.

Authors'abstracts

Mashukov A.O. *Efficiency hospital state of rehabilitation of patients with color carcer.* PhD (Med.) Odesa, 2011 [In Ukrainian].